# DIPLOMARBEIT

Titel der Diplomarbeit

## „The role of the putative antifeeding prophage of *Amoebophilus asiaticus* during infection"

Verfasst von

**Agnes Harreither**

angestrebter akademischer Grad

**Magistra der Naturwissenschaften (Mag.rer.nat.)**

# Table of Contents

# Chapter 1. Introduction

## 1.1. Significance and diversity of symbiosis

Symbiosis, the association of and interaction between two or more different biological species, is a central principle displaying itself in various manifestations in all domains of life. It is a ubiquitous phenomenon found in the most contrasting environments in terrestrial, marine, and freshwater ecosystems. Microorganisms arose long before the first multicellular organisms appeared on our planet and themselves provided stable, nutrient-rich habitats to be potentially inhabited by microbes. Since then, symbioses between large organisms and microbes have been an important driving force in the emergence of new life forms on Earth and the generation of biological diversity (Moran, 2006). But perhaps the most fundamental example for the importance of symbiosis in evolution can be found on a cellular level when looking at the origin of eukaryotic organelles. More than 1.5 billion years ago, the ancestors of today's plastids and mitochondria – belonging to the phyla of the *Cyanobacteria* and *Alphaproteobacteria*, respectively – established stable symbiotic relationships with their host cells, giving rise to modern eukaryotic cells (Margulis, 1981).

The concept of symbiosis has been known already since the mid-nineteenth century. It was first postulated by Simon Schwendener, based on studies on fungi and algae living in close proximity as lichens, which were previously considered to be a neglected class of plants (Sapp, 1994). However, Schwendener's work was met with controversial reception by the contemporary scientific society. Only towards the end of the 19th century, as further examples of unrelated organisms living together in intimate, but not merely parasitic associations were described, the dogma of symbiosis gained more and more acceptance. The term "symbiosis" itself was originally defined by Heinrich Anton de Bary as "the living together of unlike organisms" (de Bary, 1879), a rendition which has not lost its general validity up to the present.

According to the current understanding, symbiosis is used to address a broad range of associations, which can be classified according to the following criteria:

*Effects on the fitness of host and symbiont*
Based on the mutual effects on the fitness of host and symbiont, three distinct categories of symbiosis can be distinguished: mutualism, commensalism, and parasitism (Sapp, 1994). While both partners benefit in a mutualistic relationship, as it is for example observed in the aphid endosymbiont *Buchnera aphidicola* (Munson *et al.*, 1991), commensalism describes an association in which only one involved partner benefits, and the effect on the other partner is neutral. Parasitism, on the other side, occurs when one symbiotic partner increases its own fitness by exploiting the other partner. In general, bacterial human pathogens fall into the last category and have drawn attention to this type of symbiosis in the past decades, so that countless well-studied examples exist. However, the borders of this classification are not always clear and absolute, and a shift from one type to another is possible.

*Location of the symbiont*
Ectosymbionts reside on the body surface of the host, which also includes internal surfaces in larger organisms such as the digestive tract. In contrast, endosymbionts live within the body or cells of their host. Intracellular endosymbionts can either be found directly within the cytosol or surrounded by host-derived membranes.

INTRODUCTION

*Obligate versus facultative relationships*

Symbiosis can be obligate for the host, for the symbiont, for both of them, or neither, depending on the degree of specialisation (Moran, 2006).

Symbiotic relationships are as diverse as they are fascinating. One particular point of interest are bacterial endosymbionts of eukaryotic hosts, ranging from unicellular eukaryotes, such as amoebae, to insects, mammals, and other complex organisms. Corresponding to the vast diversity found in these associations, also a variety of mechanisms for host-symbiont interactions exists, and our knowledge in this field is far from complete.

## 1.2. Bacterial endosymbionts of free-living amoebae

Free-living amoebae are ubiquitous protozoa which can be found in a broad range of natural habitats, including soil, water, and air, and have also been isolated from anthropogenic environments, for example cooling towers and air-conditioning systems. Because of their importance as predators of prokaryotic and eukaryotic microorganisms, amoebae are generally considered to be essential players in controlling microbial community composition (Rodríguez-Zaragoza, 1994). However, some bacteria have developed mechanisms to escape the amoebal phagocytosis, adapt to the intracellular environment and replicate within the eukaryotic host, leading to either transient or stable associations. A variety of transient, or facultative, associations with amoebae is known in particular for human pathogens, for example *Legionella pneumophila* (Kwaik, 1996; Bozue & Johnson, 1996; Newsome *et al.*, 1985; Rowbotham, 1986). Stable associations of bacteria with amoebae result in long-term symbiotic relationships and have been described for members of the *Alphaproteobacteria* (Birtles *et al.*, 2000; Fritsche *et al.*, 1999; Horn *et al.*, 1999), *Betaproteobacteria* (Horn *et al.*, 2002), *Gammaproteobacteria* (Horn *et al.*, 1999), *Chlamydiae* (Amann *et al.*, 1997; Birtles *et al.*, 1997; Fritsche *et al.*, 2000; Horn *et al.*, 2000), and *Bacteroidetes* (Horn *et al.*, 2001). This phylogenetic diversity of bacterial endosymbionts suggests that the capability to exploit free-living amoebae as hosts has evolved independently several times within the *Bacteria* (Molmeret *et al.*, 2005). Most amoebal endosymbionts are closely related to other obligate intracellular bacteria, some of which are well-known pathogens of animals and humans, for example *Rickettsia* spp. and pathogenic members of the *Chlamydiae*. It is therefore hypothesised that many endosymbionts of free-living amoebae share common ancestors with intracellular human pathogenic bacteria, and that the amoebae may have acted as "training ground" for these ancestors supporting the evolution of mechanisms for intracellular survival (Molmeret *et al.*, 2005).

## 1.3. *Amoebophilus asiaticus*

*Amoebophilus asiaticus*, a Gram-negative bacterium assigned to the phylum of the *Bacteroidetes*, is an obligate endosymbiont of *Acanthamoeba* sp. Microscopic analysis of *A. asiaticus* revealed rod-shaped cells with a length of 1.0–1.5 μm and cell diameter of 0.3–0.5 μm (Horn *et al.*, 2001). Within the *Acanthamoeba* host cells, *A. asiaticus* resides directly in the cytoplasm and is closely associated with host cell ribosomes (Horn *et al.*, 2001; Schmitz-Esser *et al.*, 2010). Since no beneficial effects for the host are known, *A. asiaticus* is considered to be a parasite. With 88 % 16S rRNA gene sequence identity, *Cardinium hertigii*, an obligate intracellular parasite of insects, is the closest described relative of *A. asiaticus* (Zchori-Fein *et al.*, 2004). The *C. hertigii* strain cEper1 is a reproductive manipulator capable of inducing cytoplasmic incompatibility (CI) in its host, the parasitic wasp *Encarsia pergandiella* (Hunter *et al.*, 2003). Both symbionts, *A. asiaticus* and *C. hertigii*, belong to a

monophyletic group within the otherwise phylogenetically diverse phylum of the *Bacteroidetes* (Sunagawa *et al.*, 2009; Schmitz-Esser *et al.*, 2010).

## 1.3.1. Genomic features of *Amoebophilus asiaticus*

Elucidating the symbiotic relationship between *A. asiaticus* and its *Acanthamoeba* host has been a research endeavour at the Department of Microbial Ecology (University of Vienna) and its collaboration partners in the past decade. Genome analysis of the *A. asiaticus* strain 5a2, which was recovered from amoebae isolated from lake sediment in Austria (Schmitz-Esser *et al.*, 2008), has provided an abundance of insights into possible mechanisms for host cell interaction. The genome of *A. asiaticus* consists of one circular chromosome with a size of 1.9 Mbp, has a G+C content of 35 mol% and encodes 1557 proteins, corresponding to a coding density of 82 %. No evidence for plasmids was found during genome assembly and pre-analysis with pulsed-field gel electrophoresis (Schmitz-Esser *et al.*, 2010). While obligate mutualistic symbionts of insects with an intracellular lifestyle usually show an extreme reduction in genome size, typically below 1 Mbp (Moran *et al.*, 2008), the *A. asiaticus* genome is only moderately reduced by comparison. Even its closest relative, *C. hertigii*, has a much smaller genome with an 887 kb chromosome and a 58 kb cryptic plasmid (Penz *et al.*, 2012).

Notwithstanding the mild degree of genome reduction in numerical terms, *A. asiaticus* has very restricted biosynthetic capabilities. Phosphofructokinase, for example, the key enzyme for the glycolysis (or Embden-Meyerhof-Parnass) pathway, is not encoded in the genome, although most of the other enzymes required for glycolysis are present. It is assumed that the enzymatic repertoire is used in the opposed direction for gluconeogenesis rather than glycolysis, since *A. asiaticus* also lacks specific sugar uptake systems, but does encode fructose bisphosphatase, the key enzyme for gluconeogenesis. The complete tricarboxylic acid cycle and the oxidative branch of the pentose phosphate pathway are absent. In addition, pathways for the biosynthesis of cofactors, nucleotides, and *de novo* synthesis of most amino acids are missing in the genome of *A. asiaticus*, and no functional respiratory chain was detected. Taken together, these metabolic limitations suggest that energy generation via substrate level phosphorylation can only be achieved after the uptake of substrates from the amoeba host (Schmitz-Esser *et al.*, 2010). A similarly high dependency on host cell metabolism is also known from other intracellular bacteria (Wernegreen, 2005). Accordingly, the genome of *A. asiaticus* encodes 82 putative transport proteins for the uptake of different essential metabolites from the host (Schmitz-Esser *et al.*, 2010).

Corresponding to the strict dependency on its *Acanthamoeba* host, *A. asiaticus* is equipped with a large repertoire of proteins that are presumably used for interaction with the host. Outstanding among these proteins is the copious amount of proteins with eukaryotic-like domains (n = 129; 8 % of all genes) like ankyrin repeats, TRP/SEL1 repeats, leucine-rich repeats, or F- and U-box domains (Schmitz-Esser *et al.*, 2010). It is known from bacterial pathogens that these domains are substantial for the interplay between host and symbiont by mediating protein-protein interactions (Al-Khodor *et al.*, 2008; Caturegli *et al.*, 2000; Cazalet *et al.*, 2004; Habyarimana *et al.*, 2008; Kubori *et al.*, 2008; Newton *et al.*, 2007; Pan *et al.*, 2008; Voth *et al.*, 2009). In particular, *A. asiaticus* encodes an unmatched number of proteins (n = 26) which are able to interfere with the eukaryotic ubiquitin system (Schmitz-Esser *et al.*, 2010). Ubiquitination and deubiquitination play essential roles in the regulation of the eukaryotic cell cycle. For example, proteasomal degradation of proteins, cell cycle progression, signal transduction, and transcriptional regulation are controlled by the ubiquitin system (Welchman *et al.*, 2005). 15 proteins with F-box domains and 9 proteins containing an U-box domain are present in the

genome of *A. asiaticus* (Schmitz-Esser *et al.*, 2010). Both of these domains are common to eukaryotic ubiquitinating enzymes and have been identified also in other bacterial genomes (Angot *et al.*, 2007). *A. asiaticus* encodes two putative ubiquitin-specific proteases (USPs); Aasi_0770 and Aasi_1805 (Schmitz-Esser *et al.*, 2010). Remarkably, these USPs are the first described prokaryotic proteins in the CA clan, C19 family of USPs (Rytkönen *et al.*, 2007). Both are shorter than their eukaryotic homologues, but apart from the catalytic region, USPs are generally variable in size and degree of sequence conservation (Nijman *et al.*, 2005; Renatus *et al.*, 2006). In the USPs of *A. asiaticus*, catalytic center and other functionally important residues are highly conserved, and both USP genes are transcribed during an infection of amoebae (Schmitz-Esser *et al.*, 2010).

The genome of *A. asiaticus* 5a2 contains 354 transposase encoding elements (Schmitz-Esser *et al.*, 2010), which is unusually high compared to the average percentage of below 3 % in most bacterial genomes (Siguier *et al.*, 2006). In *A. asiaticus*, 93 % of these mobile genetic elements could be assigned to 16 insertion sequence (IS) elements belonging to eight different IS element families (Schmitz-Esser *et al.*, 2011). IS elements are considered to be essential mediators of genome plasticity due to their ability to disrupt genes and induce genome rearrangements (Seshadri *et al.*, 2003; Parkhill *et al.*, 2003). Furthermore, they can influence the expression of adjacent genes (Mahillon & Chandler, 1998) or mobilise them as composite transposons (Tan, 1999; Wagner, 2006). PCR analysis showed that some of the IS elements of *A. asiaticus* 5a2 are also present in the three closely related strains EIDS3, US1, and WR (98.9 %, 99.2 %, and 98.5 % 16S rRNA gene sequence identity to 5a2, respectively). This suggests that IS elements have been part of the *A. asiaticus* genome already for a longer time during recent evolutionary divergence. Transcriptional activity was experimentally shown for 13 *A. asiaticus* IS elements, sometimes producing contiguous transcripts of the IS element itself plus adjacent downstream genes. However, no indications for recent transpositional activity were found, and no large rearrangements of the genome seem to have occurred lately. It is assumed that the IS elements of *A. asiaticus* may have played an important role in shaping the genome during the adaptation to an intracellular lifestyle, but are nowadays mostly inactive and in the stage of degradation (Schmitz-Esser *et al.*, 2011).

## 1.3.2. The life cycle of *Amoebophilus asiaticus*

*A. asiaticus* starts to enter its *Acanthamoeba* host approximately six hours after contact, also referred to as hours *post infection* (h *p.i.*). From then on, the number of symbionts per infected host cell rises continuously, suggesting intracellular replication. Around 140 h *p.i.*, most infected *Acanthamoeba* cells are already densely filled with *A. asiaticus* and begin to lyse, setting the symbiont free so that the infection can start over again (Tsao, 2011).

During the intracellular replication phase, the morphology of *A. asiaticus* changes from short, coccoid rods in the beginning to a much more elongated shape at approximately 72 h *p.i.* and becomes shorter again towards the end of the infection cycle. In addition, infection experiments showed that the freshly released extracellular form of *A. asiaticus* exhibits a significantly higher degree of infectivity than the intracellular infection intermediate (Tsao, 2011). Taken together, the alteration in morphology and infectivity suggest that *A. asiaticus* probably has a biphasic lifestyle with an extracellular, infectious stage and an intracellular, non-infectious stage.

The exact mechanisms for attachment to and entry into the *Acanthamoeba* host are still largely unresolved. Genome analysis revealed the presence of two putative phospholipases D (Schmitz-Esser *et*

*al.*, 2010) with 40 % amino acid sequence identity to the functionally characterised phospholipase D of *Rickettsia* spp. (Renesto *et al.*, 2003; Hybiske & Stephens, 2008). It is suggested that *A. asiaticus* is taken up by the host via phagocytosis and escapes from phagosomes in a similar way as *Rickettsia* escapes from host vacuoles (Schmitz-Esser *et al.*, 2010). Among several proteins with unusual amino acid composition, one candidate protein for cell-cell recognition and adhesion was identified with atypically high serine/threonine content (18 %), a predicted signal peptide, no transmembrane helices, and several predicted O-glycosylation sites. Furthermore, a protein with up to 30 % amino acid identity to known adhesins from bacterial and eukaryotic adhesins and similar predicted secondary and tertiary structure as *Plasmodium vivax* MSP3 proteins was detected (Penz *et al.*, 2010).

### 1.3.3. The putative antifeeding prophage of *Amoebophilus asiaticus*

In general, bacterial endosymbionts of eukaryotic cells use secretion systems for the delivery of effector proteins to their hosts' cytoplasm (Tseng *et al.*, 2009). Considering the close host dependency and large number of putative effector proteins in the genome of *A. asiaticus*, it is surprising that none of the currently known type I–VI secretion systems is encoded. Only the sec-dependent pathway for transport of proteins across the inner membrane into the periplasm and three homologous proteins of the *Bacteroidetes*-specific Por secretion system are present (Penz *et al.*, 2010). The Por secretion system of *Porphyromonas gingivalis* consists of eleven proteins, six of which are homologous to gliding motility genes and five others (Sato *et al.*, 2010). Since all other components apart from the homologues of three of the gliding motility genes are absent in *A. asiaticus*, the Por secretion system is far from complete and not functional (Penz *et al.*, 2010).

However, *A. asiaticus* encodes a cluster of 13 genes (Aasi_1072 to Aasi_1806; Figure 1.1) with predicted operon structure and weak similarity to the type six secretion system (T6SS; Schmitz-Esser *et al.*, 2010). One protein in particular, Aasi_1801, has 63 % amino acid identity to the EvpJ protein belonging to the T6SS of *Edwardsiella tarda*, a member of the *Enterobacteriaceae* (Zheng & Leung, 2007). In addition to Aasi_1081, five other proteins with homologues in the T6SS were identified: a homologue of EvpI (VgrG; Aasi_1080), three phage-tail associated proteins (Aasi_1074: gp18, Aasi_1077: gp19, Aasi_1082: gp25), and a protein with similarity to EvpH (Aasi_1042) located close to but outside the gene cluster (Penz *et al.*, 2010). Although it was initially suspected that the gene cluster might be a derived T6SS, in-depth analysis revealed much stronger similarity to the antifeeding prophage (afp) of *Serratia entomophila*.

*S. entomophila* is an insect pathogen affecting the larvae of the New Zealand grass grub *Costelytra zealandica* (Coleoptera: Scarabaeidae). Following infection, the bacteria colonise the digestive tract of the larvae, leading to an inactivity in food intake and clearance of the normally dark coloured gut to a characteristic amber tone, which gave the disease its name, "amber disease" (Jackson *et al.*, 1993). A decrease of digestive enzymes is also observed (Jackson, 1995). In the final stage of the infection, the bacteria invade the haemocoel and eventually cause death of the larvae (Jackson *et al.*, 2001). Essential for the virulence of *S. entomophila* is the 153 kb amber disease associated plasmid (pADAP; Glare *et al.*, 1993). pADAP contains a cluster of 18 genes encoding a prophage which is morphologically similar to phage-tail (R-type) bacteriocins (Hurst *et al.*, 2004; Yang *et al.*, 2006) and has been named antifeeding prophage (afp) after the antifeeding behaviour in infected grass grub larvae. The afp proteins constitute a filamentous structure, which is supposedly used as a protein secretion apparatus for the delivery of toxins to the host (Hurst *et al.*, 2004; Hurst *et al.*, 2007). Similar

toxin-delivering prophages have been found also in various *Photorhabdus* spp. and interestingly in several marine bacteria, including members of the *Bacteroidetes* (Penz *et al.*, 2010).
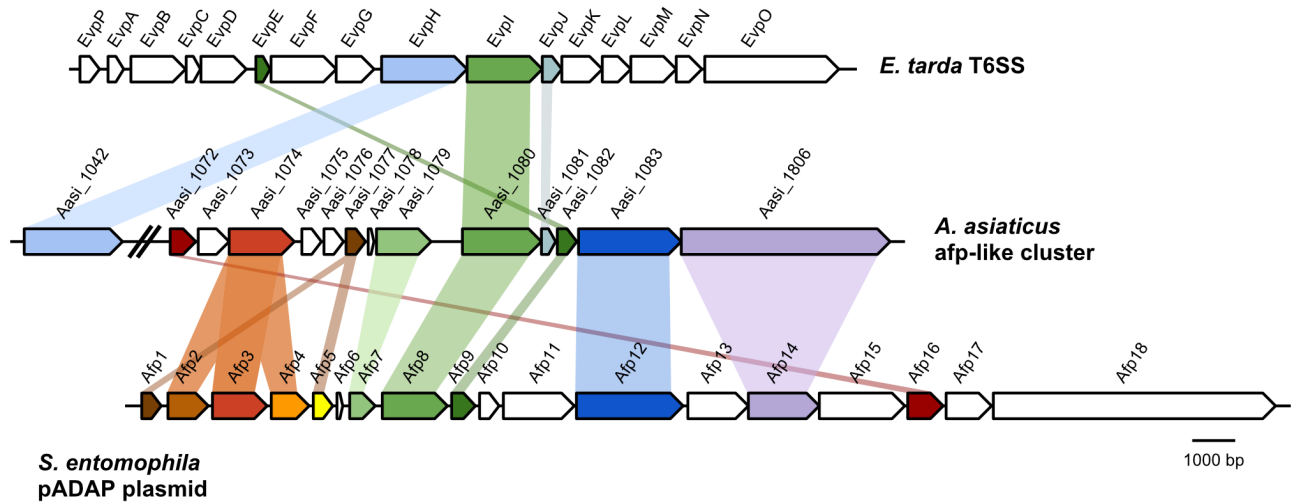


**Figure 1.1** Schematic representation of the genomic organisation of the afp-like gene cluster of *A. asiaticus* (depicted in the middle) compared to a typical type six secretion system (T6SS) of *E. tarda* and the afp cluster on the pADAP plasmid of *S. entomophila*. Homologous genes are shown in identical colours, while genes with no homologs in the other clusters are depicted in white. Gene names for *E. tarda* and *S. entomophila* and locus tags for *A. asiaticus* are given above the respective genes. Modified from Penz *et al.*, 2010.

In *A. asiaticus*, eight of the 13 genes of the afp-like cluster are similar to components of the *S. entomophila* afp, and the two gene clusters are also largely syntenic (Penz *et al.*, 2010). Based on these similarities, it is very likely that the *A. asiaticus* gene cluster represents an afp rather than a derived T6SS. Penz *et al.* (2010) proposed that the putative afp of *A. asiaticus* might be used as a protein secretion apparatus for the delivery of effectors encoded within the afp-like gene cluster, or a general protein secretion device. Recent data available from an ongoing project regarding the ultrastructure of *A. asiaticus* revealed cytoplasmic phage tail sheath-like filamentous structures in the extracellular, infectious intermediate of the symbiont, which could represent the assembled afp (Thomas Penz, Department of Microbial Ecology; personal communication). Similar structures have been found also in other members of the *Bacteroidetes*, especially in different *Cardinium* spp. (Persson *et al.*, 2009; Penz *et al.*, 2012).

## 1.4. Aims of this study

A lot of research has been done in the past decade to better understand the interactions between endosymbionts of amoebae and their eukaryotic hosts. While much is known about the developmental stages of the *Chlamydiae* and members of the *Legionellaceae*, the infection cycle of *A. asiaticus* was described only recently (Tsao, 2011). Remarkably, *A. asiaticus* can be observed in two distinct infection intermediates, which are different in both morphology and degree of infectivity. Results from previous and ongoing projects studying the symbiotic relationship between *A. asiaticus* and its host suggest that the putative afp might act as a secretion device. However, the link between the afp-like gene cluster in

the genome and cytoplasmic filamentous structures discovered by means of transmission electron microscopy was so far missing. Furthermore, the relative expression level of afp genes in the different infection intermediates was yet to be analysed to show a possible involvement of the prophage in the process of infecting the amoebal cells. In addition, samples from defined infection time points and a purification of phage particles were required to gain more detailed insights into the ultrastructure of *A. asiaticus*. The aims of this diploma thesis can therefore be summarised as follows:

1. Cloning, heterologous expression, and purification of selected proteins from the afp-like gene cluster with the long-term goal to produce antibodies for immunofluorescence to close the gap between the gene cluster and microscopically observed structures and visualise their intracellular localisation. The prophage tail sheath protein (Aasi_1074) and VgrG homologue (Aasi_1080) were used for this approach.
2. Develop, evaluate, and optimise reverse transcription quantitative real-time PCR (RT-qPCR) assays targeting the prophage tail sheath protein (Aasi_1074) and a housekeeping gene, the beta-subunit of the RNA polymerase (Aasi_1396), as reference gene, for relative quantification of prophage tail sheath transcripts.
3. Apply these assays to quantify the relative expression levels of Aasi_1074 at selected time points of the infection cycle, with focus on possible differential expression in the proposed different infection intermediates of *A. asiaticus*.
4. Sample preparation for standard transmission electron microscopy and cryo-electron microscopy. This involved the fixation of an infected *Acanthamoeba* culture at several different infection time points and purification of prophage particles by ultracentrifugation. Microscopic analysis was done by collaboration partners at the University of Ljubljana and the California Institute of Technology.

# Chapter 2. Materials and Methods

Laboratory work was in general done at the Department of Microbial Ecology (University of Vienna) with the following exceptions: (1) An Experion™ Automated Electrophoresis System (Bio-Rad), which is located at the Department of Marine Biology (University of Vienna), was used for quantitative and qualitative analysis of RNA samples. (2) For scanning of Quant-iT™ PicoGreen® dsDNA quantification assays done in 96-well microplates, the Tecan Infinite M200 microplate reader at the Department of Terrestrial Ecosystem Research (University of Vienna) was used.

## 2.1. Equipment and software

**Table 2.1** Technical equipment, including corresponding software.

| Machine (type) | Software (version) | Manufacturer |
| --- | --- | --- |
| Optima™ L-100 XP (ultracentrifuge) | Optima eXPert (1.03) | Beckman Coulter |
| SW 41 Ti (swing-out rotor used with ultracentrifuge) | — | Beckman Coulter |
| Microbiological incubator KB 115 | — | BINDER |
| MB-102 ThermoCell (incubation/mixing block) | — | Bioer Technology |
| CFX96 Touch™ Real-Time PCR Detection system (thermal cycler & optical reaction module) | CFX Manager (2.1) | Bio-Rad |
| T100™ (thermal cycler) | — | Bio-Rad |
| Experion™ Automated Electrophoresis System | — | Bio-Rad |
| MicroPulser™ (electroporation apparatus) | — | Bio-Rad |
| Mini-PROTEAN® 3 Cell (SDS-PAGE system) | — | Bio-Rad |
| PowerPac Basic (electrophoresis power supply) | — | Bio-Rad |
| SmartSpec™ 3000 (visible spectrophotometer) | — | Bio-Rad |
| Sub-Cell GT (agarose gel electrophoresis system) | — | Bio-Rad |
| Sub-Cell GT UV-Transparent Gel Tray | — | Bio-Rad |
| UST-C30M-8R (UV transilluminator) | Argus X1 (4.1) | Biostep |
| accu-jet® pro (pipetting aid) | — | BRAND |
| 5804 R (microcentrifuge) | — | Eppendorf |
| Eppendorf Research® Pipettes (various sizes) | — | Eppendorf |
| MiniSpin® plus (microcentrifuge) | — | Eppendorf |
| Perfection V700 Photo Scanner (used for scanning protein gels) | EPSON Scan (3.83US) | Epson |
| Analogue Orbital Shaker 3019 | — | GFL |
| Incubation/Inactivation Water Bath 1004 | — | GFL |
| Mikro 20 (microcentrifuge) | — | Hettich Lab Technology |
| Mikro 22 R (microcentrifuge) | — | Hettich Lab Technology |
| Rotina 35 R (microcentrifuge) | — | Hettich Lab Technology |
| RCT Basic (magnetic stirrer/hot plate) | — | IKA-Werke |

## MATERIALS AND METHODS

| | | |
|---|---|---|
| LaminAir Model 1.2 (laminar flow hood) | — | JOUAN Nordic A/S |
| Neubauer hemocytometer (counting chamber) | — | Marienfeld |
| Hybridisation oven | — | Memmert |
| Milli-Q Water Purification System | — | Millipore |
| Filtration tower | — | Millipore |
| Fritted glass base (2.5 cm diameter) + conical rubber stopper + aluminium spring clamp | — | Millipore |
| Innova™ 2300 platform shaker | — | New Brunswick Scientific |
| Analytical Plus (analytical balance) | — | Ohaus |
| C-5050 Zoom (digital camera, used with UV transilluminator) | — | Olympus |
| Vacuum/Pressure Pump DOA-P730-BN | — | Pall |
| UV Sterilising PCR Workstation | — | PEQLAB |
| BIO 101/Savant FastPrep™ FP120 (cell lysis/homogenizer) | — | Qbiogene |
| BL3100 (balance) | — | Sartorius |
| BL6100 (balance) | — | Sartorius |
| Suction flask (100 mL), glass | — | SCHOTT |
| Vortex Genie 2 | — | Scientific Industries |
| Infinite® M200 (microplate reader) | i-control™ (1.6) | Tecan |
| Haake® DC 10-P5/U (heating circulator) | — | Thermo Scientific |
| NanoDrop ND-1000 (UV-visible spectrophotometer) | ND-1000 (3.2) | Thermo Scientific |
| Galaxy Mini Microcentrifuge C12XX (benchtop centrifuge) | — | VWR |
| inoLab® pH Level 1 (pH meter) | — | WTW |
| Axio Imager M1 (epifluorescence microscope) | — | Zeiss |
| Axioplan 2 imaging (epifluorescence microscope) | AxioVision (4.7) | Zeiss |
| AxioCam HRc (digital camera, used with Axioplan 2 imaging epifluorescence microscope) | — | Zeiss |
| Axiovert 25 (inverted microscope) | — | Zeiss |
| LSM 510 META (confocal laser scanning microscope) | LSM 510 (3.2) | Zeiss |

A comprehensive list of all manufacturers and laboratory suppliers, including the address and website of the headquarters and abbreviated company names used throughout this document is given in the appendix (Table A.1).

Quantitative real-time PCR data were analysed with Bio-Rad's CFX Manager software (version 2.1). Statistical analysis was done with the R programming language (version 2.14.1; R Development Core Team, 2011) or LibreOffice Calc (version 3.5; LibreOffice contributors and/or their affiliates, 2012). Figures were prepared with the R programming language, the R package ggplot2 (version 0.8.9; Wickham, 2009), Inkscape (version 0.48; Inkscape contributors, 2011) and/or the GNU Image Manipulation Program (version 2.6; Kimball *et al.*, 2010).

## 2.2. Consumables

For DNA and RNA work, RNase-, DNase- and (human) DNA-free reaction tubes were used out of new, sealed packages that were opened only on designated work benches. Work benches, pipettes, pipette tip boxes, and other items in the working area were cleaned with DNA AWAY or RNase AWAY (Carl Roth) prior to work. PCR consumables, such as plates, tubes, and pipette tips, were additionally radiated with UV light for 30 min before pipetting.

Consumables for amoeba cultivation were opened only in a laminar flow hood (LaminAir Model 1.2; Jouan Nordic A/S). The outer surface of cell culture flasks, reaction tubes, and pipette tip boxes was sterilised by thorough rinsing with 70 % (v/v) ethanol immediately before moving them into the laminar flow hood. Sterile packaging of serological pipettes, syringes, syringe filters and other items was checked for integrity before use and only removed in the laminar flow hood.

Consumables used for work with *Escherichia coli* were opened either in a laminar flow hood, or next to a lit bunsen burner to avoid contamination.

**Table 2.2** Consumables.

| Consumable | Manufacturer |
| --- | --- |
| Hard-Shell® Thin-Wall 96-Well Skirted PCR Plates (used for qPCR) | Bio-Rad |
| Microseal® 'B' Film, adhesive (used for qPCR) | Bio-Rad |
| 0.6 mL reaction tubes | Biozym |
| 0.2 mL PCR tubes | Biozym |
| Premium Tips (pipette tips with filters), various sizes | Biozym |
| Injekt® single-use syringes, 3 mL | Braun |
| Omnifix® single-use syringes, 30 and 50 mL | Braun |
| Sterican® needles, various sizes | Braun |
| 50 mL reaction tubes | Carl Roth |
| Microscope slides, cut edges, frosted end | Carl Roth |
| Pipette tips without filters, various sizes | Carl Roth |
| PCR plates, 96-well, skirted (used for standard PCR) | Eppendorf |
| PCR film, adhesive (used for standard PCR) | Eppendorf |
| 1.5 mL reaction tubes | Greiner Bio-One |
| 2 mL reaction tubes | Greiner Bio-One |
| 15 mL reaction tubes | Greiner Bio-One |
| 50 mL reaction tubes | Greiner Bio-One |
| Microplates, 96-well, flat bottom, chimney, black | Greiner Bio-One |
| Semi-micro cuvette, 1.6 mL, 10 × 10 × 45 mm (for use with SmartSpec™ 3000 visible spectrophotometer) | Greiner Bio-One |
| Microscope slides, polytetrafluoroethylene coated, black mask with 10 wells | Marienfeld |
| Glass coverslips, 24 × 50 mm | Marienfeld |

| | |
|---|---|
| MF-Millipore™ membrane filters, 0.025 µm | Millipore |
| Polycarbonate membrane filter, black, 0.22 µm | Millipore |
| FastPrepTM Lysing Matrix A tubes (used without ceramic sphere) | MP Biomedicals |
| Nalgene syringe filters, 0.2 µm | Nalgene |
| Electroporation cuvettes, 0.2 cm | NEPA GENE |
| Standard cell culture flasks, Nunclon™Δ surface, vent/close cap, 25 cm² | Nunc |
| TripleFlask™ cell culture flasks, Nunclon™Δ surface, vent/close cap, 500 cm² | Nunc |
| Cellulose acetate membrane filters, 0.45 µm | Sartorius |
| Minisart® NML syringe filters, 5.0 µm | Sartorius |
| Glass bottles, various sizes | SCHOTT |
| Iwaki® cell culture flasks, 25 cm² | Sterilin |
| Petri dishes, 90 mm | Sterilin |
| Cell culture flasks, standard cap, 182.5 cm² | VWR |
| Serological pipettes, 10 and 25 mL | VWR |

## 2.3. Molecular biology kits

**Table 2.3** Molecular biology kits.

| Kit | Manufacturer |
|---|---|
| Ambion® TURBO DNA-free™ Kit | Invitrogen |
| Quant-iT™ PicoGreen® dsDNA Reagent and Kit | Invitrogen |
| SuperScript™ III First-Strand Synthesis System for RT-PCR | Invitrogen |
| TOPO® XL PCR Cloning Kit | Invitrogen |
| NEBNext® dA-Tailing Module | New England Biolabs |
| NEBNext® Quick Ligation Module | New England Biolabs |
| DNeasy® Blood & Tissue Kit | QIAGEN |
| QIAprep® Spin Miniprep Kit | QIAGEN |
| QIAquick® Gel Extraction Kit | QIAGEN |
| QIAquick® PCR Purification Kit | QIAGEN |
| RevertAid™ First Strand cDNA Synthesis Kit | Thermo Scientific |

## 2.4. Primers and probes

Primers used for standard PCR and quantitative real-time PCR are listed in Table 2.4 and 2.5, respectively.

**Table 2.4** Primers used in standard PCR.

| Name | Sequence | Length (nt) | Specificity | Reference |
|---|---|---|---|---|
| ISCaa15 Forward | 5′-AGC ATG GCT TGT TGG AGA GT-3′ | 20 | *A. asiaticus* ISCaa15 gene | Schmitz-Esser *et al.*, 2011 |
| ISCaa15 Reverse | 5′-CGC TCT TGA TCC GTA AGC TC-3′ | 20 | *A. asiaticus* ISCaa15 gene | Schmitz-Esser *et al.*, 2011 |
| ISCaa4 Forward | 5′-AGA GGT AGA CAG CGC TAC CAG-3′ | 21 | *A. asiaticus* ISCaa4 gene | Schmitz-Esser *et al.*, 2011 |
| ISCaa4 Reverse | 5′-TAG CTT GGC CAT TAG CAG GT-3′ | 20 | *A. asiaticus* ISCaa4 gene | Schmitz-Esser *et al.*, 2011 |
| ISCaa5 Forward | 5′-GCC TTA TAC TTT GGC GGA CA-3′ | 20 | *A. asiaticus* ISCaa5 gene | Schmitz-Esser *et al.*, 2011 |
| ISCaa5 Reverse | 5′-TGC ACT ACC AGC AGG CAT AG-3′ | 20 | *A. asiaticus* ISCaa5 gene | Schmitz-Esser *et al.*, 2011 |
| M13 Forward | 5′-GTA AAA CGA CGG CCA G-3′ | 16 | MCS of many TOPO vectors | TOPO XL® PCR Cloning Kit Manual |
| M13 Reverse | 5′-CAG GAA ACA GCT ATG AC-3′ | 17 | MCS of many TOPO vectors | TOPO XL® PCR Cloning Kit Manual |
| T7 Promoter Primer | 5′-TAA TAC GAC TCA CTA TAG GG-3′ | 20 | MCS of many pET-21 vectors | Novagen pET-21 a-d(+) Vector Map |
| T7 Terminator Primer | 5′-GCT AGT TAT TGC TCA GCG G-3′ | 19 | MCS of many pET-21 vectors | Novagen pET-21 a-d(+) Vector Map |
| pGEX 5′ Sequencing Primer | 5′-GGG CTG GCA AGC CAC GTT TGG TG-3′ | 23 | MCS of all pGEX vectors | GST Gene Fusion System Handbook |
| pGEX 3′ Sequencing Primer | 5′-CCG GGA GCT GCA TGT GTC AGA GG-3′ | 23 | MCS of all pGEX vectors | GST Gene Fusion System Handbook |
| TOPO Seq F | 5′-AGC TTG GTA CCG AGC T-3′ | 16 | pCR-XL-TOPO® vector | Christian Baranyi (pers. comm.) |
| TOPO Seq R | 5′-TCT AGA TGC ATG CTC GA-3′ | 17 | pCR-XL-TOPO® vector | Christian Baranyi (pers. comm.) |
| pET-21b Aasi_1074 F | 5′-GAG CTC CAT GCC AGA AAA TTT AAA AAC TCC GGG CG-3′ | 35 | *A. asiaticus* (prophage tail sheath gene) | Thomas Penz (pers. comm.) |
| pET-21b Aasi_1074 R | 5′-CTC GAG ACT TCC TTC TTG TCC GCC CAT CTT TTG-3′ | 33 | *A. asiaticus* (prophage tail sheath gene) | Thomas Penz (pers. comm.) |
| pGEXHis Aasi_1074 F | 5′-GTC GAC ATG CCA GAA AAT TTA AAA ACT CCC GGC G-3′ | 34 | *A. asiaticus* (prophage tail sheath gene) | Thomas Penz (pers. comm.) |
| pGEXHis Aasi_1074 R | 5′-GCG GCC GCG TTA GTG GTG GTG GTG GTG GTG ACT CCT TCT TG TCC GCC CAT CTT TTG-3′ | 57 | *A. asiaticus* (prophage tail sheath gene) | Thomas Penz (pers. comm.) |

| pET-21b Aasi_1080 F | 5′-GAG CTC CAT GAG CAC TTC CGC AAC TTC TAG-3′ | 30 | *A. asiaticus* (rpoB gene) | Thomas Penz (pers. comm.) |
| pET-21b Aasi_1080 R | 5′-CTC GAG AAT TTA TTT GTA CTA TAG TTC C-3′ | 28 | *A. asiaticus* (rpoB gene) | Thomas Penz (pers. comm.) |
| Aasi_1074 F2 | 5′-TCC TGC ACA ATA TCA AAA CTG C-3′ | 22 | *A. asiaticus* (prophage tail sheath gene) | Thomas Penz (pers. comm.) |
| Aasi_1074 R2 | 5′-GGT GCT ATC CAT ACG CCT CTA C-3′ | 22 | *A. asiaticus* (prophage tail sheath gene) | Thomas Penz (pers. comm.) |
| Aasi_1396 STD F | 5′-CAG TCT GGC AGT CTT CT GTT G-3′ | 22 | *A. asiaticus* (rpoB gene) | Thomas Penz (pers. comm.) |

**Table 2.5** Primers used in quantitative real-time PCR. All primers listed in this table are so far unpublished and were designed by Thomas Penz (personal communication).

| Name | Sequence | Length (nt) | Specificity |
| --- | --- | --- | --- |
| Aasi_1074 qPCR F1 | 5′-GTG GTG CAG ATT GCT ACA TCA T-3′ | 22 | *A. asiaticus* (prophage tail sheath gene) |
| Aasi_1074 qPCR R1 | 5′-AGT CGG GCA TAA GCA ACA TAG T-3′ | 22 | *A. asiaticus* (prophage tail sheath gene) |
| Aasi_1396 qPCR F2 | 5′-ACT AGG TAC GCC ACC TGA AAA A-3′ | 22 | *A. asiaticus* (rpoB gene) |
| Aasi_1396 qPCR R2 | 5′-AAG TTA CTC CCC TTT CCA CAC A-3′ | 22 | *A. asiaticus* (rpoB gene) |

Oligonucleotide probes listed in Table 2.6 were used for fluorescence *in situ* hybridisation (FISH; see Section 2.10.1). EUB338mix, an equimolar mixture of the three probes EUB338, EUB338 II and EUB338 III, was used to target all currently known *Bacteria* with the best possible coverage. Probes were in general single-labeled with 5(6)-Carboxyfluorescein-N-hydroxysuccinimide ester (FLUOS), Cy3, or Cy5. EUB338mix-FLUOS was sometimes used as double-labeled probe.

**Table 2.6** Probes used for rRNA-targeted fluorescence *in situ* hybridisation. All probes were hybridised at 20 % formamide concentration.

| Name | Sequence | Length (nt) | Specificity | Reference |
| --- | --- | --- | --- | --- |
| EUB338 | 5′- GCT GCC TCC CGT AGG AGT -3′ | 18 | most *Bacteria* | Amann *et al.*, 1990 |
| EUB338 II | 5′- GCA GCC ACC CGT AGG TGT -3′ | 18 | *Planctomycetales* | Daims *et al.*, 1999 |
| EUB338 III | 5′- GCT GCC ACC CGT AGG TGT -3′ | 18 | *Verrucomicrobiales* | Daims *et al.*, 1999 |
| Aph1180 | 5′- CTG ACC TCA TCC CCT CCT -3′ | 18 | *A. asiaticus* | Horn *et al.*, 2001 |
| EUK516 | 5′- ACC AGA CTT GCC CTC C -3′ | 16 | *Eukarya* | Amann *et al.*, 1990 |
| Acant412a | 5′- ACT CTT ATC GAG CGC CTG -3′ | 18 | *Acanthamoeba* sp. | — |

All primers and probes were synthesised by Thermo Fisher Scientific.

## 2.5. Restriction enzymes

**Table 2.7** Restriction enzymes by Thermo Scientific.

| Name | Restriction site |
|------|------------------|
| SacI | 5′- GAGCTC-3′ |
| XhoI | 5′- CTCGAG-3′ |
| SalI | 5′- GTCGAC-3′ |
| NotI | 5′- GCGGCCGC-3′ |

## 2.6. Buffers, solutions, and other chemicals

Chemicals were purchased in *pro analysis* or molecular biology grade. All solutions were prepared using distilled, UV-light treated, filtered, deionised water (Milli-Q Water Purification System), with the exception of PCR reagents, where double distilled water was used. pH was adjusted with NaOH and/or HCl (Carl Roth). If not stated otherwise, buffers and media were sterilised by autoclaving at 121 °C and $1013 \times 10^5$ Pa for 20 min and stored at room temperature.

### 2.6.1. Agarose gel electrophoresis

**Table 2.8** 10× Tris/Borate/EDTA (TBE) buffer (pH 8.3). Not autoclaved.

| Name | Final concentration (mmol L$^{-1}$) | Amount for 1 L (g) |
|------|-------------------------------------|--------------------|
| Tris (Carl Roth) | 890 | 107.8 |
| Boric acid (Carl Roth) | 890 | 55.0 |
| EDTA disodium salt dihydrate (Carl Roth) | 20 | 7.4 |
| Water | | fill up to 1 L |

**Table 2.9** 50× Tris/Acetate/EDTA (TAE) buffer (pH 8.3–8.7). Not autoclaved.

| Name | Final concentration (mmol L$^{-1}$) | Amount for 1 L |
|------|-------------------------------------|----------------|
| Tris (Carl Roth) | 2000 | 242 g |
| Acetic acid (Carl Roth) | 1000 | 57.1 mL |
| EDTA disodium salt dihydrate (Carl Roth) | 50 | 18.6 g |
| Water | | fill up to 1 L |

**Table 2.10** DNA ladders by Thermo Scientific.

| Name | Range (bp) |
|---|---|
| GeneRuler™ 1 kb DNA Ladder | 250—10000 |
| GeneRuler™ 50 bp DNA Ladder | 50—1000 |

## 2.6.2. Sodium dodecyl sulfate polyacrylamide gel electrophoresis

**Table 2.11** 10 % sodium dodecyl sulfate (SDS) solution. Not autoclaved. For use in buffers for sodium dodecyl sulfate polyacrylamide gel electrophoresis and fluorescence *in situ* hybridisation.

| Name | Final concentration | Amount for 50 mL |
|---|---|---|
| Sodium dodecyl sulfate (SDS; Carl Roth) | 10 % (w/v) | 5.0 g |
| Water | | fill up to 50 mL |

**Table 2.12** Lower buffer. pH was adjusted to 8.8 with HCl (Carl Roth).

| Name | Final concentration | Amount for 500 mL |
|---|---|---|
| Tris (Carl Roth) | 1.5 mol L$^{-1}$ | 90.8 g |
| 10 % SDS solution | 0.4 % (w/v) SDS | 20 mL |
| Water | | fill up to 500 mL |

**Table 2.13** Upper buffer. pH was adjusted to 6.8 with HCl.

| Name | Final concentration | Amount for 500 mL |
|---|---|---|
| Tris (Carl Roth) | 0.5 mol L$^{-1}$ | 30.3 g |
| 10 % SDS solution | 0.4 % (w/v) SDS | 20 mL |
| Water | | fill up to 500 mL |

**Table 2.14** 10 % ammonium persulfate (APS) solution. Not autoclaved. Aliquots were prepared and stored at −20 °C.

| Name | Final concentration | Amount for 50 mL |
|---|---|---|
| Ammonium peroxydisulphate (Carl Roth) | 10 % (w/v) | 5.0 g |
| Water | | fill up to 50 mL |

**Table 2.15** 4× SDS-PAGE Loading Buffer. pH was adjusted to 6.8 with HCl. Not autoclaved. Aliquots were prepared and stored at −20 ℃.

| Name | Final concentration | Amount for 100 mL |
| --- | --- | --- |
| Tris (Carl Roth) | 200 mmol L$^{-1}$ | 2.42 g |
| SDS (Carl Roth) | 8 % (w/v) | 8.0 g |
| Bromophenol blue (Carl Roth) | | 0.2 g (a spatula tip full) |
| Glycerol (Carl Roth) | 40 % (w/v) | 40 mL |
| DL-Dithiothreitol (DTT; Sigma-Aldrich) | 400 mmol L$^{-1}$ | 6.2 g |
| Water | | fill up to 100 mL |

**Table 2.16** 10× SDS-PAGE running buffer. Not autoclaved.

| Name | Final concentration | Amount for 1 L (g) |
| --- | --- | --- |
| Tris (Carl Roth) | 250 mmol L$^{-1}$ | 30.2 |
| Glycine (Carl Roth) | 1918 mmol L$^{-1}$ | 144.0 |
| SDS (Carl Roth) | 1 % (w/v) | 10.0 |
| Water | | fill up to 1 L |

**Table 2.17** Coomassie brilliant blue staining solution. Not autoclaved.

| Name | Final concentration | Amount for 1 L |
| --- | --- | --- |
| Methanol (Carl Roth) | 50 % (v/v) | 500 mL |
| Acetic acid (Carl Roth) | 10 % (v/v) | 100 mL |
| Coomassie Brilliant Blue G-250 (Carl Roth) | 3.2 mmol L$^{-1}$ | 2.76 g |
| Water | | fill up to 1 L |

**Table 2.18** Destaining solution. Not autoclaved.

| Name | Final concentration | Amount for 1 L |
| --- | --- | --- |
| Acetic acid (Carl Roth) | 5 % (v/v) | 50 mL |
| Ethanol, denatured (AustrAlco) | 20 % (v/v) | 200 mL |
| Water | | fill up to 1 L |

## 2.6.3. *E. coli* cultivation

**Table 2.19** Lysogeny broth (LB; pH 7.0–7.5).

| Name | Amount for 1 L (g) |
| --- | ---: |
| Tryptone (Oxoid) | 10.0 |
| Yeast extract (Oxoid) | 5.0 |
| NaCl (Carl Roth) | 5.0 |
| Water | fill up to 1 L |

**Table 2.20** Ampicillin stock solution (100 mg mL$^{-1}$). Ampicillin solution was filter sterilised (0.2 μm filter), but not autoclaved, and stored at −20 °C.

| Name | Final concentration | Amount for 1 mL |
| --- | :---: | ---: |
| Ampicillin sodium salt (Sigma-Aldrich) | 100 mg mL$^{-1}$ | 100 mg |
| Ethanol, denatured (AustrAlco) | 50 % (v/v) | 0.5 mL |
| Water | | 0.5 mL |

**Table 2.21** Kanamycin stock solution (100 mg mL$^{-1}$). Kanamycin solution was filter sterilised (0.2 μm filter), but not autoclaved, and stored at −20 °C.

| Name | Final concentration | Amount for 1 mL |
| --- | :---: | ---: |
| Kanamycin sulfate (Sigma-Aldrich) | 100 mg mL$^{-1}$ | 100 mg |
| Water | | 1.0 mL |

Antibiotics were added to liquid LB medium shortly before use.

For solid LB, 15–20 g agar (Sigma-Aldrich) was added to 1 L medium prior to autoclaving. The autoclaved medium was poured into 90 mm petri dishes (Sterilin) as long as it was still warm. If required, warm but not hot LB was supplied with antibiotics before pouring plates.

**Table 2.22** dYT medium (pH 7.0). Used for preparation of electrocompetent *E. coli*.

| Name | Amount for 1 L (g) |
| --- | ---: |
| Tryptone (Oxoid) | 16.0 |
| Yeast extract (Oxoid) | 10.0 |
| NaCl (Carl Roth) | 5.0 |
| Water | fill up to 1 L |

**Table 2.23** 10 % glycerol solution. Autoclaved at 110 °C. Used for preparation of electrocompetent *E. coli*.

| Name | Final concentration | Amount for 1 L |
|---|---|---|
| Glycerol (Carl Roth) | 10 % (v/v) | 100 mL |
| Water | | fill up to 1 L |

## 2.6.4. *Acanthamoeba* cultivation

**Table 2.24** Trypticase Soy Broth with Yeast Extract (TSY; pH 7.3).

| Name | Amount for 1 L (g) |
|---|---|
| Tryptone soy broth (Oxoid) | 30.0 |
| Yeast extract (Oxoid) | 10.0 |
| Water | fill up to 1 L |

**Table 2.25** Peptone Yeast Glucose Medium (PYG; pH 6.5). Autoclaved at 110 °C.

| Name | Final concentration (mmol L$^{-1}$) | Amount for 1 L |
|---|---|---|
| Proteose peptone (Oxoid) | | 20.0 g |
| Glucose (Carl Roth) | | 18.0 g |
| Yeast extract (Oxoid) | | 2.0 g |
| MgSO4 · 7 H2O (Sigma-Aldrich) | 4.0 | 980 mg |
| Na3C6H5O7 · 2 H2O (Merck) | 3.4 | 1.0 g |
| Na2HPO4 · 2 H2O (Carl Roth) | 2.0 | 355 mg |
| KH2PO4 (Sigma-Aldrich) | 1.7 | 340 mg |
| Fe(NH4)2(SO4)2 · 6 H2O (Sigma-Aldrich) | 0.05 | 20 mg |
| Water | | fill up to 1 L |

**Table 2.26** 10× Page's Amoebic Saline (PAS; pH 6.9).

| Name | Final concentration (mmol L$^{-1}$) | Amount for 1 L |
|---|---|---|
| NaCl (Carl Roth) | 20 | 1.2 g |
| MgSO4 · 7 H2O (Sigma-Aldrich) | 0.16 | 40 mg |
| CaCl2 · 2 H2O (Avantor) | 0.27 | 40 mg |
| Na2HPO4 · 2 H2O (Carl Roth) | 10 | 1420 mg |
| KH2PO4 (Sigma-Aldrich) | 10 | 1360 mg |
| Water | | fill up to 1 L |

## 2.6.5. Nucleic acids extraction and RNA work

Distilled water for RNA work was treated with 0.1 % (v/v) diethylpyrocarbonate (DEPC, Sigma-Aldrich) to inactivate RNases (Blumberg, 1987). Following the addition of DEPC, the water was stirred overnight (o/n) under a fume hood, and remaining DEPC was deactivated by autoclaving twice at 121 °C. Alternatively, commercially available distilled nuclease-free water (Life Technologies) was sometimes used instead of DEPC-treated water.

Ethanol was purchased in HPLC Gradient Grade (Carl Roth). 70 % and 75 % dilutions were prepared with DEPC-treated water in 50 mL reaction tubes. Isopropanol and chloroform (both Carl Roth) were purchased in *pro analysis* grade, and dedicated aliquots for RNA work were prepared. Glycogen (20 mg mL$^{-1}$; Thermo Scientific) and sodium acetate solution (Thermo Scientific)  were purchased in RNA grade.

## 2.6.6. Fluorescence *in situ* hybridisation

**Table 2.27** Sodium chloride solution.

| Name | Final concentration (mol L$^{-1}$) | Amount for 1 L (g) |
|---|---|---|
| NaCl (Carl Roth) | 5.0 | 292.2 |
| Water | | fill up to 1 L |

**Table 2.28** Tris/HCl buffer. pH was adjusted to 8.0 with Hcl.

| Name | Final concentration (mol L$^{-1}$) | Amount for 1 L (g) |
|---|---|---|
| Tris (Carl Roth) | 1.0 | 121.1 |
| Water | | fill up to 1 L |

**Table 2.29** Paraformaldehyde (PFA) solution. Filter sterilised, not autoclaved.

| Name | Final concentration | Amount for 50 mL |
|---|---|---|
| Formaldehyde, 37 % solution (Carl Roth) | 4 % (v/v) | 5.4 mL |
| Water | | fill up to 50 mL |

**Table 2.30** Ethylenediaminetetraacetic acid (EDTA) solution. pH was adjusted to 8.0 with NaOH (Carl Roth).

| Name | Final concentration (mol L$^{-1}$) | Amount for 250 mL (g) |
|---|---|---|
| EDTA disodium salt dihydrate (Carl Roth) | 0.5 | 46.5 |
| Water | | fill up to 250 mL |

## 2.6.7. Transmission electron microscopy sample fixation

**Table 2.31** Phosphate buffer. pH was adjusted to 7.2 with HCl and NaOH, and the solution was filter sterilised, autoclaved, and stored at 4 °C. For use in the standard TEM sample fixation protocol.

| Name | Final concentration (mmol L⁻¹) | Amount for 50 mL (g) |
|---|---|---|
| NaH2PO4 · 2 H2O (Carl Roth) | 56 | 0.44 |
| Na2HPO4 · 2 H2O  (Carl Roth) | 206 | 0.83 |
| Water | | fill up to 50 mL |

**Table 2.32** Glutaraldehyde solution. Not autoclaved. The solution was stored at 4 °C. For use in the standard TEM sample fixation protocol.

| Name | Final concentration | Amount for 5 mL |
|---|---|---|
| Glutaraldehyde, 25 % solution (Sigma-Aldrich) | 7 % (v/v) Glutaraldehyde | 1.4 mL |
| Water | | 3.6 mL |

**Table 2.33** NaCl/Tris buffer. pH was adjusted to 7.4 with HCl and NaOH, and the solution was autoclaved. Used for lysis buffer (Table 2.36).

| Name | Final concentration (mmol L⁻¹) | Amount for 50 mL |
|---|---|---|
| NaCl (Carl Roth) | 150 | 438 mg |
| Tris (Carl Roth) | 50 | 303 mg |
| Water | | fill up to 50 mL |

**Table 2.34** Lysozyme solution. Used for lysis buffer (Table 2.36). The solution was prepared shortly before use and temporarily stored on ice.

| Name | Amount for 250 µL |
|---|---|
| Lysozyme human (Sigma-Aldrich) | 1.25 mg |
| NaCl/Tris buffer (Table 2.33) | 250 µL |

**Table 2.35** 25× Protease inhibitor solution. Used for lysis buffer (Table 2.36). The solution was prepared shortly before use and temporarily stored on ice.

| Name | Amount for 1 mL |
|---|---|
| cOmplete Mini EDTA-free Protease Inhibitor Cocktail Tablets (Roche) | 1 tablet |
| Water | 1 mL |

**Table 2.36** Lysis buffer. For use in the phage sheath preparation protocol.

| Name | Amount for 2.5 mL (µL) |
|---|---:|
| Lysozyme solution (Table 2.34) | 100 |
| DNase I Amplification Grade (1 u µL⁻¹) (Sigma-Aldrich) | 10 |
| CelLytic™ B 10× Cell Lysis Reagent (Sigma-Aldrich) | 125 |
| Triton™ X-100 (Sigma-Aldrich) | 25 |
| 25× protease inhibitor solution (Table 2.35) | 100 |
| NaCl/Tris buffer (Table 2.33) | 2150 |

# 2.7. General methods

## 2.7.1. Quantification of nucleic acids

DNA and RNA concentrations were in general determined by photometric analysis using a NanoDrop ND-1000 spectrophotometer. This device measures absorbance over a broad range of wavelengths and, based on the absorbance at 230, 260 and 280 nm, allows calculation of the concentration and estimation of the purity of nucleic acids samples. Absorption measurements, however, are in general biased by the presence of nucleotides and (fragmented) single-stranded nucleic acids molecules, relatively insensitive, and susceptible to interference with contaminants such as phenol or proteins (Quant-iT™ PicoGreen® dsDNA Reagent and Kits Handbook, Invitrogen). If a more precise quantification of nucleic acids is essential or desired, for example for qPCR standards (see Section 2.16.4), a different method is therefore preferable.

## 2.7.2. Agarose gel electrophoresis

Agarose gels were prepared by melting the required amount of LE Agarose (Biozym) in 1× Tris/Borate/EDTA (TBE) or 1× Tris/Acetate/EDTA (TAE) buffer in a microwave. In general, TBE buffer (Table 2.8) was used. TAE buffer (Table 2.9) was chosen instead of TBE for gel extractions to reduce the risk of inhibition in subsequent enzymatic steps. Use of TAE gels instead of TBE is indicated in the respective sections throughout this document. 6× DNA Loading Dye (Thermo Scientific) was used to load the samples. DNA ladders are listed in Table 2.10. TBE gels were stained postrun with ethidium bromide (Sigma-Aldrich; 100 µL of 1 % (w/w) solution per 1 L water). TAE gels were stained postrun with SYBR Green I (Lonza; 50 µL of 10000× solution in 300 mL 1× TAE).

Images of agarose gels were prepared with the GNU Image Manipulation Program by performing the following steps: conversion to greyscale colour mode, colour inversion, contrast adjustment, image cropping and rotation.

## 2.7.3. Sodium dodecyl sulfate polyacrylamide gel electrophoresis

Gels for sodium dodecyl sulfate polyacrylamide gel electrophoresis (SDS-PAGE) were prepared as specified in Table 2.37 and 2.38. Amounts are sufficient for two gels (8.0 cm × 7.3 cm). At first, separating gel was prepared, pipetted into assembled gel cassettes, and overlaid with isopropanol (Carl Roth) to generate a smooth surface. After polymerisation, the isopropanol was removed, followed by

addition of stacking gel on top of separating gel, and insertion of combs. The polymerised gels were either immediately used for SDS-PAGE, or stored at 4 °C, wrapped in wet paper towels, for 1–2 days.

**Table 2.37** 12.5 % separating gel for SDS-PAGE.

| Name | Amount for 2 gels |
| --- | --- |
| Lower buffer (Table 2.12) | 2 mL |
| Water | 2.66 mL |
| 30 % acrylamide-bisacrylamide solution (Carl Roth) | 3.33 mL |
| 10 % APS (Table 2.14) | 40 µL |
| TEMED (Carl Roth) | 8 µL |

**Table 2.38** Stacking gel for SDS-PAGE.

| Name | Amount for 2 gels |
| --- | --- |
| Upper buffer (Table 2.13) | 0.63 mL |
| Water | 1.63 mL |
| 30 % acrylamide-bisacrylamide solution (Carl Roth) | 0.38 mL |
| 10 % APS (Table 2.14) | 17.5 µL |
| TEMED (Carl Roth) | 10 µL |

Samples were mixed with 4× SDS-PAGE Loading Buffer (Table 2.15), heated to 95 °C for 1 min, subsequently treated with 50 u Novagen® Benzonase® Nuclease (Merck) for 1–2 h and again briefly heated to 95 °C shortly before loading. PageRuler™ Prestained Protein Ladder (Thermo Scientific) was used as length standard. Gels were run in 1× SDS running buffer (Table 2.16) at 20 mA and max. 110 V. Staining of the gels was done by gentle shaking in Coomassie brilliant blue staining solution (Table 2.17) for at least 2 h, followed by destaining involving repeated exchange of destaining solution (Table 2.18) until no further discolouring was observed.

Images of polyacrylamide gels were acquired using a standard scanner (Epson) and cropped and rotated using the GNU Image Manipulation Program, if required.

## 2.8. Cultivation of amoebae

### 2.8.1. General

Axenic cell cultures of amoebae are highly susceptible to contamination. It is therefore crucial to take measures to reduce the risk of accidentally introducing fungi or other contaminants and avoid undesired transfer of bacterial endosymbionts from one culture to another via aerosols. Culture flasks were for this reason opened exclusively in laminar flow hoods, except for cases in which the complete content of the culture was not needed for further incubation and immediately processed, as for example for RNA extraction. Additionally, work with symbiont-free and symbiont-containing cultures as well as cultures harbouring different endosymbionts was either temporally or spatially separated. If

both symbiont-free and symbiont-containing cultures had to be handled in the same laminar flow hood, symbiont-free cultures were always opened first and never kept open in the flow hood at the same time as infected cultures.

Growth media were prepared in large batches of 3–5 litres at once and aliquoted into 250 mL glass bottles (Schott) before autoclaving, then stored at room temperature in the dark, involving regular examination of the stocks by eye for contamination. Separate bottles were used for symbiont-free and symbiont-containing cultures, and small residual amounts of medium in bottles that had been opened in the laminar flow simultaneously with cultures were discarded.

At the beginning of this diploma thesis, all cultures were screened for presence or absence and identity of bacterial endosymbionts by FISH and insertion element specific PCR. Furthermore, the cultures were monitored regularly by FISH during the course of the experiments.

## 2.8.2. Organisms

**Table 2.39** Amoebae maintained in axenic cultures.

| Organism | Endosymbiont |
| --- | --- |
| *Acanthamoeba* sp. | *Amoebophilus asiaticus* 5a2 |
| *Acanthamoeba* sp. | none (symbiont-free) |

## 2.8.3. Cultivation techniques

*Acanthamoeba* sp. harbouring *Amoebophilus asiaticus* 5a2 and symbiont-free *Acanthamoeba* sp. were maintained as adherent cultures in 25 cm² cell culture flasks (Nunc) containing 10 mL Trypticase Soy Broth with Yeast Extract (TSY; Table 2.24) or Peptone Yeast Glucose Medium (PYG; Table 2.25) at 27 °C in the dark. PYG was used exclusively for backup cultures, as it had been shown previously that symbiont-free amoebae grew significantly better in PYG than in TSY. Replication rates of amoebae infected with *A. asiaticus* are lower than those of uninfected amoebae, but similar in both media (Tsao, 2011). Infections with *A. asiaticus*, however, are progressing faster in TSY compared to PYG. More amoebae can be infected by the same number of bacteria, and higher numbers of intracellular symbionts are observed (Tsao, 2011). Therefore, cultures for infection experiments were prepared and maintained in TSY for several weeks before starting the infection. *Acanthamoeba* cultures were monitored by light microscopy on a regular basis and passaged at confluency by 1:10 dilution with fresh medium every five to ten days, depending on the condition of the cultures. Cyst formation can be an indicator for unbeneficial growth conditions, for example lack of nutrients, changing pH or temperature during incubation. If an unusually high percentage of amoebal cysts was observed, the cultures were diluted only 2- to 3-fold with fresh medium to avoid an excessive reduction of cell numbers and allow faster recovery of the cultures.

For infection experiments involving RNA extraction, larger volumes of cultures were needed to retrieve higher cell numbers of both amoebae and endosymbionts. 1–2 small cultures were transferred into 500 cm² TripleFlask™ cell culture flasks (Nunc) and filled up with TSY medium to a final volume of 150 mL. The medium of symbiont-free amoebae was exchanged regularly until 2–3 days before the

infection was started to obtain well-growing cultures consisting almost exclusively of trophozoites densely covering the bottom surfaces of the cell culture flasks. In cultures of amoebae harbouring *A. asiaticus*, the medium was not exchanged during the last week before the infection to ensure an abundant presence of extracellular endosymbionts.

## 2.9. Extraction of genomic DNA from amoeba cultures

Total DNA, including genomic DNA (gDNA) of both amoebae and their endosymbionts, was extracted using the DNeasy® Blood & Tissue Kit (QIAGEN). Amoebae were detached from the culture flask's surface by vigorous shaking, and 2 mL were harvested by centrifugation at room temperature (6 min, 4727 × g). DNA was isolated according to the manufacturer's protocol for spin-column based purification of total DNA from animal tissues, only that 2 × 50 µL of PCR water were used for elution instead of the provided elution buffer AE. DNA concentrations were determined with a NanoDrop ND-1000 spectrophotometer (Thermo Scientific). All DNA was stored at –20 °C.

## 2.10. Screening of amoeba cultures

### 2.10.1. Fluorescence *in situ* hybridisation

FISH with a general bacterial probe and a symbiont-specific probe allows quick screening of amoeba cultures for the presence or absence of certain bacterial endosymbionts. A combination of the probes EUB338mix (targeting all *Bacteria*) and Aph1180 (specific for *A. asiaticus*) was used for detection of *A. asiaticus*. For more information about probes see Table 2.6.

Amoebae were detached from the cell culture flask's surface by vigorous shaking. Following harvesting of 2 mL of the culture by centrifugation at room temperature (6 min, 4727 × g), the pellet was resuspended in 150 µL 1× Page's Amoebic saline (PAS; Table 2.26). Residual traces of medium were removed by washing the pellet in 500 µL 1× PAS. The resulting pellet was resuspended in 150 µL 1× PAS. 20 µL per well of the cell suspension were applied to a polytetrafluoroethylene coated FISH slide and incubated at room temperature for 20 min, allowing the amoebae to attach to the glass surface. After carefully removing the liquid droplets without touching the wells' surface with the pipette tip, 20 µL of 4 % paraformaldehyde solution (PFA; Table 2.29) were added to each well for cell fixation and incubated for 10 min at room temperature. The PFA solution was carefully removed, followed by washing 1–2× with 20 µL of distilled water. Slides with fixed samples were dried at room temperature or in an incubator with slightly elevated temperature until the wells were completely dry. Hybridisations were conducted as previously described (Daims *et al.*, 2005).

For microscopic analysis, FISH slides were embedded in an anti-fadent solution (Citifluor AF1), and a coverslip was put on top. Epifluorescence microscopes (Axio Imager M1 and Axioplan 2 imaging; both microscopes by Zeiss) were used for quick visualisation, and a confocal laser scanning microscope (LSM 510 META; Zeiss) for image acquisition.

### 2.10.2. IS element specific PCR

Because it is not possible to discriminate between different *A. asiaticus* strains with FISH due to their high 16S rRNA sequence similarity, an IS element specific PCR based on the presence or absence of certain IS elements (Schmitz-Esser *et al.*, 2011) was performed to distinguish between the strains 5a2,

# MATERIALS AND METHODS

EIDS3, and US1. Table 2.40 gives an overview of the occurrence of selected IS elements in the genome of these three strains.

**Table 2.40** Occurrence of IS elements in *A. asiaticus* 5a2, EIDS3, and US1.

| IS element in *A. asiaticus* 5a2 | *A. asiaticus* EIDS3 | *A. asiaticus* US1 |
|---|---|---|
| ISCaa4 | — | — |
| ISCaa5 | + | + |
| ISCaa15 | + | — |

Genomic DNA of amoebae and their endosymbionts was isolated as described in Section 2.10. 1 µL of DNA (100 ng µL$^{-1}$) per reaction was subjected to PCR (Table 2.41 and 2.42) with the following primers: (1) ISCaa4F/ISCaa4R, targeting a 602 bp fragment of IS element ISCaa4, (2) ISCAA5F/ISCaa5R, targeting a fragment of 423 bp length of ISCaa5, and (3) ISCaa15F/ISCaa15R, for amplification of a 419 bp fragment of ISCaa15 (see Table 2.4 for more information about IS element primers). In order to validate the results, DNA previously isolated from cultures harbouring strains EIDS3 and US1, and from symbiont-free amoebae, was analysed by PCR with the same primers (1–3). PCR was controlled with agarose gel electrophoresis (1 % agarose, 120 V, 60 min).

**Table 2.41** Components in one IS element-PCR reaction.

| Reagent | Amount (µL) |
|---|---|
| 10× Taq Buffer with KCl (Thermo Scientific) | 5.0 |
| dNTP Mix (2 mmol L$^{-1}$ each) (Thermo Scientific) | 5.0 |
| MgCl2 (25 mmol L$^{-1}$) (Thermo Scientific) | 4.0 |
| Primer Forward (50 pmol µL$^{-1}$) | 1.0 |
| Primer Reverse (50 pmol µL$^{-1}$) | 1.0 |
| Taq DNA Polymerase (recombinant, 5 u µL$^{-1}$) (Thermo Scientific) | 0.2 |
| Template DNA | 1.0 |
| PCR water | 32.8 |

**Table 2.42** IS element-PCR thermal cycling programme.

| Repeats | Temperature (°C) | Time (min) | Comments |
|---------|------------------|------------|----------|
| 1× | 95 | ∞ | hot start |
| 1× | 95 | 05:00 | |
| 35× | 95 | 00:30 | |
| | 63.7 | 00:30 | |
| | 72 | 00:37 | |
| 1× | 72 | 10:00 | |
| 1× | 4 | ∞ | final hold |

## 2.11. Cloning of selected afp proteins

Two proteins of the afp-like cluster of *A. asiaticus*, the prophage tail sheath, Aasi_1074, and the VgrG homologue, Aasi_1080, were cloned for heterologous protein expression in *E. coli*. For this purpose, two different expression vectors, pET-21b and pGEX-4T-3, were chosen which both possess an inducible lac promoter to allow selective induction of the expression of the cloned proteins. In pET-21b, a polyhistidine tag (6× His tag) is already included in the vector sequence. pGEX-4T-3 does not possess a 6× His tag, only a glutathione S-transferase (GST) tag, but the reverse primers for pGEX cloning contained again the sequence for a His tag so that a fusion protein with His tag would be expressed. Based on this His tag, purification and refolding of proteins expressed in inclusion bodies can be done in one step using affinity chromatography (Hochuli *et al.*, 1988).

To obtain functional proteins, it is essential that the expression vectors contain the desired insert *in frame* and in the correct orientation. Forward and reverse primers therefore contained sequences to introduce restriction sites adjacent to the insert on both ends. Following cloning into pCR-XL-TOPO® and digestion with two different restriction enzymes, the insert can be cloned into the chosen expression vectors in the correct orientation. To avoid undesired restriction of the insert itself, enzymes were chosen where no restriction sites were present in the target sequences. In addition to the restriction sites, 1–2 bases were included in the primer sequences, if required, so that the insert would be *in frame*.

### 2.11.1. Competent *E. coli* strains

**Table 2.43** Competent *Escherichia coli* strains.

| Organism | Strain | Detailed description | Manufacturer |
|----------|--------|---------------------|--------------|
| *Escherichia coli* | TOP10 | One Shot® Top10 Chemically Competent *E. coli* | Invitrogen |
| *Escherichia coli* | BL21 | Electrocompetent *E. coli* | — |
| *Escherichia coli* | C41 | Electrocompetent *E. coli* | — |
| *Escherichia coli* | C43 | Electrocompetent *E. coli* | — |

One Shot® TOP10 Chemically Competent *E. coli* (Invitrogen) were used for the propagation of pCR-XL-TOPO® plasmids. Electrocompetent *E. coli* were prepared with the following protocol and used for the propagation of pET-21b/pGEX-4T-3 and heterologous protein expression.

*Preparation of electrocompetent E. coli*

50 mL dYT Medium were inoculated with *E. coli* of the desired strain and grown o/n at 37 °C on a platform shaker (200 rpm). All solutions and consumables (10 % glycerol solution, autoclaved distilled water, reaction tubes, glass pipettes) were pre-cooled to 4 °C o/n. On the next day, 750 mL dYT Medium were inoculated with 50 mL o/n culture and grown at 37 °C to an OD600 of 0.5–0.7, followed by cooling for 15 min on ice. All subsequent steps were conducted at 4 °C or on ice. The cells were harvested by centrifugation at 4 °C (15 min, 3270 × g) in 50 mL tubes. The pellet was washed with 50 mL of pre-cooled water and again centrifuged (4 °C, 15 min, 3270 × g). The resulting pellet was washed with 10 % ice cold glycerol solution and centrifuged (4 °C, 15 min, 3270 × g). After discarding the supernatant, the same volume of 10 % glycerol solution as the volume of the cell pellet (approximately 1–2 mL) was used to carefully resuspend the pellet. 100 μL aliquots were prepared and stored at –80 °C in screw cap tubes.

## 2.11.2. Amplification of target sequences

*High Fidelity PCR Enzyme Mix*

Initially, the amplification of prophage tail sheath (Aasi_1074) with the primer pairs (1) pET-21b Aasi_1074 F/pET-21b Aasi_1074 R and (2) pGEXHis Aasi_1074 F/pGEXHis Aasi_1074 R was attempted using the High Fidelity PCR Enzyme Mix (Thermo Scientific). This enzyme mix is a combination of standard *Taq* DNA Polymerase and a thermostable DNA polymerase with proofreading activity and altogether has a four times lower error rate than standard *Taq* DNA Polymerase. Four parallel reactions of 50 μL each were conducted for both primer pairs. The PCR was controlled by analysing small volumes (5 μL each) of the PCR products with agarose gel electrophoresis (1 % agarose, 120 V, 60 min). For neither of the primers, any PCR product could be obtained. This required switching to a different high fidelity polymerase.

*TaKaRa™ Ex Taq™ DNA Polymerase*

TaKaRa™ Ex Taq™ DNA Polymerase (TaKaRa Biotechnology) is specially intended for the amplification of longer and difficult templates. It possesses an additional 3´→5´ proofreading activity for improved fidelity (4.5× lower mutation rate than standard *Taq* DNA Polymerase). Aasi_1074 was amplified with the same primers (1) and (2) and in four parallel reactions as described for the High Fidelity PCR Enzyme Mix. Reaction mix and thermal cycling programme are given in Table 2.44 and 2.45.

**Table 2.44** Components in one PCR reaction using TaKaRa™ Ex Taq™ Polymerase.

| Reagent | Amount (µL) |
| --- | --- |
| 10× Ex Taq™ Buffer with MgCl2 (20 mmol L⁻¹) (TaKaRa Biotechnology) | 5.0 |
| dNTP Mix (2.5 mmol L⁻¹ each) (TaKaRa Biotechnology) | 4.0 |
| Primer Forward (50 pmol µL⁻¹) | 1.0 |
| Primer Reverse (50 pmol µL⁻¹) | 1.0 |
| TaKaRa™ Ex Taq™ Polymerase (5 u µL⁻¹) (TaKaRa Biotechnology) | 0.25 |
| *A. asiaticus* 5a2 gDNA (100 ng µL⁻¹) | 1.0 |
| PCR water | 37.75 |

**Table 2.45** Thermal cycling programme for amplification of Aasi_1074 (TaKaRa™ Ex Taq™ Polymerase).

| Repeats | Temperature (°C) | Time (min) | Comments |
| --- | --- | --- | --- |
| 1× | 94 | ∞ | hot start |
| 1× | 94 | 05:00 | |
| 35× | 95 | 00:30 | |
| | 69.2 | 00:30 | |
| | 72 | 01:33 | |
| 1× | 72 | 10:00 | |
| 1× | 4 | ∞ | final hold |

PCR was controlled with agarose gel electrophoresis (1 % agarose, 120 V, 60 min). Remaining PCR products of Aasi_1074 for cloning into pET-21b and pGEX-4T-3 were then pooled from the four parallel reactions per template (total volume after gel electrophoresis: approximately 180 µL) and purified with the QIAquick® PCR Purification Kit (QIAGEN) according to the manufacturer's protocol.

*Phusion® High-Fidelity DNA Polymerase*

Phusion® DNA Polymerase (New England Biolabs), a *Pyrococcus furiosus*-like enzyme fused with a processivity-enhancing domain, has 3′→5′ exonuclease activity and produces blunt ends. Its error rate is 50× lower than that of standard *Taq* DNA Polymerase. Aasi_1074 and Aasi_1080 were amplified with Phusion® DNA Polymerase with the primers (1) pET-21b Aasi_1074 F/pET-21b Aasi_1074 R and (2) pET-21b Aasi_1080 F/pET-21b Aasi_1080 R. Reaction mix and thermal cycling programme are given in Table 2.46 and 2.47. Four parallel reactions per target were conducted. PCR was controlled with agarose gel electrophoresis (1 % agarose, 120 V, 60 min).

## MATERIALS AND METHODS

**Table 2.46** Components in one PCR reaction using Phusion® Polymerase.

| Reagent | Amount (µL) |
|---|---|
| 5× Phusion® HF Buffer with MgCl2 (7.5 mmol L⁻¹) (New England Biolabs) | 10.0 |
| Deoxynucleotide Solution Mix (10 mmol L⁻¹ each) (New England Biolabs) | 1.0 |
| Primer Forward (50 pmol µL⁻¹) | 1.0 |
| Primer Reverse (50 pmol µL⁻¹) | 1.0 |
| Phusion® High-Fidelity DNA Polymerase (2 u µL⁻¹) (New England Biolabs) | 0.5 |
| *A. asiaticus* 5a2 gDNA (100 ng µL⁻¹) | 1.0 |
| PCR water | 35.5 |

**Table 2.47** Thermal cycling programme (Phusion® Polymerase).

| Repeats | Temperature (°C) | Time (min) | Comments |
|---|---|---|---|
| 1× | 98 | ∞ | hot start |
| 1× | 98 | 01:00 | |
| 35× | 98 | 00:05 | |
| | 69.2 | 00:15 | |
| | 72 | 00:45 | |
| 1× | 72 | 10:00 | |
| 1× | 4 | ∞ | final hold |

### *dA-tailing*

TOPO® XL cloning requires PCR products with 3′-deoxyadenosine (dA) overhangs. Because Phusion® Polymerase, unlike *Taq* polymerases, does not incorporate a non-templated single deoxyadenosine monophosphate (dAMP) on the 3′ end of PCR products, the addition of a 3′-dA has to be done in a separate step. For this purpose, the NEBNext® dA-Tailing Module (New England Biolabs) was used. Following the purification of PCR products pooled from four parallel PCR reactions with the QIAquick® PCR Purification Kit (QIAGEN) according to the manufacturer's protocol, the 3′-dA tailing reaction was conducted in a reaction volume of 50 µL at 37 °C for 30 min. Components of the reaction mix are given in Table 2.49. 3′-dA tailed products were purified with the QIAquick® PCR Purification Kit (QIAGEN) and subsequently used for TOPO® XL cloning.

**Table 2.48** Components in one 3′-dA tailing reaction.

| Reagent | Amount (µL) |
|---|---|
| 10× NEBNext® dA-Tailing Reaction Buffer (New England Biolabs) | 5.0 |
| Klenow Fragment (New England Biolabs) | 3.0 |
| Template DNA | 15.0 |
| PCR water | 27.0 |

## 2.11.3. Cloning into pCR-XL-TOPO® and chemical transformation of *E. coli*

Invitrogen's TOPO® XL PCR Cloning Kit is designed for one-step cloning of PCR products into the vector pCR-XL-TOPO® (provided in the kit). Topoisomerase I is covalently bound to the linearised plasmid and mediates ligation of 3′-dA tailed PCR products with the 3′-deoxythymidine overhangs of the vector. pCR-XL-TOPO® contains a lethal *E. coli* gene, ccdB, which is disrupted by ligation of a PCR product into the vector so that only transformants containing a recombinant plasmid will survive.

TOPO® XL cloning of Aasi_1074 and Aasi_1080 and subsequent chemical transformation of *E. coli* One Shot® TOP10 cells (provided in the TOPO® XL Cloning Kit) were done according to the manufacturer's protocol (TOPO® XL PCR Cloning Kit; Life Technologies, 2012), with the only modification that 4 instead of 2 µL Cloning Reaction were used. Transformed cells were plated on selective medium (LB containing 50 mg L$^{-1}$ kanamycin) to inhibit growth of *E. coli* that failed to take up plasmids, and incubated at 37 °C o/n.

## 2.11.4. Screening and growing of recombinant clones

The approximate length of inserts was determined by PCR with M13 Forward and M13 Reverse primers, binding to regions flanking the MCS of the pCR-XL-TOPO® vector. PCR was controlled with agarose gel electrophoresis (1 % agarose, 120 V, 60 min).

**Table 2.49** Components in one M13-PCR reaction.

| Reagent | Amount (µL) |
| --- | --- |
| 10× Taq Buffer with KCl (Thermo Scientific) | 5.0 |
| dNTP Mix (2 mmol L$^{-1}$ each) (Thermo Scientific) | 5.0 |
| MgCl2 (25 mmol L$^{-1}$) (Thermo Scientific) | 4.0 |
| Primer M13 Forward (50 pmol µL$^{-1}$) | 1.0 |
| Primer M13 Reverse (50 pmol µL$^{-1}$) | 1.0 |
| Taq DNA Polymerase (recombinant, 5 u µL$^{-1}$) (Thermo Scientific) | 0.2 |
| Template DNA | colony picked from plate |
| PCR water | 33.8 |

**Table 2.50** M13-PCR thermal cycling programme.

| Repeats | Temperature (°C) | Time (min) | Comments |
| --- | --- | --- | --- |
| 1× | 95 | ∞ | hot start |
| 1× | 95 | 05:00 | |
| 35× | 95 | 00:30 | |
| | 63.7 | 00:30 | |
| | 72 | variable | 1 min per 1 kb target length |
| 1× | 72 | 10:00 | |
| 1× | 4 | ∞ | final hold |

For each plasmid, two clones with inserts of correct length were inoculated in liquid LB amended with 50 mg L$^{-1}$ kanamycin and incubated at 37 °C on a platform shaker (200 rpm) o/n.

## 2.11.5. Isolation of plasmids

pCR-XL-TOPO® plasmids were isolated from 5 mL *E. coli* o/n culture with the QIAprep® Spin Miniprep Kit (QIAGEN) according to the manufacturer's recommendations, with the only modification that 30 µL PCR water instead of the provided buffer were used for elution.

Sequences of the inserts were controlled by Sanger sequencing (Microsynth Austria GmbH; Vienna, Austria) with the primers TOPO Seq F/TOPO Seq R, M13 Forward/M13 Reverse, and the specific primers used for amplification of the target sequences. Visualisation of the DNA sequences of sequenced plasmids was done with FinchTV (v1.4.0; Geospiza, Inc., 2006). Sequences were subsequently aligned with reference sequences from the *A. asiaticus* 5a2 genome to check for insertions, deletions, or mismatched bases. For this purpose, the EMBOSS Needle – Pairwise Sequence Alignment Tool, which is part of the European Molecular Biology Open Software Suite (EMBOSS) and applies the Needleman-Wunsch algorithm for global alignment of nucleotide and/or protein sequences, was used (Rice *et al.*, 2000) via a graphical user interface provided by the European Bioinformatics Institute (URL http://www.ebi.ac.uk/Tools/psa/emboss_needle/, European Bioinformatics Institute, 2012).

## 2.11.6. Cloning into pET-21b and pGEX-4T-3

*Restriction by double digest*

Empty pET-21b and pGEX-4T-3 plasmids were available at the Department of Microbial Ecology. pCR-XL-TOPO® plasmids containing inserts for cloning into pET-21b and empty pET-21b vectors were digested with SacI and XhoI. pCR-XL-TOPO® plasmids with inserts for cloning into pGEX and empty pGEX-4T-3 vectors were digested with SalI and NotI. Restrictions were conducted as double digest in general buffers. 10× Buffer Tango was used for SacI/XhoI, and 10× Buffer O was used for SalI/NotI (all restriction enzymes and buffers by Thermo Scientific). Table 2.51 lists the components of one restriction reaction.

**Table 2.51** Components in one restriction reaction (double digest).

| Reagent | Amount |
|---|---|
| 10× Buffer Tango/Buffer O (Thermo Scientific) | 5.0 µL |
| Restriction enzyme 1 | 3.0 µL |
| Restriction enzyme 2 | 3.0 µL |
| Template DNA (plasmid) | 1–2 µg |
| PCR water | fill up to 50 µL |

The restriction products were analysed on a TAE gel (1 % agarose, 120 V, 60 min), stained with SYBR® Green I (Lonza). Vector and insert were identified based on their length and extracted from the gel with the QIAquick® Gel Extraction Kit (QIAGEN) according to the manufacturer's protocol, with the following modifications: (1) QIAGEN MinElute spin columns were used instead of the

columns provided in the kit. (2) 600 μL buffer QG were added to the gel slices instead of only 300 μL. (3) Independent from the colour of the pH indicator, sodium acetate was added. (4) 200 μL isopropanol were used. (5) Elution was done with 15 μL PCR grade water.

*Restriction by two subsequent digestions*

If the restriction by double digest was not successful, a different approach of two subsequent reactions with a purification step in between was used. 1–2 μg plasmid DNA were digested with 3 μL of the restriction enzyme *A* in 5 μL of the specific buffer for enzyme *A* in a final reaction volume of 50 μL for 90 min at 37 °C. After heat inactivation of the enzyme according to the manufacturer's recommendations, followed by a purification step (QIAGEN PCR Purification Kit) and elution in 30 μL PCR water, a second restriction was conducted. 3 μL of restriction enzyme *B* and 5 μL of the respective buffer were added to the purified plasmid. The reactions were filled up to a volume of 50 μL with PCR water, then incubated at 37 °C for 90 min. Following heat inactivation and another PCR purification, the restriction products were analysed on a TAE gel and purified as described for the restriction by double digest.

*Ligation with Thermo Scientific T4 ligase*

50–75 ng of empty vector and 150 ng of the respective insert were mixed in 2 μL 10× T4 DNA ligase Buffer. Following the addition of 2 μL T4 DNA Ligase (5 u μL$^{-1}$; buffer and enzyme by Thermo Scientific), the reaction (total volume: 20 μL) was incubated at 22 °C for 30 min for ligation, then stored temporarily on ice or at –20 °C. Before transformation, the ligated plasmids were dialysed against distilled water through a 0.025 μm membrane filter (Millipore) for 15 min.

*Ligation with NEBNext® Quick T4 DNA Ligase*

NEBNext® Quick T4 DNA Ligase (New England Biolabs) was tested as an alternative ligase for pET-21b Aasi_1074 and pET-21 Aasi_1080. 50–75 ng of empty pET-21b and 150 ng of the respective insert were mixed in 5 μL 5× NEBNext Quick Ligation Reaction Buffer. 2.5 μL Quick T4 DNA Ligase (New England Biolabs) were added, and the reaction (total volume: 25 μL) was incubated at 20 °C for 20 min for ligation. Storage conditions and dialysis step were identical as described for the Thermo Scientific T4 ligase.

*Screening of ligated expression vectors*

To control if the ligation was successful and estimate the length of the insert, a PCR with T7 or pGEX primers (see Section 2.11.8) was sometimes performed after dialysis.

## 2.11.7. Transformation by electroporation

The complete dialysed ligation reaction was added to an aliquot of electrocompetent *E. coli* on ice and incubated at 0 °C for 30 min, followed by electroporation (12.5 kV cm$^{-1}$) in pre-cooled 0.2 cm electroporation cuvettes. 250 μL of S.O.C. Medium (Life Technologies) were added, and the cells were incubated at 37 °C on a platform shaker (200 rpm) for 1 h. 50 and 150 μL of the cells were plated on LB containing 100 mg L$^{-1}$ ampicillin and incubated at 37 °C o/n.

## 2.11.8. Screening and growing of recombinant clones

Following the same principle as already described for M13-PCR of pCR-XL-TOPO® plasmids, the length of inserts in pET-21b and pGEX-4T-3 vectors was checked by PCR with T7 Promoter Primer/T7 Terminator Primer and pGEX 5′ Sequencing Primer/pGEX 3′ Sequencing Primer, respectively.

MATERIALS AND METHODS

Annealing temperature was 56 °C for T7-PCR and 55 °C for pGEX-PCR. PCR was controlled with agarose gel electrophoresis (1 % agarose, 120 V, 60 min).

**Table 2.52** Components in one T7/pGEX-PCR reaction.

| Reagent | Amount (µL) |
|---|---|
| 10× Taq Buffer with KCl (Thermo Scientific) | 5.0 |
| dNTP Mix (2 mmol L⁻¹ each) (Thermo Scientific) | 5.0 |
| MgCl2 (25 mmol L⁻¹) (Thermo Scientific) | 4.0 |
| Primer Forward (50 pmol µL⁻¹) | 1.0 |
| Primer Reverse (50 pmol µL⁻¹) | 1.0 |
| Taq DNA Polymerase (recombinant, 5 u µL⁻¹) (Thermo Scientific) | 0.2 |
| Template DNA | colony picked from plate |
| PCR water | 33.8 |

**Table 2.53** T7/pGEX-PCR thermal cycling programme.

| Repeats | Temperature (° C) | Time (min) | Comments |
|---|---|---|---|
| 1× | 95 | ∞ | hot start |
| 1× | 95 | 05:00 | |
| 35× | 95 | 00:30 | |
| | 56/55 | 00:30 | |
| | 72 | variable | 1 min per 1 kb target length |
| 1× | 72 | 10:00 | |
| 1× | 4 | ∞ | final hold |

Two clones per construct were inoculated in liquid LB amended with 100 mg L⁻¹ ampicillin and incubated at 37 °C on a platform shaker o/n. Plasmids were isolated as described in Section 2.11.5 and sequenced by Sanger sequencing (Microsynth) with T7 and pGEX primers, as well as the specific primers used for target amplification.

## 2.12. Heterologous protein expression in *E. coli*

### 2.12.1. Heterologous protein expression

All cloning vectors, including empty pET-21b and pGEX-4T-3 as controls, were freshly transformed into *E. coli* BL21 and grown on ampicillin plates o/n. One colony per plasmid was inoculated in 5 mL liquid LB+ampicillin and grown until an OD600 of 0.6 was reached, as determined with a visible spectrophotometer. 2 mL of the culture were harvested by centrifugation (1 min, 20000 × g) and resuspended in 2 mL LB+ampicillin, then stored at 4 °C o/n. On the next day, 300 µL of this suspension were freshly inoculated in 5 mL LB+ampicillin and grown until the cells were in logarithmic phase (OD600 of 0.5–0.7).

Heterologous protein expression was induced by adding 5 µL of a 1 mmol L⁻¹ solution of isopropyl-β-D-1-thiogalactopyranoside (IPTG; Thermo Scientific). After 4–5 h, 2 × 2 mL were harvested by centrifugation (1 min, 20000 × g). One pellet was resuspended in SDS-PAGE loading dye and subsequently analysed with SDS-PAGE, the other pellet was stored at –20 °C for later use for an inclusion body test.

### 2.12.2. Inclusion body test

For subsequent purification steps, it is essential to know if proteins are expressed in inclusion bodies or as soluble proteins. Following cell lysis, inclusion bodies can be easily separated from cell debris by centrifugation, but as the contained proteins are misfolded, an additional re-folding step is required to obtain functional proteins. Soluble proteins, on the other hand, cannot be easily harvested by centrifugation and therefore require a different purification protocol.

To test whether the proteins were expressed in inclusion bodies, the cell pellets harvested after heterologous protein expression were resuspended in 200 µL 1× TE buffer amended with 20 µL protease inhibitor solution (cOmplete; Roche). 30 µL CelLytic™ B 10× Cell Lysis Reagent (Sigma-Aldrich) were added. After incubation for 10 min at room temperature and three freeze/thaw cycles, 6 µL lysozyme solution (from chicken; Sigma-Aldrich; 100 mg in 1 mL water) were added. Following centrifugation at 4 °C and 20000 × g for 30 min, the supernatant, containing soluble proteins, was transferred to a fresh tube. The pellet, which contained the inclusion bodies, was resuspended in the same volume 1× TE buffer as the volume of the supernatant. 45 µL of each fraction, pellet and supernatant, were mixed with 15 µL SDS-PAGE loading dye and analysed by SDS-PAGE.

## 2.13. Infection of *Acanthamoeba* sp. with *A. asiaticus*

In asynchronous cultures of *Acanthamoeba* sp. harbouring *A. asiaticus*, all different stages of an infection cycle are present. However, to study selected infection time points, it is essential to set up a synchronous infection. This can be achieved by infecting previously symbiont-free amoebae with freshly released extracellular *A. asiaticus*. Originally used in virology, the term *multiplicity of infection* (MOI) is defined as the ratio of infectious agents to infection targets. In this particular case, the MOI refers to the number of *A. asiaticus* used for an infection, divided by the number of amoebae.

## 2.13.1. Harvesting of freshly released extracellular *A. asiaticus*

Without detaching the amoebae, the desired volume of supernatant from *Acanthamoeba* sp. cultures harbouring *A. asiaticus* 5a2 was filtered through a 5.0 μm filter into 50 mL reaction tubes to remove floating amoebae from the medium containing extracellular symbionts. Bacterial cells were pelleted by centrifugation at room temperature (5 min, 10595 × g) and resuspended in an appropriate amount of TSY medium. A method for quantification of harvested amoebae and symbionts is described in the following sections.

## 2.13.2. Quantification of amoebal cells

Amoebal cells were quantified by counting using a Neubauer hemocytometer and an Axiovert 25 inverse phase contrast microscope (Zeiss; 10× objective, no immersion). After detaching the amoebae by shaking, a small amount of the culture was transferred to a 2 mL reaction tube. 12 μL were pipetted into each of the two counting chambers, and the number of cells within the four large counting grids of both chambers was determined to calculate the concentration (Equation 2.1).

**Equation 2.1** Equation to calculate the concentration of amoebal cells (in cells per mL) based on quantification with a Neubauer hemocytometer. Counting grid area = 8 × 1 mm². Depth of chamber = 0.1 mm.

$$cells\,mL^{-1} = \frac{counted\,cell\,number}{counting\,grid\,area\,(mm^2) \times depth\,of\,chamber\,(mm)} * 1000$$

## 2.13.3. Quantification of bacterial cells

4′,6-diamidino-2-phenylindole (DAPI) is a fluorescent stain which is able to pass cell membranes and bind to AT-rich regions of DNA. DAPI staining can be done very fast, which is an essential prerequisite for quantification in the context of infection experiments. It has to be taken into consideration, however, that both living and dead cells are stained upon treatment with DAPI, meaning that the actual number of living, infectious cells is presumably somewhat lower than the calculated cell number. Still, the achieved accuracy is sufficient for determination of the MOI. Since DAPI is light sensitive, it has to be handled with care to avoid bleaching.

Samples were stained on a black 0.22 μm polycarbonate membrane filter (Millipore) mounted on a 0.45 μm cellulose acetate support filter (Sartorius). For this purpose, a filtration tower was set up as follows: (1) A fritted glass base (2.5 cm diameter) was placed in the neck of a 100 mL suction flask, with a hollow conical rubber stopper in between. (2) The support filter was situated on top of the glass base, soaked with 1× PAS, and (3) covered by the black 0.22 μm filter. (4) The filtration tower was placed on the glass base equipped with the two filters and secured with an aluminium clamp. (5) The intake line of a vacuum/pressure pump was connected to the suction flask, with an interposed Woulfe bottle to avoid spilling of DAPI solution. All glass parts were rinsed and flamed before setting up the filtration device.

Depending on the expected amount of harvested cells, a 1:1000 to 1:50000 dilution of 1–5 μL of the suspension in sterile 1× PAS was prepared (by default, 1 μL in 5 mL PAS, yielding a dilution factor of 5000). When isolating symbionts for large-scale infections intended for RNA extraction, the concentration of the cell suspension was usually much higher, and the dilutions were made in 50 mL PAS to avoid pipetting of volumes smaller than 1 μL.

5 mL of the diluted cell suspension were added to the filtration tower. A vacuum (250 mmHg pressure) was applied until the liquid had been aspirated completely, then the pump was turned off. Residual traces of the sample on the funnel and neck of the tower were rinsed down with 5 mL $1\times$ PAS, which was again aspirated by applying vacuum. After switching off the pump, 400–500 µL of DAPI solution (Carl Roth; 1:1000 dilution in $1\times$ PAS) were added onto the filter, the tower was covered with aluminium foil, and the sample was incubated for staining for 5 min in the dark. The DAPI solution was aspirated by applying vacuum, followed by a rinsing step with 5 mL $1\times$ PAS and another aspiration step. The filtration tower was disassembled, and the black polycarbonate filter, which contained the stained sample, was carefully placed on a glass microscope slide. A droplet of anti-fadent solution (Citifluor AF1) was added, and a coverslip was put on top. The slide was stored in the dark until microscopic analysis.

The number of cells was determined using an Axioplan 2 imaging epifluorescence microscope with a $10\times10$ counting grid (Zeiss; $100\times$ objective, oil immersion). 10 random positions within the stained area of the filter were chosen, and all cells in the grid were counted. Based on the average number of cells per grid, the concentration was calculated (Equation 2.2). Knowing the concentrations of symbiont-free amoebae and extracellular *A. asiaticus*, the required volume of symbiont suspension for the desired MOI was calculated.

**Equation 2.2** Equation to calculate the concentration of bacterial cells (in cells per mL) based on quantification by DAPI staining and visualisation by epifluorescence microscopy. *MF* microscopic factor; MF = 11264; calculated by dividing the membrane area exposed to filtration (176 mm²) through the grid area ($1.5625 \times 10^{-4}$ mm²); *DF* dilution factor.

$$cells\,mL^{-1} = average\ number\ of\ cells\ per\ grid \times MF \times DF$$

## 2.13.4. Preliminary infection experiments

Three preliminary infection experiments were performed, in which two different MOIs, 50 and 500, and several different time points throughout a complete infection cycle between 4 and 168 hours *post infection* (h *p.i.*) were investigated. One small culture (10 mL, in a 25 cm² cell culture flask) per time point was used and discarded after sampling, instead of repeatedly taking samples from one larger culture, which would most probably have an indeterminable influence on the progression of the infection, because: (1) Repeated sampling requires reiterative disruption of the incubation at 27 °C and detaching of the amoebae for each sampling. (2) In addition, a constant reduction of the residual culture volume (or dilution, if fresh medium was added) would result.

Symbiont-free *Acanthamoeba* sp. were harvested from approximately 50 mL culture (TSY) and quantified as described in Section 2.13.2. Six 25 cm² cell culture flasks, each containing $2 \times 10^6$ of the harvested amoebae and filled up with TSY to a final volume of 10 mL, were prepared and incubated for at least 30 min at room temperature to let the amoebae attach. Symbionts were isolated from *Acanthamoeba* sp. infected with *A. asiaticus* (100 mL total culture volume) and quantified as specified in Sections 2.13.1 and 2.13.3. In the first test infection, three cultures were infected with a MOI of 50, and the remaining three with a MOI of 500, while for the subsequent two experiments only a MOI of 500 was used. The infection was monitored with FISH (probes: EUBmix, Aph1180, EUK516). Time points analysed with FISH were 24, 48, and 72 h *p.i.* in the first experiment and 4, 24, 48, 72, 96, and 168 h *p.i.* in the subsequent two infections.

## 2.13.5. Modifications for high-yield RNA extraction

*Selection of time points*

Based on the results of the preliminary experiments, three time points representing early (12 h *p.i.*), intermediate (68 h *p.i.*), and late (140 h *p.i.*) stages of the infection cycle, were chosen for RNA extraction and subsequent analysis with RT-qPCR.

*Upscaling of the infection setup*

As high-yield RNA extraction requires substantially large amounts of cultures, the experimental setup had to be modified for upscaling. An additional test infection in 182.5 cm² cell culture flasks (VWR) containing $12 \times 10^6$ amoebae in 60 mL TSY showed that the progression of the infection was identical to what had been observed in previous experiments with 25 cm² flasks, confirming that larger flasks were an equally suitable alternative.

*Removing non-attaching amoebae prior to infection*

Ideally, well-grown symbiont-free amoebae forming a monolayer on the bottom of the cell culture flask are used for infection experiments. In praxis, not all amoebae have the ability to attach; some degree of cyst formation, although mostly so low that it could be considered neglectable, was always observed. To remove non-attaching amoebae, the cultures were pre-treated prior to harvesting by carefully decanting the supernatant (without shaking) and adding fresh medium for detaching.

*Removing non-infectious symbionts*

It is futile to differentiate between symbionts that are already attached to and in the process of entering their eukaryotic host, and bacterial cells that are located in the vicinity of an amoeba, but not attached yet, by FISH and epifluorescence or laser scanning microscopy. Separating infectious from non-infectious *A. asiaticus* when isolating extracellular symbionts for infection is impossible. To circumvent this problem, unattached (and thus presumably non-infectious) symbionts were removed by decanting the supernatant and adding fresh medium as described above immediately before RNA extraction and harvesting cells for FISH for the samples at 12 h *p.i.* For later time points, the washing step was done at 24 h *p.i.* for practical reasons.

*Selection of MOI*

The washing step also has implications for choosing an appropriate MOI, as it reduces the amount of symbionts and thereby may affect the extraction yield in regard of bacterial RNA. Consequently, a relatively high MOI of 1000 was selected for the earliest time point, 12 h *p.i.* For the later time points, MOI 500 was used, as a higher number of symbionts could be expected due to intracellular replication.

The final setup of the infection experiment, including three biological replicates for all sampling time points, is shown in Figure 2.1.
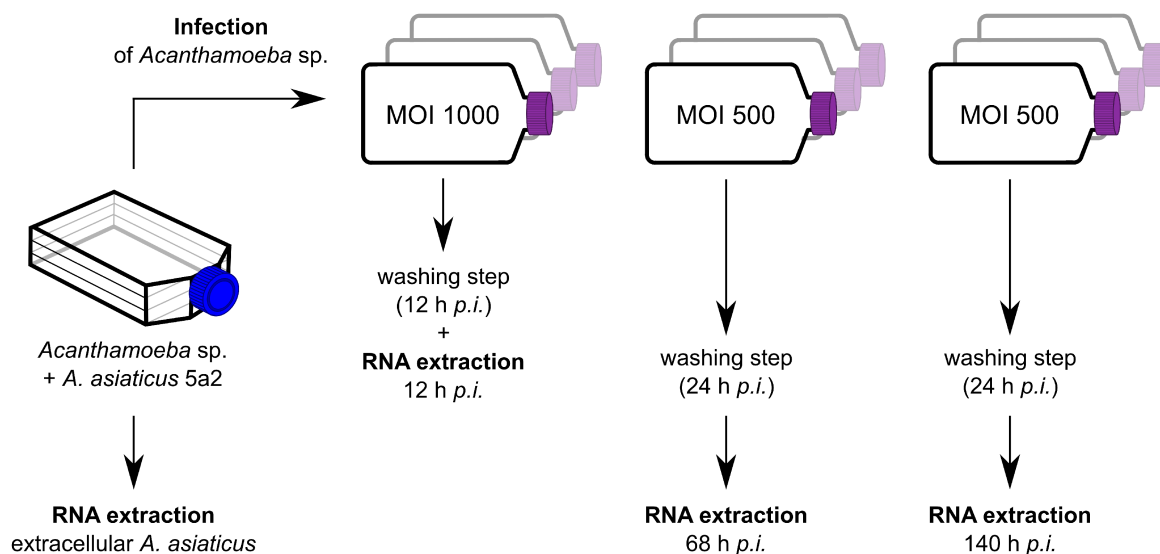
**Figure 2.1** *A. asiaticus* was isolated from an *Acanthamoeba* sp. culture and used to infect previously symbiont-free *Acanthamoeba* sp. Three biological replicates per investigated time point (12, 68, and 140 h *p.i.*) were prepared. MOI 1000 was used for 12 h p.i., and MOI 500 for the other cultures. Non-infectious *A. asiaticus* was removed by a washing step 12 or 24 h *p.i.* RNA was extracted from extracellular *A. asiaticus* and the infected cultures at the indicated time points.

## 2.13.6. Modifications for transmission electron microscopy sample preparation

A separate infection was set up as described for the preliminary experiments, with a high MOI of 5000 to ensure saturation of the infection. At 17 and 24 h *p.i.*, 15 mL of the cultures were harvested and preserved as specified in Section 2.17.1.

## 2.14. RNA extraction

Total RNA was isolated from three different kinds of samples: (1) Selected time points during an infection cycle, as described in detail in Section 2.13.5. (2) Extracellular *A. asiaticus* harvested from running cultures of *Acanthamoeba* sp. infected with *A. asiaticus*. Symbionts used for setting up the synchronous infection and for RNA extraction were isolated simultaneously and from the same cultures. (3) Symbiont-free *Acanthamoeba* sp. The same cultures were used as for the infection cycle, but symbiont-free amoebae for RNA extraction were harvested at a different time than for the infection.

### 2.14.1. General guidelines for working with RNA

Because RNA is labile and highly susceptible to degradation, the introduction of RNases from exogenous sources and their endogenous presence within samples has to be reduced to a minimum. RNases are ubiquitous and very stable (Nielsen, 2011). While autoclaving at 121 °C is sufficient to inactivate many other enzymes, as for example DNases, RNases are insensitive to these temperatures. However, they can be permanently inactivated by treating solutions with diethylpyrocarbonate (DEPC). All consumables (reaction tubes and filtered pipette tips) were purchased free of RNases and used out of sealed packages. At the Department of Microbial Ecology, a designated work bench

intended only for working with RNA is available. Work bench, pipettes and other surfaces were thoroughly cleaned with RNase AWAY solution (Carl Roth). As RNA is more stable at lower temperatures, samples were kept on ice between working steps and immediately transferred to –80 °C for storage as soon as work was finished. Repeated thawing and freezing of samples was avoided.

## 2.14.2. Phenol-based extraction of RNA

The TRIzol® Reagent (Life Technologies) is a commercially available phenol-based reagent for isolation of total RNA or simultaneous isolation of DNA, RNA, and proteins from one sample.

*Cell lysis/homogenisation*

50 mL of the culture were harvested by centrifugation at room temperature (6409 × g, 3 min). After discarding the supernatant, the pellet was resuspended in 750 µL TRIzol® Reagent and immediately transferred to a 2 mL FastPrep™ Lysing Matrix A tube (MP Biomedicals), from which the ¼ inch ceramic spheres had been removed before. Bead beating was done for 30 seconds at 4.5 m s⁻¹ with a BIO 101/Savant FastPrep™ FP120 device (Qbiogene).

*RNA extraction*

Following cell lysis by bead beating, RNA was extracted with TRIzol® Reagent according to the manufacturer's protocol for RNA isolation, starting from the "Phase separation" step. The exact step-by-step protocol is given in Section A.1. All reagents were added in the same amounts as specified in the protocol per 1 mL TRIzol® Reagent, although only 750 µL of the reagent were used. Addition of RNase-free glycogen as a carrier during RNA precipitation is optionally recommended for small sample quantities, but as the amount of harvested cells was estimated to be high enough, this step was left out. The RNA pellet was dissolved in 100 µL RNase-free water. At variance with the protocol, no heating step was performed after dissolving the pellet.

## 2.14.3. DNase treatment

Co-isolated DNA was removed from the RNA samples by DNase I digestion with the Ambion® TURBO DNA-free™ Kit (Invitrogen). 10 µg nucleic acids, as determined with a NanoDrop ND-1000 spectrophotometer, were digested in a total reaction volume of 50 µL. As the input amount of nucleic acids was relatively high, the manufacturer's recommendations for rigorous DNase treatment (intended for samples that contain more than 200 µg of nucleic acids per mL) were followed. The slightly adapted protocol is given in Section A.2.

## 2.14.4. Ethanol precipitation of RNA

Although the TURBO DNA-free™ Kit is designed to efficiently remove the DNase and divalent cations after the digestion, an additional de-salting step by ethanol precipitation was included to improve the purity of the DNA-free RNA. The complete amount of RNA recovered after DNase treatment (approximately 50 µL) was filled up with water to a volume of 200 µL and amended with 20 µL of sodium acetate (3 mol L⁻¹; Thermo Scientific) and 2 µL of RNase-free glycogen (5 mg mL⁻¹; Thermo Scientific). 660 µL ethanol were added. Following incubation for 30 min at –80 °C, the mixture was centrifuged at 4 °C (21255 × g, 10 min). The pellet was washed with 1 mL of 70 % ethanol and again centrifuged at 4 °C (21255 × g, 10 min). After removing the supernatant, the pellet was air-dried for maximal 5 min and resuspended in 5–10 µL RNase-free water. The step-by-step protocol can be found in Section A.3.

## 2.14.5. Quality control by microfluidics-based electrophoretic analysis

The integrity of DNA-free RNA was assessed with an Experion™ Automated Electrophoresis System (Bio-Rad). Experion™ HighSens Analysis Kit and Chips were used according to the manufacturer's recommendations. RNA samples were thawed on ice and diluted with nuclease-free water. 5 ng RNA per sample were applied to the chip.

# 2.15. First strand cDNA synthesis

## 2.15.1. Endogenous DNA contamination in RNA samples

After DNase treatment, all RNA samples were analysed with a control PCR using the primers Aasi_1074 F2 and Aasi_1074 R2 to detect remaining traces of DNA. In addition, DNase-treated RNA spiked with 100 ng of genomic DNA was applied to the same PCR assay to test for PCR inhibitory substances. The PCR was controlled with agarose gel electrophoresis (2.5 % agarose, 120 V, 60 min).

**Table 2.54** Components in one PCR reaction for endogenous DNA contamination testing.

| Reagent | Amount (µL) |
|---|---|
| 10× Taq Buffer with KCl (Thermo Scientific) | 5.0 |
| dNTP Mix (2 mmol L⁻¹ each) (Thermo Scientific) | 5.0 |
| MgCl2 (25 mmol L⁻¹) (Thermo Scientific) | 4.0 |
| Primer Aasi_1074 F2 (50 pmol µL⁻¹) | 1.0 |
| Primer Aasi_1074 R2 (50 pmol µL⁻¹) | 1.0 |
| Taq DNA Polymerase (recombinant, 5 u µL⁻¹) (Thermo Scientific) | 0.2 |
| RNA | 2.0 |
| PCR water | 31.8 |

**Table 2.55** Thermal cycling programme for endogenous DNA contamination testing.

| Repeats | Temperature (°C) | Time (min) | Comments |
|---|---|---|---|
| 1× | 95 | ∞ | hot start |
| 1× | 95 | 05:00 | |
| 35× | 95 | 00:30 | |
| | 61.9 | 00:30 | |
| | 72 | 00:12 | |
| 1× | 72 | 10:00 | |
| 1× | 4 | ∞ | final hold |

## 2.15.2. Reverse transcription of RNA

cDNA was synthesised with the SuperScript™ III Reverse Transcriptase and SuperScript™ III First-Strand Synthesis System for RT-PCR (Invitrogen). In the beginning, a different system, the RevertAid™ First Strand cDNA Synthesis Kit (Thermo Scientific), was tested, but soon abandoned in favour of the SuperScript™ kit. Random Priming (Feinberg & Vogelstein, 1983) with hexamer primers was used. Unless the commonly employed alternative priming strategy for reverse transcription, oligo(dT) priming, random priming does not discriminate against non-polyadenlyated RNAs and is therefore better suited for cDNA synthesis of bacterial RNAs. Specific primers would be a third strategy for cDNA synthesis to selectively amplify one or few targets of interest.

Reactions were set up in a final volume of 25 µL with the following components: 5 µL of template RNA (100 ng µL$^{-1}$), 4 µL of random hexamer primers (50 ng µL$^{-1}$), 6.25 µL of dNTP mix (2 mmol L$^{-1}$), 5 µL of 5× first-strand buffer, 2.5 µL of dithiothreitol (DTT, 0.1 mol L$^{-1}$), 1 µL of RNaseOUT™ (20 U µL$^{-1}$), and 1 µL of SuperScript III reverse transcriptase (200 U µL$^{-1}$; all reaction components by Invitrogen). All steps were carried out according to the manufacturer's recommendations for the SuperScript™ III Reverse Transcriptase. After heat inactivation, the cDNA was put on ice and stored at –20 °C.

All samples were reverse transcribed in three technical replicates. Additionally, a no-reverse transcriptase control with identical reaction components as described above but the enzyme replaced by 1 µL of DEPC-treated water was performed for each sample. Mastermixes were prepared to minimise tube-to-tube variations. To check the kit for contaminations, a no-template control (NTC) with DEPC-treated water instead of template RNA was included in every batch of reverse transcription. No-reverse transcriptase controls were subsequently analysed with qPCR to test the samples for detectable amounts of residual endogenous DNA. The NTC was also subjected to qPCR.

# 2.16. Quantitative real-time PCR

## 2.16.1. General

For the development of quantitative real-time PCR (qPCR) assays for relative quantification of antifeeding prophage tail sheath (Aasi_1074) mRNAs, the beta-subunit of the RNA polymerase gene (Aasi_1396), was selected as reference gene. The iQ™ SYBR® Green Supermix (Bio-Rad), which contains the DNA-binding dye SYBR Green I as reporter, was chosen in favour over a fluorescent reporter probe based approach. This Supermix is provided aliquoted and pre-mixed to ensure optimal performance and repeatability. For each qPCR run, a mastermix of Supermix and respective primers was prepared to reduce statistical variations between single reactions. qPCR was performed with a CFX96 Touch™ Real-Time PCR Detection System (Bio-Rad). The primer pairs Aasi_1074 qPCR F1/Aasi_1074 qPCR R1, targeting a 141 bp fragment of the antifeeding prophage tail sheath gene Aasi_1074 and Aasi_1396 qPCR F2/Aasi_1396 qPCR R2, targeting a 167 bp fragment of the reference gene Aasi_1396, were used. qPCR reactions were carried out in Hard Shell® Thin-Wall 96-Well Skirted PCR Plates (Bio-Rad) with white shell and clear wells in a reaction volume of 50 µL. Reaction components and cycling programme for qPCR are given in Table 2.56 and 2.57. A melting curve, starting at 55 °C and increasing the temperature by 0.5 °C each 10 sec up to a temperature of 95 °C, was performed after each qPCR run to assess the specificity of the amplification.

**Table 2.56** Components in one qPCR reaction.

| Reagent | Aasi_1074 (µL) | Aasi_1396 (µL) |
|---|---|---|
| 2× iQ™ SYBR® Green Supermix (Bio-Rad) | 25.0 | 25.0 |
| Primer Aasi_1074 qPCR F1 (10 pmol µL⁻¹) | 1.0 | — |
| Primer Aasi_1074 qPCR R1 (10 pmol µL⁻¹) | 1.0 | — |
| Primer Aasi_1396 qPCR F2 (10 pmol µL⁻¹) | — | 1.0 |
| Primer Aasi_1396 qPCR R2 (10 pmol µL⁻¹) | — | 1.0 |
| Template DNA (cDNA) | 5.0 | 5.0 |
| PCR water | 18.0 | 18.0 |

**Table 2.57** qPCR thermal cycling programme.

| Repeats | Temperature (°C) | Time (min) | Comments |
|---|---|---|---|
| 1× | 95 | 03:00 | |
| 45× | 95 | 00:30 | |
| | 65.7 | 00:30 | optimised from 55 °C to 72 °C |
| | 72 | 00:30 | real-time detection |
| 1× | 95 | 01:00 | |
| 1× | 55 | 01:00 | |
| 80× | 55 | 00:10 | raise temperature + 0.5 °C per step (melt curve) |
| 1× | 4 | ∞ | final hold (o/n) |

Controls were included in every qPCR run. One or two replicates of NTCs (5 µL PCR of water) plus sometimes an additional NTC with 5 µL of DEPC-treated water that was used for general RNA work were always included, also during assay development. A no-target control was included when the optimised assays were applied to analyse cDNA samples. For this purpose, cDNA from symbiont-free *Acanthamoeba* sp. was used. Additional bacterial no-target controls were not considered, as the absence of symbionts other than *A. asiaticus* 5a2 within the experimental system was controlled by FISH and IS element PCR.

## 2.16.2. Assay development

qPCR conditions, including annealing temperature and primer concentrations, were optimised with genomic DNA isolated from a culture of *Acanthamoeba* sp. infected with *A. asiaticus*.

*Evaluation of primer specificity*

Primer specificity was evaluated *in silico* with Primer-BLAST, a search option of the Basic Local Alignment Search Tool (BLAST; Altschul *et al.*, 1990) provided by the National Center for Biotechnology Information for design and evaluation of primers. Following each qPCR run, the specificity was additionally checked with a melting curve (see Table 2.57).

*Optimisation of primer annealing temperature*

To obtain an approximation of a suitable annealing temperature range, a standard PCR with 35 cycles and a temperature gradient from 47 °C to 72 °C was performed. Subsequently, the annealing temperature was optimised by qPCR with a temperature gradient from 55 °C to 72 °C. gDNA (*Acanthamoeba* sp. and *A. asiaticus*) in three different amounts (0.1, 1, and 10 ng per reaction) was used as template. NTCs were included for annealing at 55 °C.

*Optimisation of primer concentrations*

Concentrations of 100, 200, 300, 400, and 500 nmol $L^{-1}$ forward and reverse primer in all possible combinations were tested using 1 ng gDNA per reaction as template. To minimise the potential effect of varying numbers of pipetting steps and/or pipetting different volumes, the qPCR mastermix was designed to contain the lowest evaluated primer concentrations (100 nmol $L^{-1}$), and equal volumes of diluted primer solutions or PCR-grade water, depending on the desired final concentrations, were added to the individual reactions. NTCs were included for a concentration of 300 nmol $L^{-1}$ for both forward and reverse primer. No technical replicates were performed.

## 2.16.3. Preparation of qPCR standards

During the evaluation, for which gDNA was exclusively used, it was decided to switch to a different kind of qPCR standard for practical reasons. Firstly, it turned out that dilutions of gDNA were not stable when stored at –20 °C over longer time periods. Apart from that, gDNA does not allow calculation of absolute copy numbers, which is on the one hand not essential for a relative quantification, but on the other hand useful to evaluate the performance of the qPCR assay.

TOPO® XL plasmids (Life Technologies) containing a 1507 bp insert with the complete prophage tail sheath gene were already available from cloning for heterologous protein expression. For the reference gene, an 851 bp fragment was amplified with the primers Aasi_1396 STD F and Aasi_1396 qPCR R2 (Table 2.58 and 2.59) and cloned into pCR-XL-TOPO® as described in Section 2.11.3.

**Table 2.58** Components in one PCR reaction for cloning of TOPO XL qPCR standards.

| Reagent | Amount (µL) |
| --- | --- |
| 10× Taq Buffer with KCl (Thermo Scientific) | 5.0 |
| dNTP Mix (2 mmol $L^{-1}$ each) (Thermo Scientific) | 5.0 |
| MgCl2 (25 mmol $L^{-1}$) (Thermo Scientific) | 4.0 |
| Primer Aasi_1396 STD F (50 pmol $\mu L^{-1}$) | 1.0 |
| Primer Aasi_1396 qPCR R2 (50 pmol $\mu L^{-1}$) | 1.0 |
| Taq DNA Polymerase (recombinant, 5 u $\mu L^{-1}$) (Thermo Scientific) | 0.2 |
| *A. asiaticus* 5a2 gDNA (100 ng $\mu L^{-1}$) | 1.0 |
| PCR water | 32.8 |

**Table 2.59** Thermal cycling programme for cloning of qPCR standards.

| Repeats | Temperature (°C) | Time (min) | Comments |
|---|---|---|---|
| 1× | 95 | ∞ | hot start |
| 1× | 95 | 05:00 | |
| 35× | 95 | 00:30 | |
| | 61.9 | 00:30 | |
| | 72 | 00:52 | |
| 1× | 72 | 10:00 | |
| 1× | 4 | ∞ | final hold |

## 2.16.4. Quantification of qPCR standards

Plasmids used as qPCR standards were quantified using the Quant-iT™ PicoGreen® dsDNA Reagent and Kit (Invitrogen) according to the manufacturer's manual, with the following modifications: The reaction volume was downscaled from 1 mL to 100 μL (50 μL of sample or standard plus 50 μL of diluted PicoGreen® dsDNA Reagent), so that the assay could be performed in black 96-well microplates (Greiner Bio-One) as previously described (Hausmann, 2012). Measurements were done with an Infinite® M200 microplate reader (Tecan). A standard dilution series of 0, 20, 40, 80, 160, 200, 400, 600, 800, and 1000 ng mL$^{-1}$ final in-well concentration was prepared. Samples were diluted with 1× TE buffer to obtain estimated concentrations within the standard range, and measured in triplicates. Standards were measured in duplicates and applied to the second and next-to-last row of the plate to compensate for biases caused by time differences of the measurements, as the microplate reader scans the plate row by row. Upon addition of 50 μL of PicoGreen® dsDNA Reagent, the content of the wells was mixed by pipetting. The plate was sealed with PCR film, covered with aluminium foil, briefly spun down and scanned with automatic optimal gain (PCR film and cover were removed from the plate before measurements).

Copy numbers were calculated based on concentration and molecular mass of each plasmid. Molecular masses were determined with the DNA/RNA/Protein/Chemical Molecular Weight Calculator (Chang Bioscience, Inc.; URL http://www.changbioscience.com/genetics/mw.html).

**Equation 2.3** Calculation of nucleic acids copy numbers in a defined volume based on known concentrations and atomic mass. Atomic mass constant 1 u = 1.660538921 × 10$^{-27}$ kg (Mohr *et al.*, 2012).

$$copy\,number = \frac{concentration\left(ng\,\mu L^{-1}\right) \times 10^{-12} \times volume\left(\mu L\right)}{atomic\,mass\left(u\right) \times atomic\,mass\,constant\left(kg\,u^{-1}\right)}$$

Calculated copy numbers of the standard dilutions series are given in Table 2.60.

**Table 2.60** Copy numbers in 5 µl of standard solution. All dilutions were tested during evaluation, but only the dilutions $10^{-3}$ to $10^{-11}$ were used in the final assay.

| Dilution | TOPO® XL Aasi_1074 clone | TOPO® XL Aasi_1396 clone |
|---|---|---|
| $10^0$ | 115200000000 | 145700000000 |
| $10^{-1}$ | 11520000000 | 14570000000 |
| $10^{-2}$ | 1152000000 | 1457000000 |
| $10^{-3}$ | 115200000 | 145700000 |
| $10^{-4}$ | 11520000 | 14570000 |
| $10^{-5}$ | 1152000 | 1457000 |
| $10^{-6}$ | 115200 | 145700 |
| $10^{-7}$ | 11520 | 14570 |
| $10^{-8}$ | 1152 | 1457 |
| $10^{-9}$ | 115 | 146 |
| $10^{-10}$ | 12 | 15 |
| $10^{-11}$ | 1 | 1 |

## 2.16.5. Evaluation of assay performance

Amplification efficiencies were evaluated by applying a dilution series of the qPCR standards to both assays. Cq values were plotted against starting template amounts. Based on the slope of the linear regression line, the qPCR efficiencies were calculated. Furthermore, dynamic range and limit of detection were determined for both assays.

## 2.16.6. Inhibition testing

To test for inhibition of the reverse transcription, different amounts of RNA template of a selected sample (140 h *p.i.*) were reverse transcribed, and a constant volume of the resulting cDNA was applied to qPCR. Furthermore, a dilution series of cDNA was analysed to detect inhibition of the qPCR. The range of the dilution series was predetermined by the concentration of the RNA extract (undiluted RNA and undiluted cDNA were included in the evaluation) and the detection limit of the qPCR. In both cases, a good linear correlation between the applied sample amounts and detected copy numbers should be observed if no inhibitory substances are present, while in the case of inhibition, no linear increase would result for rising template amounts.

## 2.16.7. Relative quantification of prophage tail sheath mRNAs at different stages of an infection

Samples were already reverse transcribed in technical triplicates, all of which were analysed by qPCR without further technical replication. Identical amounts of RNA had been used as template for reverse transcription. For qPCR, all samples were diluted 10-fold (PCR water), and 5 µL of the diluted cDNA were applied to a reaction volume of 50 µL. Standards were prepared as fresh dilution series for each

qPCR run and analysed in three technical qPCR replicates. One out of three technical reverse transcription replicates of the no-target controls (symbiont-free *Acanthamoeba* sp.) was included. No-reverse transcriptase controls were analysed for each biological sample, but without technical replication. Furthermore, NTCs of the reverse transcription and NTCs of the qPCR itself were included. To evaluate inter-plate variation, one standard was amplified in three technical replicates with the primers Aasi_1074 qPCR F1/Aasi_1074 qPCR R1 on each plate. Since a calibration curve was in any case included on each plate, no further positive controls were required.

## 2.17. Transmission electron microscopy

### 2.17.1. Conventional transmission electron microscopy

*Sample fixation*

At selected infection time points (17 and 24 h *p.i.*), 15 mL of an infected culture were harvested by centrifugation at room temperature (3 min, 3214 × g). The cell pellet was carefully resuspended in 1 mL TEM fixative solution, freshly prepared before use by mixing 500 μL phosphate buffer (Table 2.31) with 500 μL 7 % glutaraldehyde solution (Table 2.32). Samples were shipped and stored at 4 °C until transmission electron microscopy.

*Staining, embedding, and microscopic analysis*

Further steps for sample preparation (osmium tetroxide contrasting and fixation, embedding in Agar 100 resin, sectioning, and staining with uranyl acetate and Reynold's lead citrate) and transmission electron microscopy were performed by Dr. Rok Kostanjšek (University of Ljubljana).

### 2.17.2. Cryo-electron microscopy

*Sample preparation of extracellular A. asiaticus*

Extracellular symbionts were harvested from asynchronous cultures of *Acanthamoeba* sp. infected with *A. asiaticus* by centrifugation as described in Section 2.13.1.

*Sheath preparation*

In addition to samples of complete *A. asiaticus* cells, a prophage sheath preparation was done according to a slightly modified protocol based on Basler *et al.* (2012). Approximately 2.4 L of *Acanthamoeba* sp. culture harbouring *A. asiaticus* were filtered through 5.0 μm filters to separate the extracellular symbionts from the amoebae. The filtered symbiont suspension was centrifuged at room temperature (5 min, 8372 × g) in 50 mL reaction tubes and pooled into one tube by additional centrifugation steps. The cell pellet was placed on ice and resuspended in 2.15 mL pre-cooled lysis buffer (Table 2.36). Following an incubation at 37 °C for 5–10 min, the lysate was centrifuged at 4 °C (15 min, 15000 × g) to remove intact cells and cellular debris. After a final ultracentrifugation step at 4 °C (1 h, 150000 × g), the pellet was resuspended in 50 μL NaCl/Tris buffer (Table 2.33) amended with protease inhibitor (1×), and stored at –20°C.

*Plunge-freezing and microscopic analysis*

Staining, plunge-freezing, and cryo-electron microscopy were done by Mag. Karin Aistleitner (Department of Microbial Ecology, University of Vienna) and Dr. Martin Pilhofer (California Institute of Technology) at the facilities of the California Institute of Technology. A first batch of images from

the isolated prophage tail sheaths was acquired by standard transmission electron microscopy after negative staining with uranyl acetate. The remaining samples were stained with colloidal gold and plunge-frozen. Cryo-electron microscopy images were recorded as tilt series from –60 ° to +60 °, with an increment of 1 ° at 10 μm under-focus.

# Chapter 3. Results

## 3.1. Heterologous expression of selected afp proteins

Final aim of cloning and heterologous expression of the prophage tail sheath, Aasi_1074, and the VgrG homologue, Aasi_1080, of *Amoebophilus asiaticus* was the production of specific antibodies against the purified proteins for immunofluorescence. Since applications like these require that the expressed proteins are functional, it was crucial to thoroughly analyse the sequences of the inserts with focus on the following key aspects: (1) The expression vector has to contain the respective insert in full length and in the correct orientation. The correct orientation should be ensured by using a two-step cloning protocol involving a restriction step with two different restriction enzymes. (2) No frame shift mutations must occur, as this would alter the reading frame and thereby lead to a completely different translated product than the desired protein. (3) No base substitutions should be found within the coding sequence. Whether the latter point becomes apparent during translation by effectively changing the identity of an encoded amino acid is dependent on the base that is exchanged, its position within the codon, and the meaning of the respective codon. (4) The polyhistidine tag, which is either part of the vector sequence or introduced via the primers used for target amplification has to be present to enable affinity chromatography-based purification and refolding of the proteins (Hochuli *et al.*, 1988).

### 3.1.1. Cloning of afp proteins

In a first attempt to clone Aasi_1074 into pET-21b and pGEX-4T-3, two different high fidelity polymerases were tested for amplification of the target sequences: (1) High Fidelity PCR Enzyme Mix (Thermo Scientific), and (2) TaKaRa™ Ex Taq™ DNA Polymerase (TaKaRa Biotechnology). PCR products were analysed with agarose gel electrophoresis. With the High Fidelity Enzyme Mix, no target amplification at all could be accomplished. PCR with a standard recombinant *Taq* Polymerase (also by Thermo Scientific), which had been done in parallel as a control, gave rise to products of correct length, indicating that the PCR generally worked, but not with the selected enzyme. Aasi_1074 was finally amplified using TaKaRa™ Polymerase and cloned into pET-21b and pGEX-4T-3.

Two clones of each construct were isolated and sequenced. Sequence analysis revealed that in all plasmids, the inserts were correctly oriented and also *in frame*, but each of them contained base substitutions. Pairwise nucleotide sequence alignments of the sequenced pET-21b and pGEX-4T-3 constructs with the reference sequence of Aasi_1074 are presented in Figure 3.1, along with the corresponding translated amino acid sequences. In both pET-21b clones, a C was found on position 209 relative to the start codon instead of a T, altering the codon from GTC (encoding valine) to GCC (encoding alanine), and a G instead of an A on position 647, altering the codon from AAT (encoding asparagine) to AGT (encoding serine). In both pGEX-4T-3 clones, a G on position 931 was substituted by an A, meaning that the codon GCA was replaced by ACA and upon translation, threonine would be incorporated instead of alanine. Due to these base substitutions and possible effects on the functionality of the proteins, the expression vectors clearly did not meet the requirements for the intended downstream applications.

**(a)**

```
    V   P   V   F   T   V   K   P   A   E   K   G   G   G   D   L
201 TGTGCCTGTCTTTACCGTTAAACCTGCAGAAAAAGGAGGTGGAGATCTTA 250   ref_seq
201 TGTGCCTGCCTTTACCGTTAAACCTGCAGAAAAAGGAGGTGGAGATCTTA 250   pET-21b clone
    V   P   A   F   T   V   K   P   A   E   K   G   G   G   D   L


    P   L   G   E   D   K   N   K   Y   V   T   R   F   R   E   N   I
601 CCATTAGGAGAAGACAAAAATAAATATGTAACTCGATTTAGAGAAAATAT 650   ref_seq
601 CCATTAGGAGAAGACAAAAATAAATATGTAACTCGATTTAGAGAAAGTAT 650   pET-21b clone
    P   L   G   E   D   K   N   K   Y   V   T   R   F   R   E   S   I


    G   L   D   N   L   T   Y   G   A   A   Y   Y   P   W   V   K
651 AGGCTTAGACAACCTAACCTATGGTGCAGCGTACTACCCTTGGGTTAAAA 700   ref_seq
651 AGGCTTAGACAACCTAACCTATGGTGCAGCGTACTACCCTTGGGTTAAAA 700   pET-21b clone
    G   L   D   N   L   T   Y   G   A   A   Y   Y   P   W   V   K
```

**(b)**

```
    L   N   V   L   P   A   A   P   A   M   A   G   L   Y   T   R
901 CTTAATGTATTGCCAGCAGCACCAGCTATGGCAGGGTTGTACACACGTAC 950   ref_seq
901 CTTAATGTATTGCCAGCAGCACCAGCTATGACAGGGTTGTACACACGTAC 950   pGEX-4T-3 clone
    L   N   V   L   P   A   A   P   A   M   T   G   L   Y   T   R
```

**Figure 3.1** Base substitutions were detected in all sequenced Aasi_1074 expression vectors. Pairwise nucleotide sequence alignment of **(a)** pET-21b and **(b)** pGEX-4T-3 clones and the reference sequence (ref_seq) of Aasi_1074 is shown. Translated protein sequences are also aligned with the nucleotide sequences. Incorrect bases and amino acids are highlighted in red, while the corresponding correct bases and amino acids are shown in blue.

It was suspected that the base substitutions were most likely caused by failure of the TaKaRa™ Polymerase used for target amplification, in spite of its allegedly low error rate. For the final cloning pipeline, Aasi_1074 and Aasi_1080 were therefore both amplified with Phusion® DNA Polymerase, which is superior in regards of fidelity to both TaKaRa™ Polymerase and the Thermo Scientific enzyme mix. When analysed with gel electrophoresis, bands with a size of approximately 1.5 kb and 1.8 kb, respectively, were obtained for Aasi_1074 and Aasi_1080, which coincides with the actual length of the target sequences. PCR products were purified and cloned into pCR-XL-TOPO®. Sequencing of two clones of each pCR-XL-TOPO® construct confirmed the absence of any base substitutions. All further results presented in Section 3.1.1 are from the second cloning using Phusion® DNA Polymerase.

*3.1.1.1. Restriction digest improvements*

For unknown reasons, problems occurred during the restriction for cloning of Aasi_1074 and Aasi_1080 amplified with Phusion® DNA Polymerase into pET-21b. In the following passage, improvement steps of the restriction protocol are described.

In the original protocol, the restriction of pET-21b and pGEX-4T-3 vectors without insert and pCR-XL-TOPO® plasmids containing the full-length sequences of Aasi_1074 and Aasi_1080 was planned to be performed as double digest. One pCR-XL-TOPO® clone per construct was selected and digested as described in Section 2.11.6. This protocol had successfully been used in the first attempt to clone Aasi_1074 into pET-21b and pGEX-4T-3, which unluckily had resulted in expression vectors with incorrect insert sequences. In the second cloning attempt, analysis of the restriction products by agarose gel electrophoresis (Figure 3.2a) showed that in case of the digestion of all pCR-XL-TOPO® plasmids, two clear bands with the corresponding sizes of the inserts and a larger band of approximately 3.5 kb, representing the TOPO vector, were obtained. The restriction of empty pET-21b, however, did not result in a distinct band on the gel but displayed itself as smear.

The restriction sites of the used restriction endonucleases, XhoI and SacI, are separated only by 32 bp on pET-21b. The most probable explanation for the unsuccessful digestion is that one of the enzymes could bind more effectively to the restriction site on the vector, thus preventing the other enzyme from performing its action. To circumvent this potential cause of the problem, two subsequent digests were conducted, with a heat inactivation and purification step in between to remove the first restriction enzyme before the second one was even added. Agarose gel electrophoresis (Figure 3.2b) showed a weak but clear band at approximately 5.5 kb for the restriction of empty pET-21, which confirmed that the digest was still not very efficient, but successful. For the restriction of the pCR-XL-TOPO® vectors, three bands were obtained; one at 1.5 kb or 1.8 kb, representing the respective insert, a second one at roughly 3.5 kb, which corresponds to the size of the empty TOPO vector, and a third one at approximately 5 kb. The latter one coincides with the size of vector plus insert and indicates a slightly reduced restriction efficiency, which can be explained by some degree of re-ligation of the vector during two-step restriction.
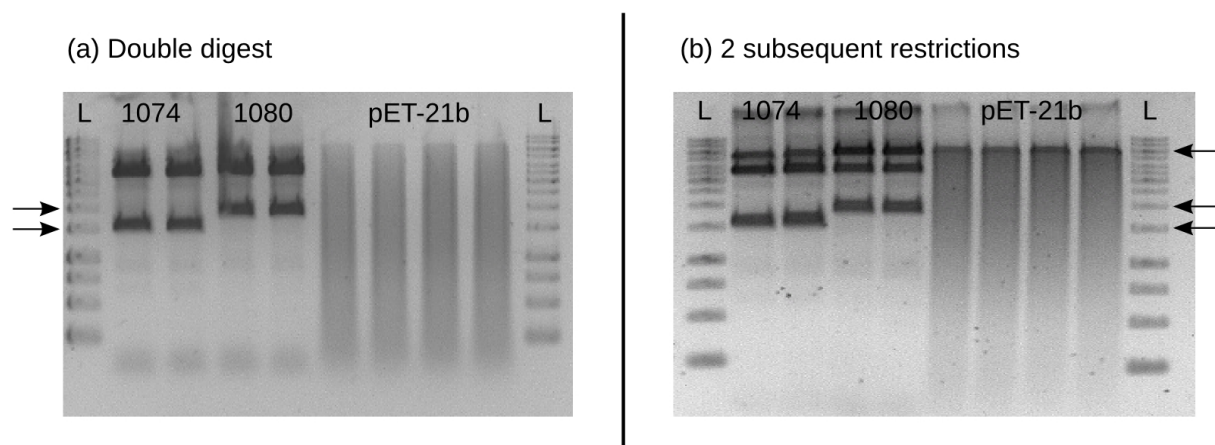
**Figure 3.2** Agarose gel electrophoresis of the restriction of pCR-XL-TOPO® plasmids containing full-length inserts of Aasi_1074 and Aasi_1080 and empty pET-21b (1 % agarose, 120 V, 60 min). *L* GeneRuler™ 1 kb DNA Ladder, arrows indicate bands with sizes of 1.5, 2.0, and 5.0 kb; *1074* pCR-XL-TOPO® vector with Aasi_1074; *1080* pCR-XL-TOPO® vector with Aasi_1080. **(a)** Double digest with XhoI and SacI in 1× Tango Buffer. Bands of the correct size were observed for the restriction of the pCR-XL-TOPO® plasmids, but the restriction of empty pET-21b was not successful. **(b)** Restriction in two subsequent steps.

### 3.1.1.2. Transformation of expression vectors

One clone of each construct, pET-21b Aasi_1074 and pET-21b Aasi_1080, was transformed into *E. coli* BL21 by electroporation. However, no growth of recombinant *E. coli* was observed for both expression vectors after incubation overnight. Restriction, ligation, and transformation were repeated with a different ligase (NEBNext® Quick T4 DNA Ligase; New England Biolabs) instead of the previously used Thermo Scientific T4 ligase. Again, the transformation remained unsuccessful, as no *E. coli* colonies could be detected on the plates even after prolonged incubation. Consequently, the ligated expression vectors were analysed by PCR with T7 Promoter Primer and T7 Terminator Primer to see if the ligation itself had worked (Figure 3.3). Both pET-21b Aasi_1074 and pET-21b Aasi_1080 ligations resulted in distinct bands at approximately 1.8 and 2.1 kb, respectively, corresponding to the length of the inserts plus 331 bp of adjacent vector sequences. Bands at the bottom of the gel lanes are most likely a mixture of primer dimers and short fragments of 331 bp length amplified from a fraction of pET-21b plasmids that do not contain an insert. It can therefore be inferred that the ligation of both expression vectors was successful, and that the absence of recombinant *E. coli* was probably caused by hindered uptake or early loss of the plasmids. The transformation was further tested with two alternative *E. coli* strains, C41 and C43, but also with these strains, it was not possible to obtain growth of recombinant *E. coli*.
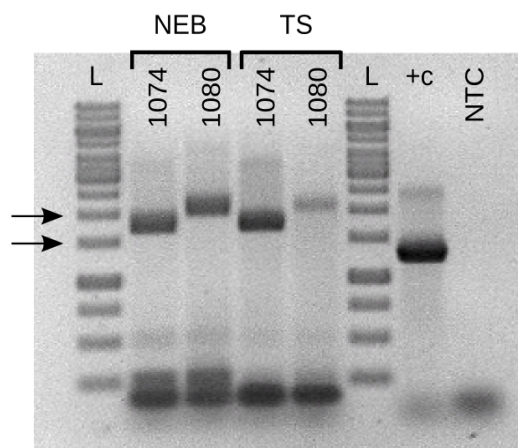
**Figure 3.3** Agarose gel electrophoresis of T7 PCR (1 % agarose, 120 V, 60 min). *L* GeneRuler™ 1 kb DNA Ladder, arrows indicate bands with sizes of 1.5 and 2.0 kb; *+c* positive control (pET-21b vector containing a full length-insert of a Ubiquitin-specific protease of *A. asiaticus*); *NTC* NTC (PCR water); *NEB* ligation with NEBNext® Quick T4 DNA Ligase (New England Biolabs); *TS* ligation with standard T4 ligase (Thermo Scientific). Bands at the bottom of gel lanes are most probably a mixture of primer dimers and 331 bp fragments amplified from pET-21b plasmids which do not contain an insert.

## 3.1.2. Heterologous protein expression

Notwithstanding the limited number and inferior sequence quality of available expression vectors, all of which contained base substitutions, heterologous expression of Aasi_1074* in pET-21b and pGEX-4T-3 was attempted in *E. coli* BL21 (the asterisk is used to indicate that at least one base substitution was present in the insert). Table 3.1 gives an overview of all used expression vectors, including the expected length of hypothetical proteins. Molecular masses of proteins were calculated using online tools from the ExPASy Bioinformatics Resource Portal (Artimo *et al.*, 2012), which is operated by the Swiss Institute of Bioinformatics, in the following way: (1) DNA sequences were translated *in silico* using the ExPASy Translate tool. (2) Molecular weight of translated sequences was subsequently determined with the ExPASy Compute pI/Mw tool.

**Table 3.1** pET-21b and pGEX-4T-3 vectors used for heterologous expression of Aasi_1074*.

| Vector | Insert | Tags | Molecular mass of protein (Da) |
|---|---|---|---|
| pET-21b | Aasi_1074* | His | 56362 |
| pGEX-4T-3 | Aasi_1074* | His, GST | 83081 |

The analysis of the cell extracts with sodium dodecyl sulfate gel electrophoresis (SDS-PAGE) is shown in Figure 3.4a. In the first two lanes, extract from *E. coli* harbouring empty pET-21b and pGEX-4T-3 plasmids, respectively, was applied to the gel. The band pattern in the lane with empty pET-21b corresponds to cellular proteins of *E. coli*, as the vector does not contain an insert, therefore no expression of heterologous proteins can be induced. In the pGEX-4T-3 lane, a very distinct band was additionally observed. This band represents the glutathione S-transferase (GST) tag of the pGEX vector, which has a size of approximately 26 kDa and is expressed upon induction with IPTG

independent from the presence of an insert in the vector. For both *E. coli* clones with pET-21b Aasi_1074*, distinct bands at approximately 56 kDa were visible, which coincides with the actual size of the prophage tail sheath protein (plus polyhistidine tag). The expression of Aasi_1074* in pGEX-4T-3 resulted in bands between 70 and 100 kDa. Since the GST tag with 26 kDa is fused to proteins expressed with the pGEX system, the observed band is also in accordance with the expected protein size (83 kDa).

Following heterologous protein expression, an inclusion body test was performed (Figure 3.4b). In all samples, the protein was detected in the pellet fraction rather than in the supernatant. It can be inferred that Aasi_1074* is expressed in inclusion bodies. In the bottom of all lanes where the pellet fraction was analysed, a band of 10–15 kDa was observed that most likely represents the lysozyme (14.3 kDa) used for the inclusion body test.
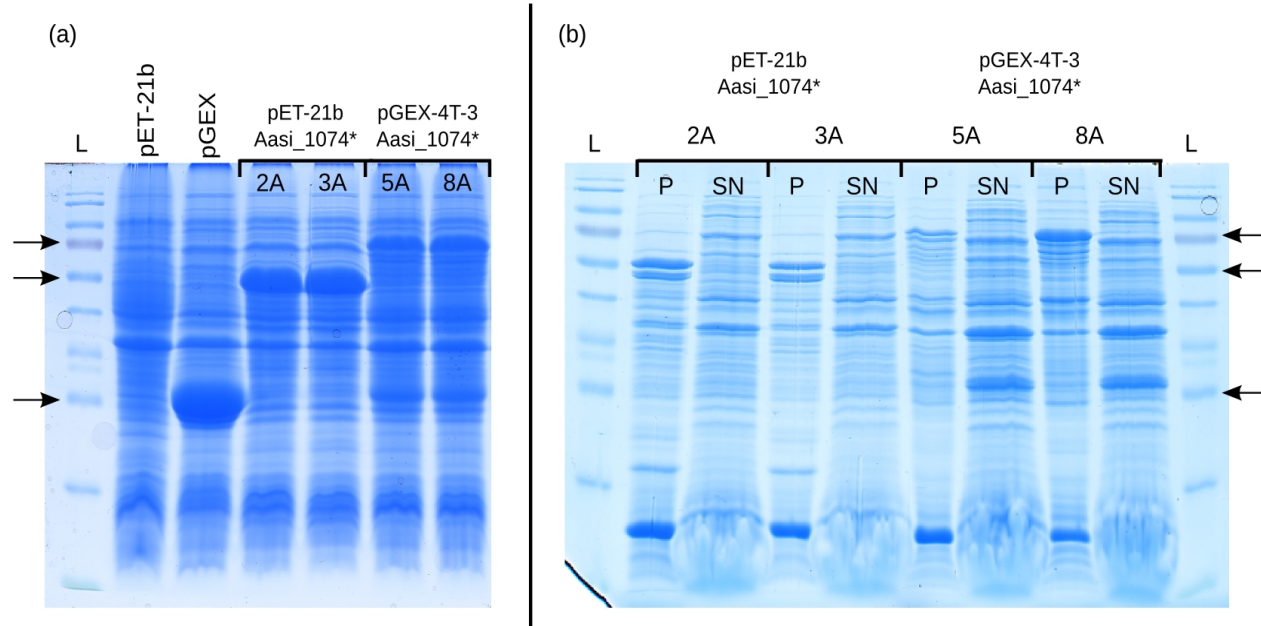


**Figure 3.4** SDS-PAGE (12.5 % separating gel, 20 mA, max. 110 V) of cell extracts after heterologous protein expression **(a)** and the Inclusion body test **(b)**. *L* PageRuler™ Prestained Protein Ladder, arrows at 25, 55, 70 kDa; *pET-21b* pET-21b empty; *pGEX* pGEX-4T-3 empty; *2A–3A* pET-21b Aasi_1074* clones; *5A–8A* pGEX-4T-3 Aasi_1074* clones. *P* pellet fraction; *SN* supernatant.

## 3.2. Infection cycle of *A. asiaticus* in *Acanthamoeba* sp.

### 3.2.1 Preliminary infection experiments

At the beginning of this diploma thesis, three preliminary infection experiments were conducted to select time points for gene expression analysis and optimise the protocol for large-scale infections intended for RNA extraction. In the first test infection, two different multiplicities of infection (MOI), 50 and 500, were compared at 24, 48, and 72 hours *post infection* (h *p.i.*). The progression of the infection was visualised with fluorescence *in situ* hybridisation (FISH). Newly infected amoebae could be detected already at 24 h *p.i.*, and the percentage of infected cells was significantly higher in samples where a MOI of 500 was used, compared to MOI 50 (data not shown). Since substantial amounts of

symbiont RNA would be required in infections for the gene expression analysis, MOI 500 was considered to be better suited. An important criterion for the decision on time points that would be analysed was the time when *A. asiaticus* actually entered its amoebal host. Discrimination between symbionts attached to the outside of their hosts' cell membrane and intracellular *A. asiaticus* is difficult, as both will result in a FISH signal within the contours of the amoebal cells. FISH samples were therefore analysed with epifluorescence microscopy by manually screening through the different focal planes from top to bottom of the amoebae. If all symbionts are found within one focal plane, it can be assumed that they are still attached to the outer surface of the amoebae. Whereas if the FISH signal indicates that the symbionts are distributed in different focal planes within individual amoebal cells, *A. asiaticus* is most likely intracellular. For this infection, *A. asiaticus* was found intracellularly in all investigated time points (data not shown). It was inferred that the entry into the host occurred at an earlier time point than 24 h, which is in accordance with a previous study on the infection cycle of *A. asiaticus* (Tsao, 2011).

In the second and third infection experiment, only a MOI of 500 was used, and samples at 4, 24, 48, 72, 96, and 168 h *p.i.* were analysed with FISH (Figure 3.5). As in the first test infection, *A. asiaticus* was detected intracellularly from 24 h on (Figure 3.5a), but not in the early infection stage at 4 h *p.i.* (data not shown). Thus, the time frame for entry could be narrowed down to between 4 and 24 h *p.i.* In later time points, the percentage of infected amoebae did not rise notably, but the number of symbionts per infected host cell increased over time because of intracellular replication (Figure 3.5b-d). At 168 h *p.i.* (Figure 3.5d), most infected amoebae were densely filled with symbionts. Furthermore, clusters of extracellular *A. asiaticus* were detected, indicating that host cell lysis was already occurring, although this could also be the result of induced cell disruption during sample preparation and FISH.

FISH analysis of samples at 15 h *p.i.*, taken from an additional test infection using 182.5 cm² cell culture flasks, confirmed that at this time point, a washing step before sample fixation could reduce the number of *A. asiaticus* to a minor extent, but not remove all of them (data not shown). It can be concluded that *A. asiaticus* is attached to its prospective host at this stage of infection, but has not invaded the amoebal cells yet.

Three infection time points were finally chosen for analysis of prophage tail sheath expression: (1) an early time point (12 h *p.i.*), where *A. asiaticus* is attached to and in the process of entering its host, (2) an intermediate stage (for practical reasons, 68 instead of 72 h *p.i.*), representing intracellularly replicating *A. asiaticus*, and (3) a late time point (140 h *p.i.*), at which some amoebae are already lysed and the infection cycle starts anew. A MOI of 500 was selected, with exception of the early time point, for which a MOI of 1000 was used.
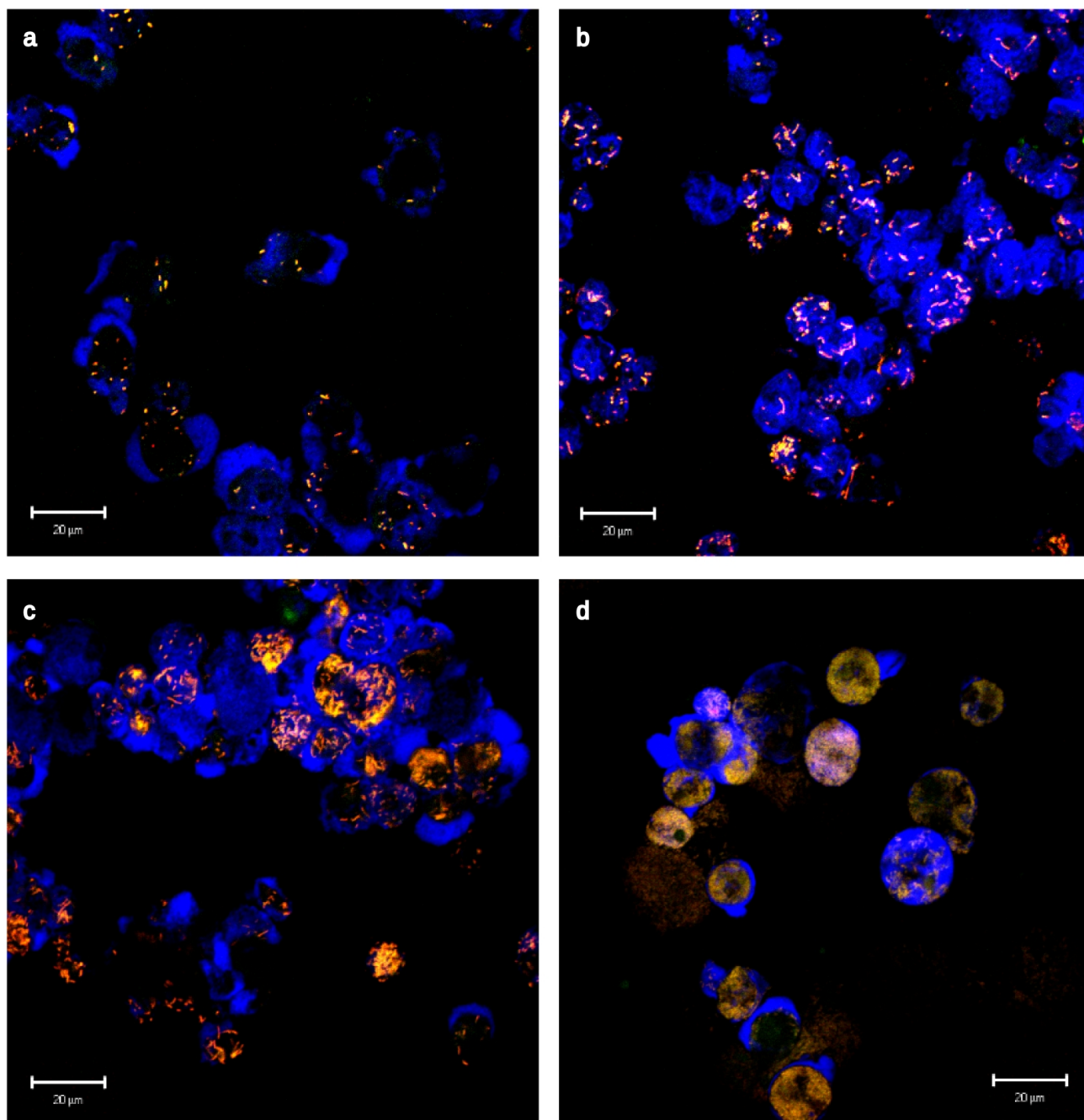
**Figure 3.5** Fluorescence *in situ* hybridisation images of *Acanthamoeba* sp. infected with *A. asiaticus* in preliminary infection experiments. Scale bars are 20 μm. **(a)** Sample taken at 24 h *p.i.*, **(b)** 48 h *p.i.*, **(c)** 72 h *p.i.*, **(d)** 168 h *p.i.* All hybridisations were performed with the probes EUB338mix (green), Aph1180 (red), and EUK516 (blue). *A. asiaticus* appears yellow or orange as a result of the combination of red and green signals. The green structures visible in the top right corner of (b) and central top region of (c) are caused by autofluorescence. Images were recorded with the help of Han-Fei Allen Tsao, Department of Microbial Ecology, University of Vienna.

## 3.2.2. Infection for RNA extraction

For RNA extraction, a large-scale infection was conducted and monitored by FISH at relevant time points (Figure 3.6). In contrast to the preliminary experiments, unattached *A. asiaticus* was removed from all cultures by a washing step either immediately before sampling (for the early time point, 12 h *p.i.*) or at 24 h *p.i.* (for later time points). Non-infectious symbionts located close to the cell membrane of an amoeba may display a similar appearance to attached symbionts in FISH images. Through this washing step, however, this possibility should be ruled out, so that whenever *A. asiaticus* is detected extracellularly in later time points, it can be inferred that lysis of amoebal cells has occurred. At 12 h *p.i.* (Figure 3.6a), *A. asiaticus* attaching to amoebal cells was observed, but no intracellular symbionts were detected. Coinciding with the results of the preliminary infection experiments, *A. asiaticus* was found intracellularly at 68 h *p.i.* (Figure 3.6b). The cell shape of *A. asiaticus* changed from short, almost coccoid rods at 12 h *p.i.* to a much more elongated form in intermediate stages of the infection. This change in shape has been previously described for *A. asiaticus* (Tsao, 2011). At the latest time point of RNA extraction, 140 h *p.i.* (Figure 3.6c), most infected amoebae were completely packed with symbionts and beginning to get lysed. Additionally, a smaller fraction of amoebae was observed that contained only a few symbionts, indicating the start of a new cycle of the infection with freshly released *A. asiaticus*.
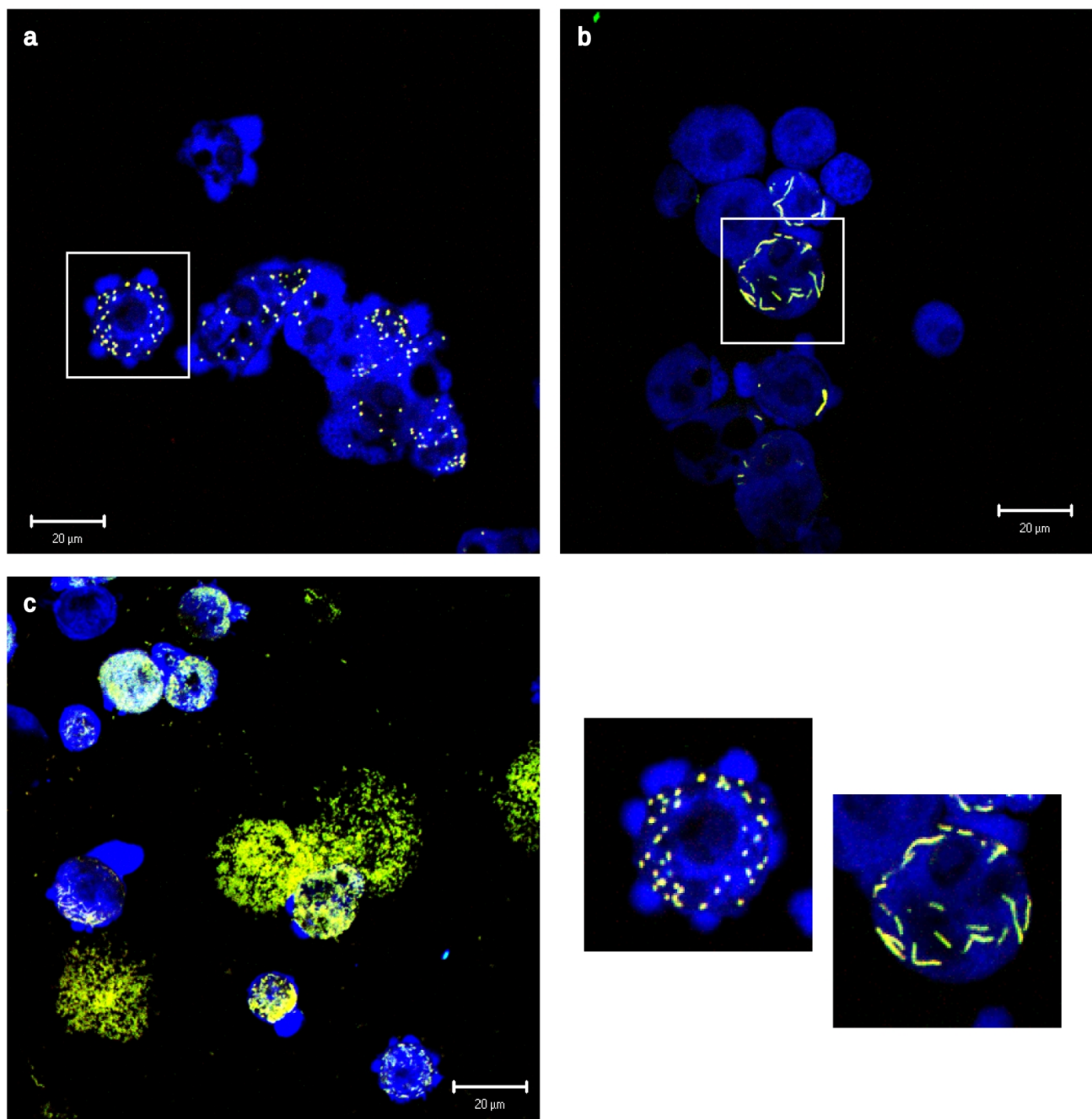
**Figure 3.6** Fluorescence *in situ* hybridisation images of *Acanthamoeba* sp. infected with *A. asiaticus* in the infection used for RNA extraction. Scale bars are 20 μm. Magnified sections are indicated with white boxes. **(a)** 12 h *p.i.*, **(b)** 68 h *p.i.*, **(c)** 140 h *p.i.* All hybridisations were performed with the probes EUBmix (double labeled with FLUOS; green), Aph1180 (red), EUK516 (blue), and Acant412a (blue). *A. asiaticus* appears yellow as a result of the overlay of red and green signals. Images were recorded with the help of Han-Fei Allen Tsao, Department of Microbial Ecology, University of Vienna.

Agnes Harreither

## 3.3. Evaluation of RNA extraction

The performance of any reverse-transcriptase quantitative real-time PCR (RT-qPCR) assay is highly dependent on the purity and integrity of the analysed RNA samples (Fleige & Pfaffl, 2006). RNA purity was assessed by measuring absorbance at 260 nm and 280 nm to detect protein contaminations and testing for residual DNA after DNase treatment. In addition, the integrity of DNase treated RNA was determined by microfluidics-based electrophoresis. The quantity of the extracted RNA can also become a limiting factor for successful and reliable RT-qPCR analysis if the yield is very low. However, as sustainable amounts of RNA were obtained for all samples, no further optimisation of the extraction protocol for higher yields was done.

### 3.3.1. Protein contamination assessment

Absorbance measurements were conducted from 10-fold dilutions, since the RNA concentration turned out to be relatively high in all extracts. The 260:280 ratios were between 1.90 and 2.08 for all samples, indicating that the RNA purity was high in terms of protein contaminations.

### 3.3.2. DNase treatment

Although the TRIzol® Reagent and protocol used are especially intended for selective extraction of RNA, certain amounts of DNA will inevitably be co-isolated. Since traces of DNA cannot be distinguished from reverse transcribed RNA (i.e., cDNA) in subsequent analysis with standard PCR or qPCR, it was crucial to remove all DNA from RNA samples. Otherwise, the perception of the quality of RNA and, consequently, cDNA samples would be clearly compromised and potentially bias the final results of the gene expression study.

Co-isolated DNA was removed by DNase I digestion. To detect residual DNA contaminations in DNase-treated RNA samples, a control PCR was performed as described in Section 2.15.1. For this purpose, all RNA samples were applied to the PCR assay pure and, additionally, mixed with 100 ng of gDNA from *Acanthamoeba* sp. + *A. asiaticus*. For pure RNA samples, no bands were expected. Contamination with DNA would result in a band at approximately 193 bp in RNA samples. Spiking allows to differentiate between negative PCR results caused by the absence of DNA within RNA samples and negative PCR results due to the presence of PCR inhibitory substances. In case of PCR inhibition, no bands would be observed for RNA spiked with gDNA, which otherwise should be present. The PCR results are shown in Figure 3.7. No obvious contaminations with DNA and no signs for PCR inhibition were detected.
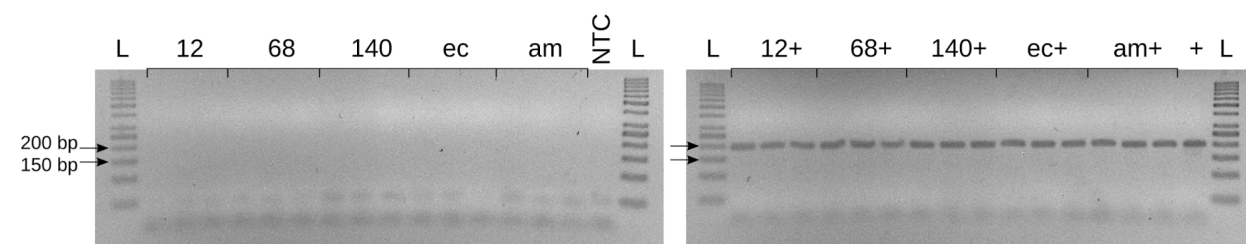
**Figure 3.7** Agarose gel electrophoresis of PCR for endogenous DNA contamination testing (2.5 % agarose, 120 V, 60 min). *L* GeneRuler™ 50 bp DNA Ladder, arrows are 150 and 200 bp; *+* positive control, 100 ng of *Acanthamoeba* sp. + *A. asiaticus* gDNA; *NTC* NTC (PCR water); *12* 12 h *p.i.*, *68* 68 h *p.i.*, *140* 140 h *p.i.*, *ec* extracellular *A. asiaticus*, *am* symbiont-free amoebae; *12+*, *68+*, *140+*, *ec+*, *140+* inhibition controls (RNA spiked with 100 ng of gDNA); for all samples 3 biological replicates were analysed in 3 adjacent lanes. Target bands have approximately 193 bp; bands at the bottom of the gels most likely represent primer dimers.

### 3.3.3. Integrity of DNA-free RNA

All DNase treated RNA samples were analysed with the Experion™ Automated Electrophoresis System (Bio-Rad). Benchmark indicators for high quality of RNA are electropherograms with pronounced peaks for ribosomal RNAs (rRNAs), with subsidence of the signal down to the base line in between. A high ratio (2:1) of 23S to 16S rRNA in prokaryotic RNA samples and 28S to 18S rRNA in RNA samples from eukaryotic organisms, respectively, is considered as evidence for the absence of degradation.

Distinct rRNA peaks were obtained for all samples, indicating that the overall quality of the RNA was satisfying. The results were highly similar between biological replicates. For RNA isolated from extracellular *A. asiaticus*, sharp 16S and 23S rRNA peaks were observed, and additionally a lower and wider peak of RNAs with a smaller size, most likely representing tRNAs. Samples from different infection time points, containing both *A. asiaticus* and *Acanthamoeba* sp. RNA, resulted in three sharp peaks for 16S, 18S, and 23S rRNA and a lower and wider peak for 28S rRNA, indicating that long RNAs might be degraded to some degree. A smaller and wider peak with two apices was observed for tRNAs and 5S rRNAs. Since the size of the target mRNAs, 1497 nt for the prophage tail sheath (Aasi_1074) and 3861 nt for the beta-subunit of the RNA polymerase as reference gene (Aasi_1396), lies below or at least between the size of 23S rRNA (2906 nt) and 28S rRNA (5070 nt), it was inferred that the integrity of these mRNAs was still maintained. As for the biological replicates, the results for the samples from different infection stages looked very much alike so that only two representative electropherograms of the analysis are shown (Figure 3.8). For samples containing a mixture of prokaryotic and eukaryotic RNA (12, 68, and 140 h *p.i.*) the ratio of 23S to 16S rRNA was not determined, because the individual peaks could not be reliably annotated by the software. For samples from extracellular *A. asiaticus*, the 23S to 16S rRNA ratio was between 1.76 and 1.79, attesting only a very low degree or even absence of degradation. Calculation of RNA quality indicators (RQI) was unfortunately not possible because only an outdated version of the Experion software was available, which does not support RQI determination.
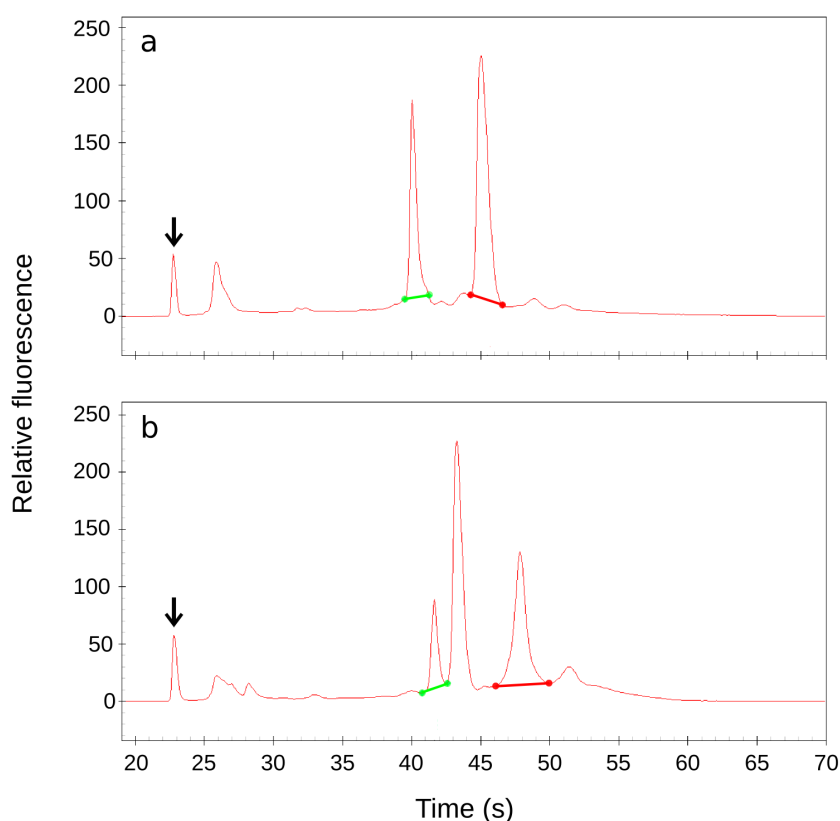
**Figure 3.8** Electropherograms from the Experion™ analysis of selected RNA samples isolated from extracellular *A. asiaticus* **(a)** and *Acanthamoeba* sp. infected with *A. asiaticus* 140 h *p.i.* **(b)**. The signal peak is marked with an arrow. 16S rRNA and 23S rRNA peak are marked with a green and red line, respectively. The small peak after the signal peak most likely consists of tRNAs and 5S rRNA.

## 3.4. qPCR assay development

### 3.4.1. Primer specificity

qPCR primers were designed by Thomas Penz (Department of Microbial Ecology, University of Vienna) using Primer3web (v4.0.0; Rozen & Skaletsky, 2000) and as a part of the process of primer design checked for specificity *in silico* with Primer-BLAST. For the primers used in the Aasi_1074 targeted assay, Aasi_1074 qPCR F1/Aasi_1074 qPCR R1, one hit for the target gene within the *A. asiaticus* 5a2 genome was found as best hit. This primer pair resulted in a second BLAST hit for possible amplification of a 4 kb fragment of *Xenorhabdus bovienii* by binding of the reverse primer to two insertion elements, with three mismatches per primer binding site. However, this result was considered as of no relevance, since the presence of *X. bovienii* in the experimental system used for this study can be excluded. The primer pair for the second assay targeting Aasi_1396, Aasi_1396 qPCR F2/Aasi_1396 qPCR R2, resulted in only one BLAST hit for *A. asiaticus*. All primers were therefore deemed as highly specific. In addition, the specificity of every qPCR run was supervised during evaluation and application of the qPCR assays by including melting curves and sometimes analysing PCR products with agarose gel electrophoresis. Melt curve results and gel images are presented in the respective context in the following sections.

## 3.4.2. Primer annealing temperature

An optimal annealing temperature for any primer pair used for PCR or qPCR can be determined experimentally as the highest temperature for which the target is specifically amplified. To get a first estimation of an appropriate temperature range, a standard PCR with temperature gradient from 47 to 72 °C was performed and checked by agarose gel electrophoresis. For both primer pairs, Aasi_1074 qPCR F1/Aasi_1074 qPCR R1 and Aasi_1396 qPCR F2/Aasi_1396 qPCR R2, distinct bands at 141 and 167 bp, respectively, coinciding with the length of the targets, were obtained up to an annealing temperature of 61.9 °C (gel images not shown). With an annealing step at 66.8 °C, only a minor decrease in the intensity of the target bands was observed, while higher temperatures of 70 °C or more led to a clear reduction of the amount of PCR product, indicating that the optimal annealing temperature might be roughly between 62 and 67 °C.

The temperature for the annealing step was subsequently fine-tuned by performing qPCR with a narrower gradient from 55 to 72 °C. Equal amounts of template (gDNA in three different starting quantities) were subjected to different annealing temperatures, and the Cq values were plotted as a function of temperature (Figure 3.9a and b). Suitable annealing temperatures will allow specific amplification of the target, while at the same time the efficiency of the reaction should be as high as possible, which is indicated by low Cq values. A definite rise in Cq values was observed for temperatures close to 70 °C or above for both assays, but unclear trends of the bending of the curves finally led to the conclusion that it was safer to select a slightly lower annealing temperature. Specificity was supervised by performing melting curves (Figure 3.9c and d). Distinct, coincident melt peaks for all samples indicate that the amplification was specific independent from the annealing temperature. In both assays, also the no-template controls (NTCs) for an annealing temperature of 55 °C showed a fluorescent signal, but with significantly higher Cq values than all gDNA samples. As the melt peaks for the NTCs occurred at a different position than for the gDNA, it was inferred that the observed fluorescence was the result of SYBR Green I binding to unspecific by-products, most probably primer dimers. NTCs for higher annealing temperatures were not included in this qPCR run, but in later evaluations steps. During initial evaluation, 61.7 °C were used for annealing in a few qPCR runs, but soon the switch was made to 65.7 °C because the specificity was not always satisfying with the lower temperature. In the final assay, 65.7 °C were used as annealing temperature for the analysis of all cDNA samples.
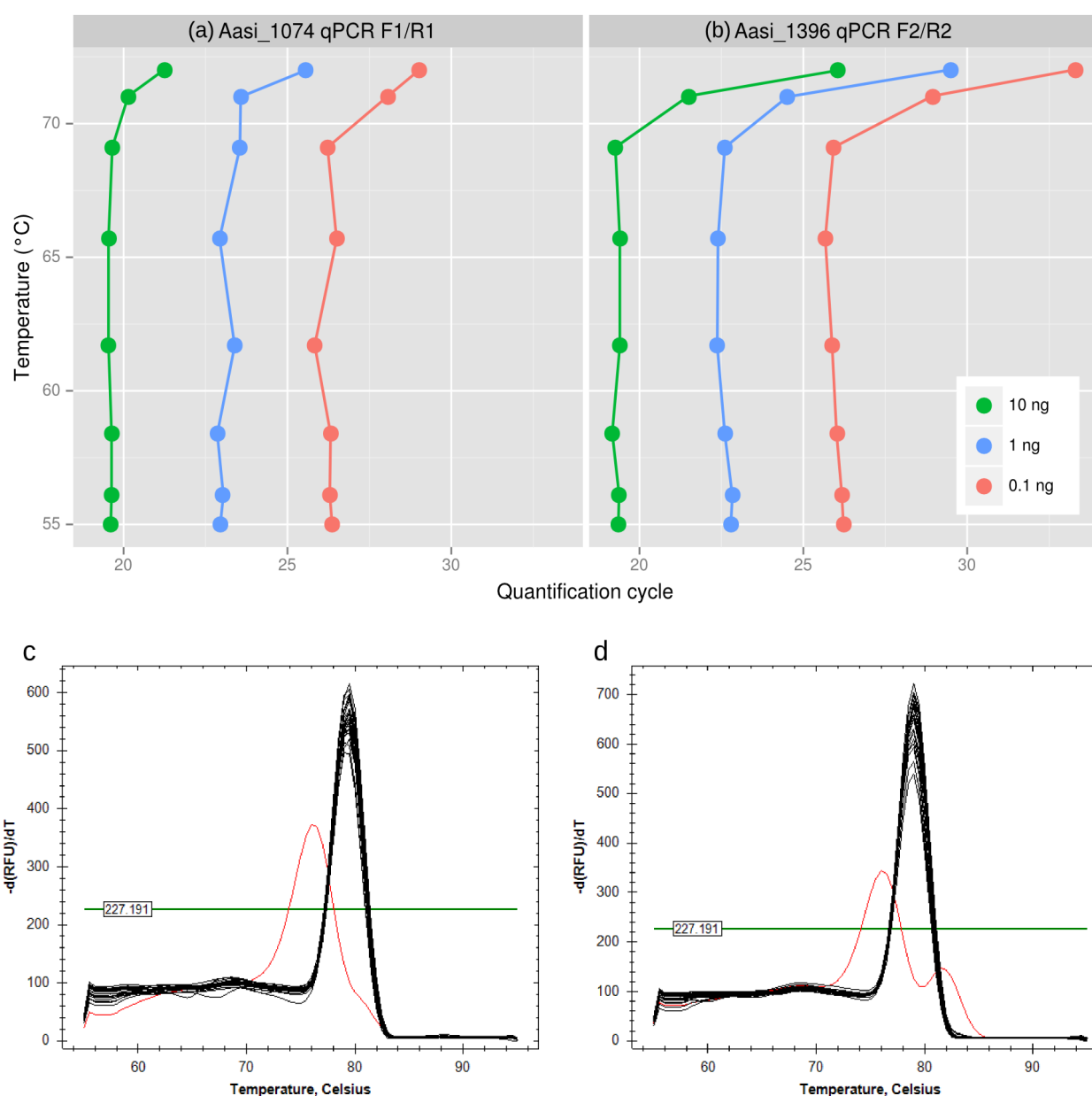
**Figure 3.9** Three different starting amounts of *Acanthamoeba* sp. + *A. asiaticus* 5a2 gDNA, 10, 1, and 0.1 ng, were subjected to qPCR assays targeting **(a)** Aasi_1074 and **(b)** Aasi_1396, using different annealing temperatures from 55 to 72 °C, and the Cq values were plotted against temperature. For better visibility, x and y axis were reversed in the plots so that a bend of the curves to the right indicates a decrease in amplification efficiency. **(c)** and **(d)** melting curves performed after the qPCR runs. Threshold is indicated by a horizontal green line, and threshold values are given. Melt peaks for specific PCR products are observed for approximately 79 °C in both assays, while the NTC (red traces) results in a shifted peak with one or two vertices at a different melting temperature.

### 3.4.3. Primer concentrations

Since the optimal concentration of the forward primer does not necessarily have to be the same as for the reverse primer, all possible combinations of 100, 200, 300, 400, and 500 nmol $L^{-1}$ were evaluated for both assays. As in the optimisation of annealing temperature, ideal primer concentrations will result in high amplification efficiencies and manifest themselves as lowest possible Cq values for the same starting template amounts. The obtained Cq values are presented in a scatterplot (Figure 3.10), where the size of the circles corresponds to the difference to the highest Cq value observed among all evaluated combinations of primer concentrations, which was the case for 100 nmol $L^{-1}$ of both forward and reverse primer. If a concentration of only 100 nmol $L^{-1}$ was employed for one of the primers, the Cq values were generally higher as in reactions where concentrations of at least 200 nmol $L^{-1}$ were used for both primers. Interestingly, for both assays, the usage of a low concentration of forward primer had a more pronounced effect than low concentrations of reverse primer. Because no significant difference was seen between all analysed scenarios of primer concentrations of 200 nmol $L^{-1}$ and higher, a combination of 200 nmol $L^{-1}$ forward and 200 nmol $L^{-1}$ reverse primer was selected for both assays. However, it has to be considered that all observed differences are actually small, ranging within less than one Cq value. The maximum difference to the highest Cq value was 0.86 for the assay targeting Aasi_1074 and 0.84 for the assay targeting Aasi_1396.
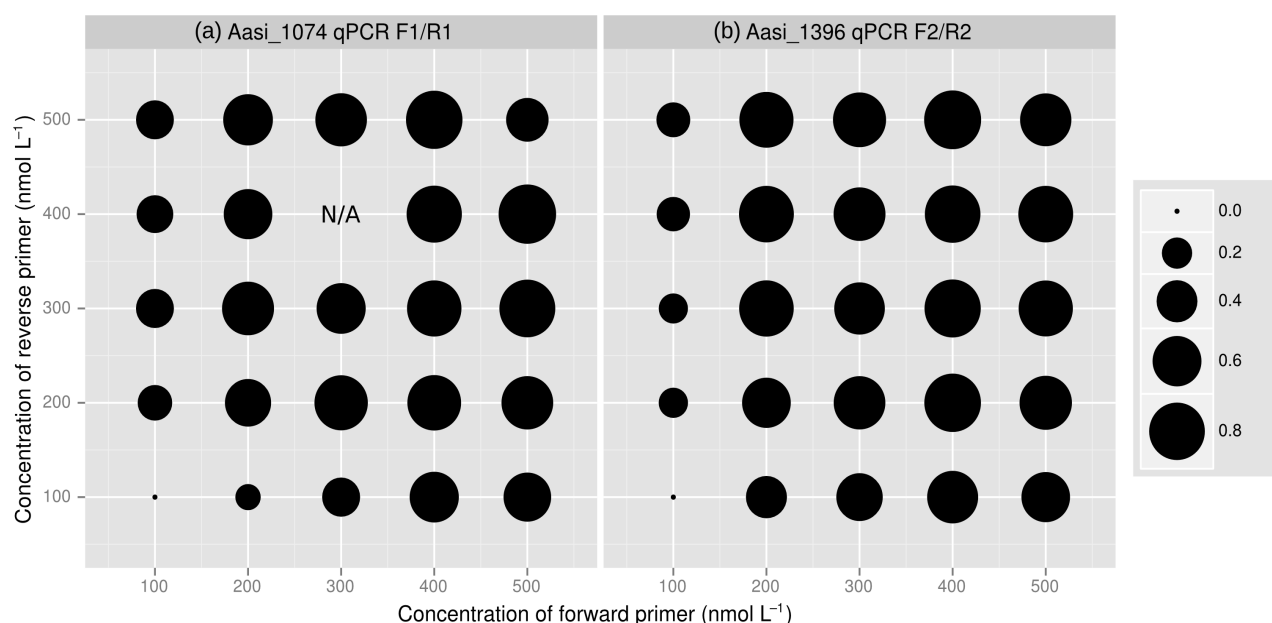


**Figure 3.10** Primer concentrations were optimised for both qPCR assays, **(a)** Aasi_1074 and **(b)** Aasi_1396, using *Acanthamoeba* sp. + *A. asiaticus* 5a2 gDNA as template. Area of circles represents the difference to the highest observed Cq value for all analysed primer concentration combinations. The combination of 300 nmol $L^{-1}$ forward primer and 400 nmol $L^{-1}$ reverse primer could not be evaluated (N/A) for the Aasi_1074-targeted assay because of a technical failure of the qPCR cycler.

### 3.4.4. Evaluation of assay performance

Benchmarks for a well-optimised qPCR assay are a linear standard curve covering a broad dynamic range and high amplification efficiencies close to 100 %. Serial dilutions of DNA with defined

concentrations and/or target copy numbers serve as standards for the assessment of assay performance. Initially, gDNA isolated from a culture of of *Acanthamoeba* sp. infected with *A. asiaticus* was tried to be established as qPCR standard (Figure 3.11), since it was already available and had been successfully used for assay optimisation. However, gDNA standards proved to have several practical drawbacks. With pre-diluted gDNA stored at –20 °C for days or even weeks, no reliable standard curves could be produced (Figure 3.11a and b), and also with freshly prepared dilutions (Figure 3.11c and d), the results were of varying quality. Therefore, the switch was made to pCR-XL-TOPO® plasmids. An additional advantage of plasmids as qPCR standards is a reliable copy number determination, which facilitates an estimation of linear dynamic range and detection limit. For the final analysis of all cDNA samples for prophage tail sheath mRNA quantification, pCR-XL-TOPO® standards were used exclusively.
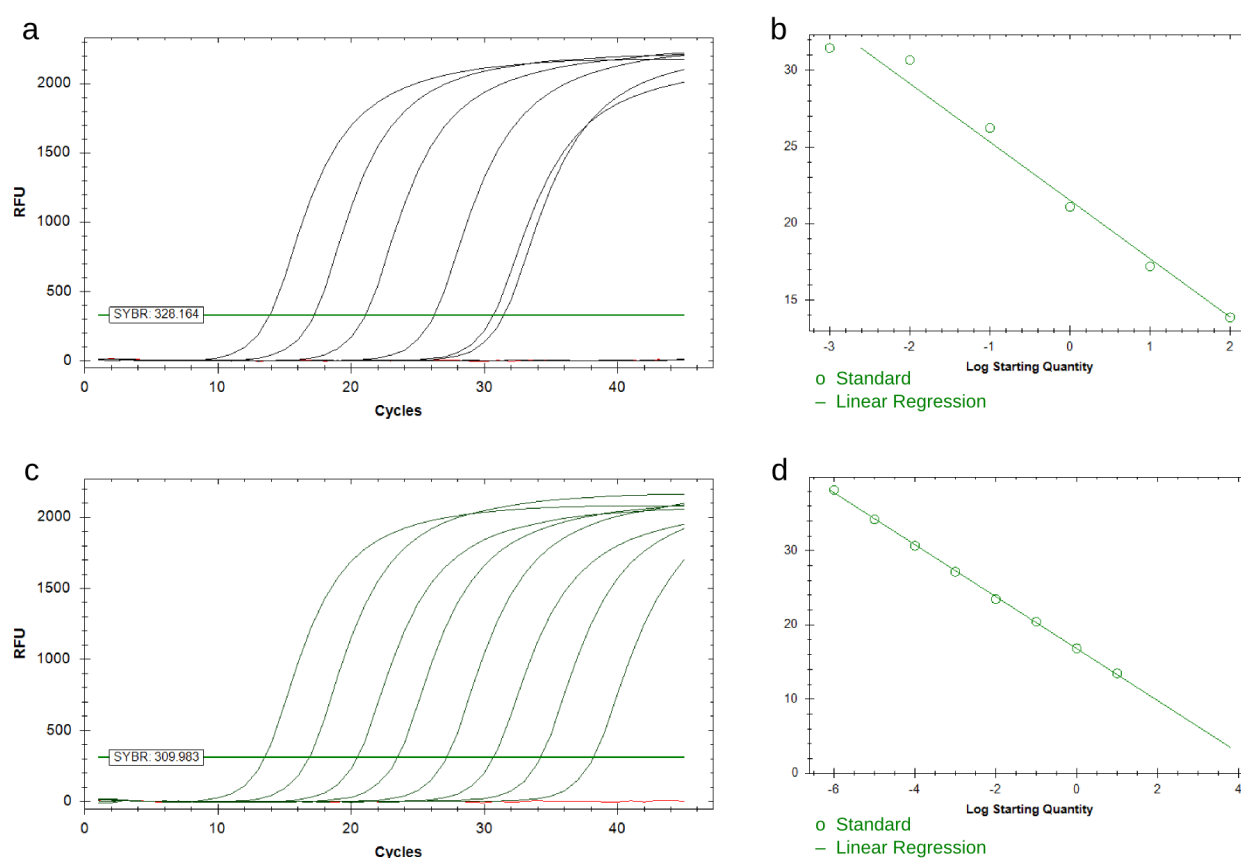


**Figure 3.11** Comparison of old and freshly prepared gDNA standard dilution series for the Aasi_1074 targeted assay. For standard curves, Cq values were plotted against starting template amounts. **(a)** and **(b)** amplification chart and standard curve with a gDNA dilution series stored at −20 °C for several days before qPCR. Threshold is indicated by a horizontal green line, and threshold values are given. Standards are not evenly spaced, and high dilutions are not amplified at all. **(c)** and **(d)** amplification chart and standard curve with a new dilution series prepared from concentrated gDNA immediately before qPCR.

### 3.4.4.1. Linear dynamic range

The ambit of starting template amounts for which accurate Cq values can be obtained and show a linear correlation to the template concentration is defined as the linear dynamic range of a qPCR assay. Linear dynamic range and qPCR efficiencies were determined by subjecting dilutions of pCR-XL-

TOPO® standards to both assays. Standards yielding fluorescence signals above threshold already during the first cycles of the qPCR were excluded from the analysis under the assumption that the starting template amounts were too high to gain reliable results. Towards the lower end of the dilution series, the range was restricted by the detection limit of the qPCR. Only dilutions for which all three technical replicates still gave a positive signal were considered for the analysis. The linear dynamic range extended from $1.2 \times 10^8$ to $1.2 \times 10^1$ copies for the assay targeting Aasi_1074 and from $1.5 \times 10^8$ to $1.5 \times 10^1$ copies for the assay targeting Aasi_1396, respectively. The mean Cq at the limit of detection (standard of lowest concentration within linear dynamic range) was 36.88 for the Aasi_1074 targeted assay and 36.87 for the Aasi_1396 targeted assay.

*3.4.4.2. qPCR efficiency*

qPCR efficiencies were calculated based on the slope of the linear regression of the Cq values obtained for all standards within linear dynamic range, plotted against starting template amounts (Figure 3.12). For the assay targeting Aasi_1074 (Figure 3.12a), an efficiency of 88.1 % (qPCR standard curve quality indicator: $R^2 = 0.999$) could be achieved, while for the assay targeting Aasi_1396 (Figure 3.12b), the efficiency was 87.6 % (qPCR standard curve quality indicator: $R^2 = 0.998$). For the relative quantification of a target gene normalised against one reference gene with two independent qPCR assays, it is recommended that both assays are comparable in their performance. As the efficiencies differed by only 0.5 %, and also linear dynamic range and mean Cq at the limit of detection were highly similar, this criterion was regarded as fulfilled.
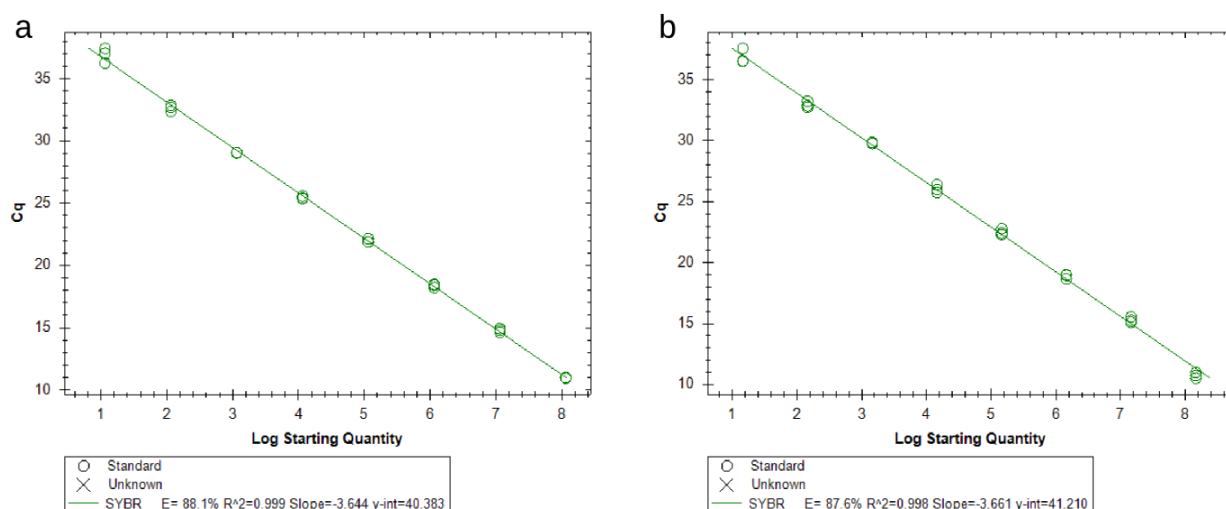


**Figure 3.12** Standard curves with pCR-XL-TOPO® standards. Cq values were plotted against starting template amounts, and qPCR efficiencies were determined by linear regression analysis. **(a)** Aasi_1074 targeted assay. qPCR efficiency = 88.1 % (qPCR standard curve quality indicator: $R^2 = 0.999$) **(b)** Aasi_1396 targeted assay. qPCR efficiency = 87.6 % (qPCR standard curve quality indicator: $R^2 = 0.998$).

## 3.4.5. Inhibition testing

Like any enzymatic reaction, reverse transcription of RNA and the qPCR reaction itself can be interfered by the presence of a variety of endogenous or exogenous inhibitors in RNA extracts. One selected sample from time point 140 h *p.i.* was tested for inhibition in these two steps with the Aasi_1396 targeted qPCR assay. It is commonly recommended to apply equal template amounts to

cDNA synthesis, but the extraction yield was different for individual samples, requiring an adjustment by dilution to the same concentration for reverse transcription. Consequently, also the amount of possible inhibitory substances would be reduced to varying degrees. The sample from 140 h *p.i.* was chosen because it had the lowest RNA concentration after DNase treatment, thus resulting in relatively high amounts of possible inhibitors in the reverse transcription reaction mix. Due to restricted availability of time and resources, no additional inhibition testing was done for the second qPCR assay.

### 3.4.5.1. RNA dilution series

Inhibition of the reverse transcription was tested by applying different amounts of 140 h *p.i.* RNA to the reverse transcription and subsequently analysing constant amounts of the resulting cDNA with qPCR. The qPCR results of the RNA dilution series are presented in Figure 3.13. A linear correlation between the amount of RNA applied to reverse transcription and the detected copy numbers was observed (linear regression quality indicator: $R^2 = 0.982$). Only 5 μL of undiluted RNA as template for reverse transcription showed clear signs of inhibition. The number of detected copy numbers was 18.5 ± 5.5 copies (ng RNA)$^{-1}$ (29 % RSD) for the undiluted sample and thereby much lower than for the first dilution, for which 60.5 ± 4.3 copies (ng RNA)$^{-1}$ (7 % RSD) were detected. In absence of inhibitory substances, the normalised detected copy numbers should theoretically be the same for all dilutions. This sample was therefore considered as an outlier and excluded from linear regression analysis. The average Aasi_1396 copy numbers, calculated without outliers, were 58.5 ± 31.7 copies (ng RNA)$^{-1}$ (54 % RSD). For reverse transcription of small RNA amounts, the normalised Aasi_1396 copy numbers were clearly below average (24.2 ± 0.9 copies (ng RNA)$^{-1}$ (4 % RSD) and 11.7 ± 1.0 copies (ng RNA)$^{-1}$ (9 % RSD) for $2.1 \times 10^{-2}$ and $6.9 \times 10^{-3}$ ng RNA, respectively). This indicates that the efficiency of the cDNA synthesis was slightly better with higher template amounts, although all evaluated RNA dilutions fit into the recommended range for the cDNA synthesis kit. For the final protocol, reverse transcription of 5 μL of RNA adjusted to a concentration of 100 ng μL$^{-1}$ was regarded as suitable.
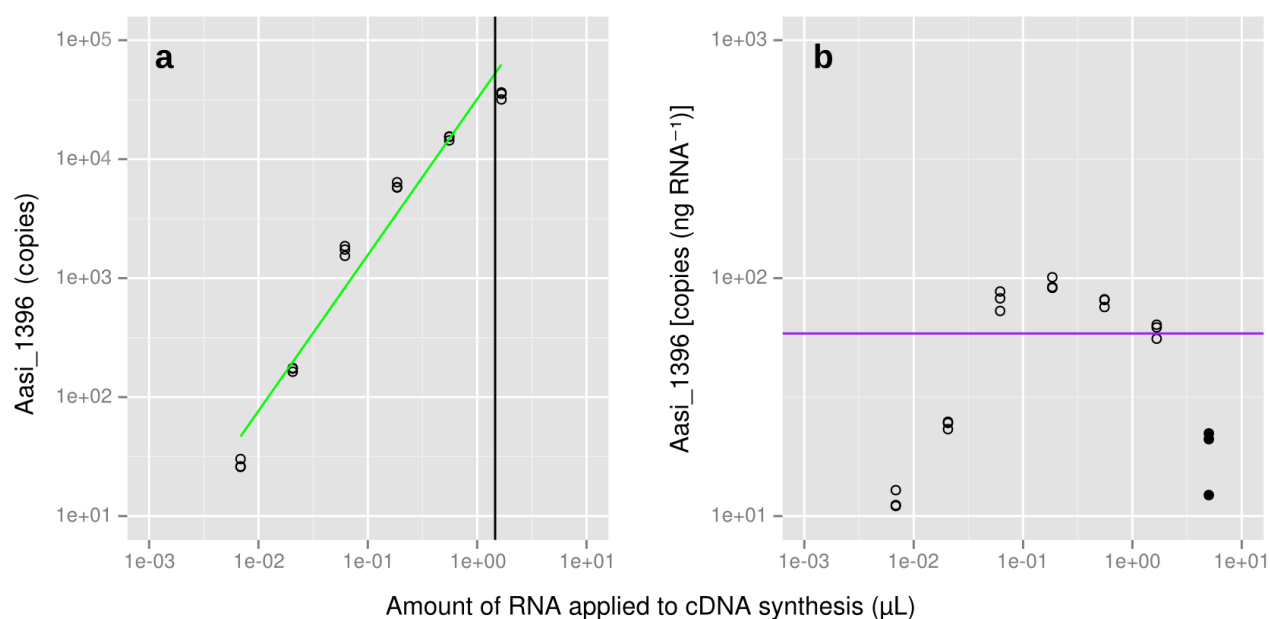
**Figure 3.13** RNA dilution series for inhibition testing on RT level. Different amounts of DNA-free RNA from time point 140 h *p.i.* (concentration: 342.5 ng μL⁻¹) were reverse transcribed, and 2.5 μL out of 25 μL cDNA solution were analysed with the qPCR assay targeting Aasi_1396. The data is plotted in two different ways: **(a)** absolute copy numbers and **(b)** copy numbers normalised against 1 ng of reverse transcribed RNA. For linear regression analysis of Aasi_1396 copy numbers against the reverse transcribed volume of RNA (shown as green line), undiluted RNA was excluded and is also not shown in the left plot. In the right plot, the horizontal purple line indicates the average Aasi_1396 copy number. qPCR results of undiluted RNA are shown as black filled circles, but were not included in the calculation of average copy numbers. Vertical black lines represent a RNA concentration of 100 ng μL⁻¹, which was used for reverse transcription in the final experimental pipeline. qPCR efficiency: 95.0 %. Dilution series linear regression quality indicator: $R^2 = 0.982$.

### 3.4.5.2. cDNA dilution series

Reaction components from the reverse transcription in the cDNA solution can have an inhibiting effect on qPCR performance. By diluting the cDNA solution and applying smaller amounts to the qPCR, the influence of potential inhibitors can be reduced. The manual for the SuperScript™ III First-Strand Synthesis System for RT-PCR (Invitrogen) recommends to use 2 μL of the cDNA solution for a PCR reaction volume of 50 μL. To test for inhibition of the qPCR reaction, a dilution series of cDNA synthesised from 5 μL undiluted RNA from the same sample as used in the RNA dilution series (140 h *p.i.*) was analysed with the Aasi_1396 targeted assay. Figure 3.14 shows the qPCR results of the cDNA dilution series. Except for the highest analysed amount of cDNA, a good linear correlation between the amount of cDNA applied to qPCR and Aasi_1396 copy numbers was seen (linear regression quality indicator: $R^2 = 0.993$), suggesting that no inhibitors were present or at least had no significant effects within this range. For the highest cDNA template amount, 2.5 μL of undiluted solution in 25 μL qPCR reaction (10 % of the total reaction volume), a normalised copy number of 37.0 ± 10.9 copies (ng RNA)⁻¹ (29 % RSD) was calculated. Compared to the average normalised Aasi_1396 copy number calculated without this outlier, 108.6 ± 11.8 copies (ng RNA)⁻¹ (11 % RSD), it was assumed that such high cDNA solution amounts as 10 % of the reaction volume had an inhibiting effect on the qPCR. For the final qPCR protocol, 0.5 μL (5 μL of a 10-fold dilution) of cDNA in 50 μL reaction volume were used.
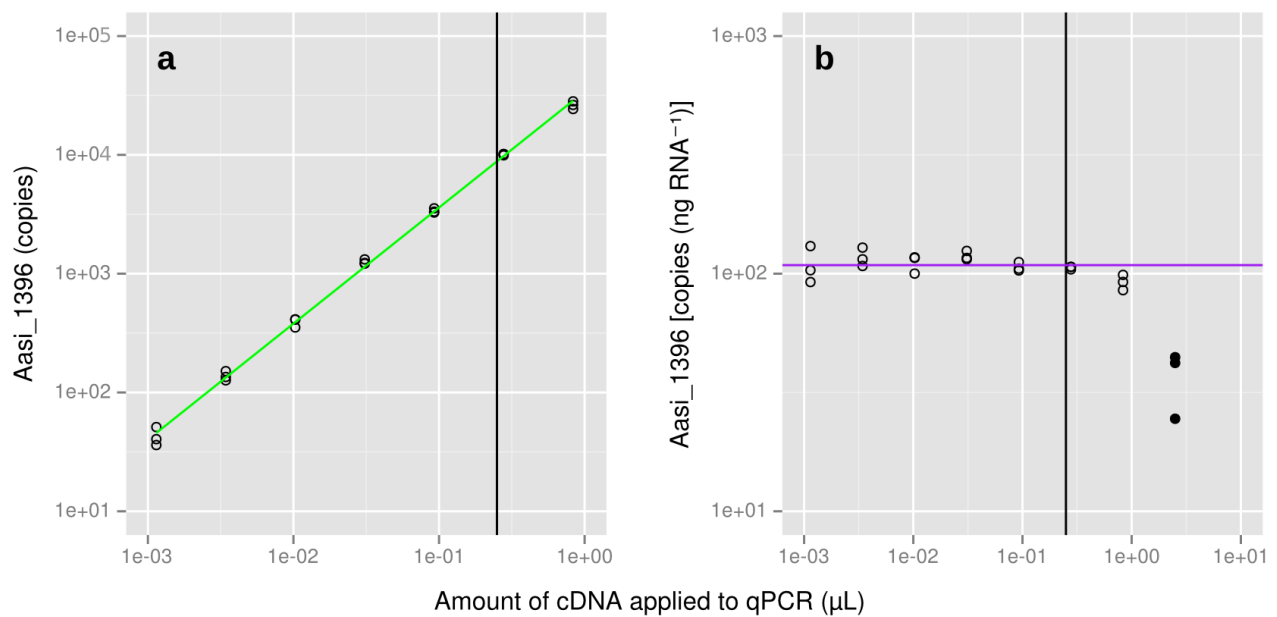
**Figure 3.14** cDNA dilution series for inhibition testing on qPCR level. 5 ng of DNA-free RNA from time point 140 h *p.i.* were reverse transcribed. Different amounts of the cDNA solution were analysed with the qPCR assay targeting Aasi_1396. The data is plotted in two different ways: **(a)** absolute copy numbers and **(b)** copy numbers relative to 1 ng of reverse transcribed RNA. Undiluted cDNA was excluded from linear regression analysis of Aasi_1396 copy numbers against the amount of cDNA applied to qPCR and is not shown in the left plot. In the right plot, the average number of Aasi_1396 copies (calculated without undiluted cDNA) is represented by a vertical purple line. qPCR results of undiluted cDNA are shown as black filled circles. Vertical black lines represent a 10-fold dilution of the cDNA solution, which was used in the final experimental pipeline. qPCR efficiency: 95.0 %. Dilution series linear regression quality indicator: 0.993.

## 3.5. Relative quantification of prophage tail sheath mRNAs

For the investigation of the expression level of one representative component of the *A. asiaticus* prophage, the prophage tail sheath gene, throughout an infection cycle, RNA was isolated at four different time points (extracellular, infectious *A. asiaticus* and 12, 68, and 140 h *p.i.*). Relative mRNA amounts were determined by RT-qPCR using the two newly established qPCR assays targeting the prophage tail sheath, Aasi_1074, and the beta-subunit of the RNA polymerase, Aasi_1396, as reference gene. After isolation of RNA from approximately 50 mL *Acanthamoeba* sp. cultures, 10 µg of the RNA extracts were subjected to DNase I digestion, followed by ethanol precipitation for RNA purity improvement. DNA-free RNA was reverse transcribed (RNA template amount: 500 ng in 25 µL total reaction volume) in technical triplicates, and 0.5 µL of cDNA solution were applied to qPCR in 50 µL PCR reaction volume. To assess and, if necessary, compensate for inter-plate variation, one standard ($10^{-2}$) was amplified with the Aasi_1074 specific primers Aasi_1074 qPCR F1/Aasi_1074 qPCR R1 in technical triplicates on each qPCR plate. Since no significant difference between the corresponding Cq values in individual runs was observed (two sample t-test; t(4) = 0.5267; p-value = 0.6262), no data correction was done. qPCR results are shown in Figure 3.15.

NTCs were included in reverse transcription and qPCR to control for introduction of exogenous DNA in these steps, which would potentially lead to an alteration of the overall qPCR results. For the reverse-transcription NTCs, amplification was never observed. With the assay targeting Aasi_1074, one out of two qPCR-NTCs (prepared with PCR water used for dilutions of standards and samples and the qPCR mastermix; red traces in Figure 3.15) was quantified with an average Cq value of 31.71 ± 0.83 (3 % RSD), while the other qPCR-NTC (prepared with purchased RNase-free water used for RNA work; traces not shown) was amplified only on one plate with a relatively high Cq of 39.44 and remained negative in other qPCR runs. However, the corresponding melt curve analysis revealed shouldered and shifted peaks, indicating that no full length products were amplified. Additionally, in the Aasi_1396 targeted assay, neither of the two NTCs showed a signal. It was inferred that the observed amplification was most probably the result of unspecific PCR products, like primer dimers, and was therefore considered as of no relevance. In both assays, the no-target control (cDNA reverse transcribed from RNA isolated from symbiont-free *Acanthamoeba* sp.) was not amplified at all (orange traces in Figure 3.15). For all samples, no-reverse transcriptase controls (reverse transcription reactions with RNA, but without enzyme; purple traces) were applied to both assays as well. A large fraction of the no-reverse transcriptase controls was not amplified, and those where amplification occurred were quantified in the same range as the lowest standard, close to or even beyond detection limits of the qPCR. When looking at the corresponding melt curves, it can be seen that the PCR products are specific, but the calculated starting template amounts are so low that any influence on the qPCR results is very unlikely.

Relative amounts of prophage tail sheath transcripts were calculated as the ratio of absolute Aasi_1074 copy numbers normalised against absolute Aasi_1396 copy numbers (Figure 3.16). The highest Aasi_1074 to Aasi_1396 transcript ratio was observed for extracellular, infectious intermediates of *A. asiaticus*, and the lowest relative level of Aasi_1074 gene expression was reached at the intracellular stage of *A. asiaticus* at 68 h *p.i.* (231-fold lower ratio than for extracellular *A. asiaticus*). During the attachment of *A. asiaticus* to its *Acanthamoeba* host at 12 h *p.i.*, the Aasi_1074 mRNA level was still four times higher than at 68 h *p.i.*, but relatively low compared to the extracellular stage of *A. asiaticus* (53-fold lower ratio of absolute copy numbers). In the late phase of the infection, at 140 h *p.i.*, the ratio of Aasi_1074 to Aasi_1396 mRNAs was starting to increase again (approximately 8-fold lower

ratio than for extracellular *A. asiaticus*, but already 30-fold higher than at 68 h *p.i.*). Taken together, these observations suggest a biphasic regulation of the expression of Aasi_1074 at the transcriptional level. While only a low level of Aasi_1074 mRNAs is present in the cells during intracellular replication of *A. asiaticus*, the relative amount of these mRNAs is significantly increased in late stages of the infection and in the extracellular, infectious intermediates.
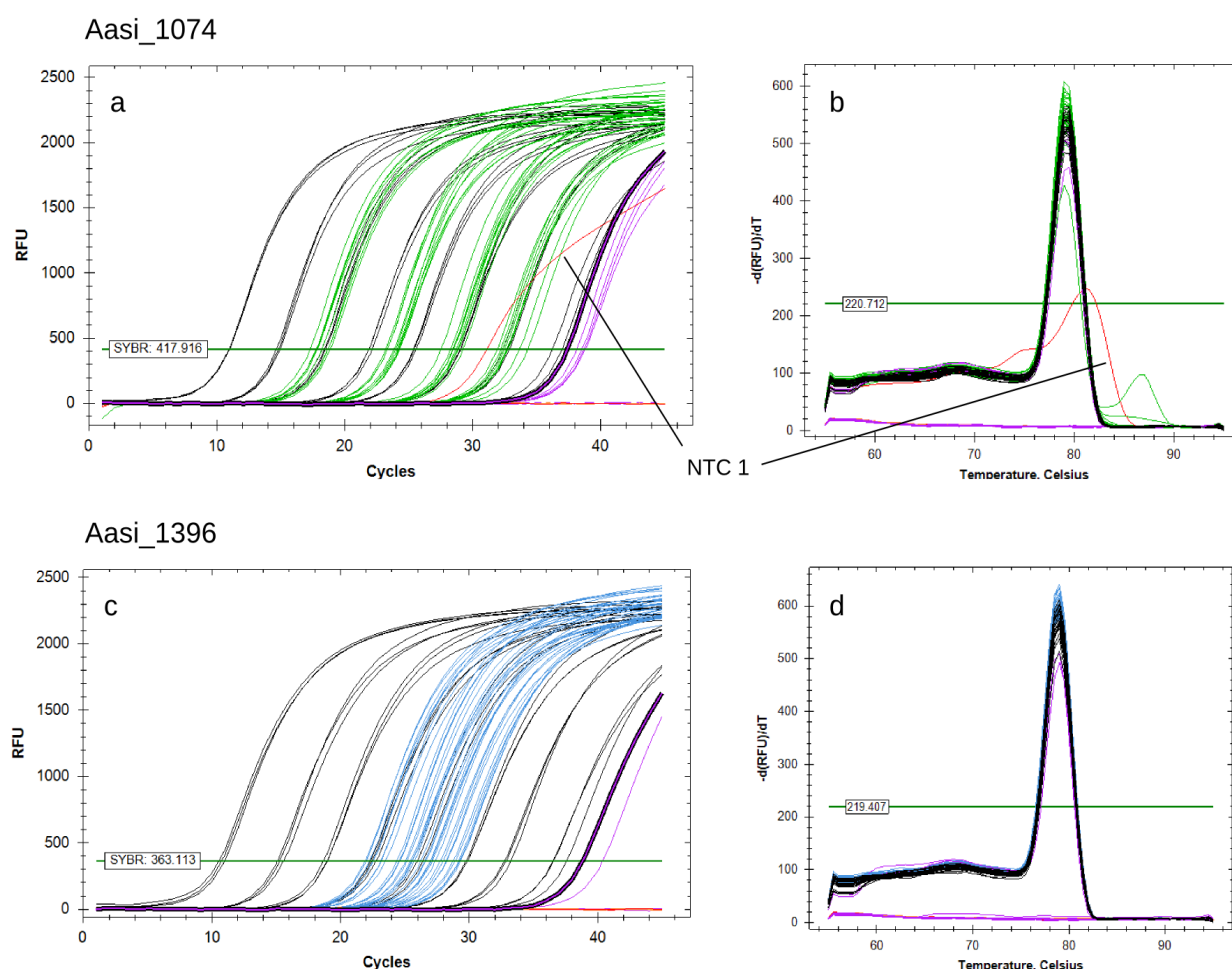


**Figure 3.15** qPCR results. Traces of standard dilution series (black), cDNA samples (green and blue for Aasi_1074 and Aasi_1396, respectively), qPCR NTCs (red), no-target controls (orange) and no-reverse transcriptase controls (purple) are shown. Threshold is indicated by a horizontal green line, and threshold values are given. $-d(RFU)\,dT^{-1}$ in melt curves is the negative first derivative of relative fluorescence units versus temperature. **(a)** traces and **(b)** melt curves of qPCR assay targeting Aasi_1074. qPCR efficiency = 88.1 % (qPCR standard curve quality indicator: $R^2$ = 0.999). **(c)** traces and **(d)** melt curves of qPCR assay targeting Aasi_1396. qPCR efficiency = 87.6 % (qPCR standard curve quality indicator: $R^2$ = 0.998). The no-reverse transcriptase controls with the lowest Cq values are highlighted in (a) and (c) (indicated by a thicker line).
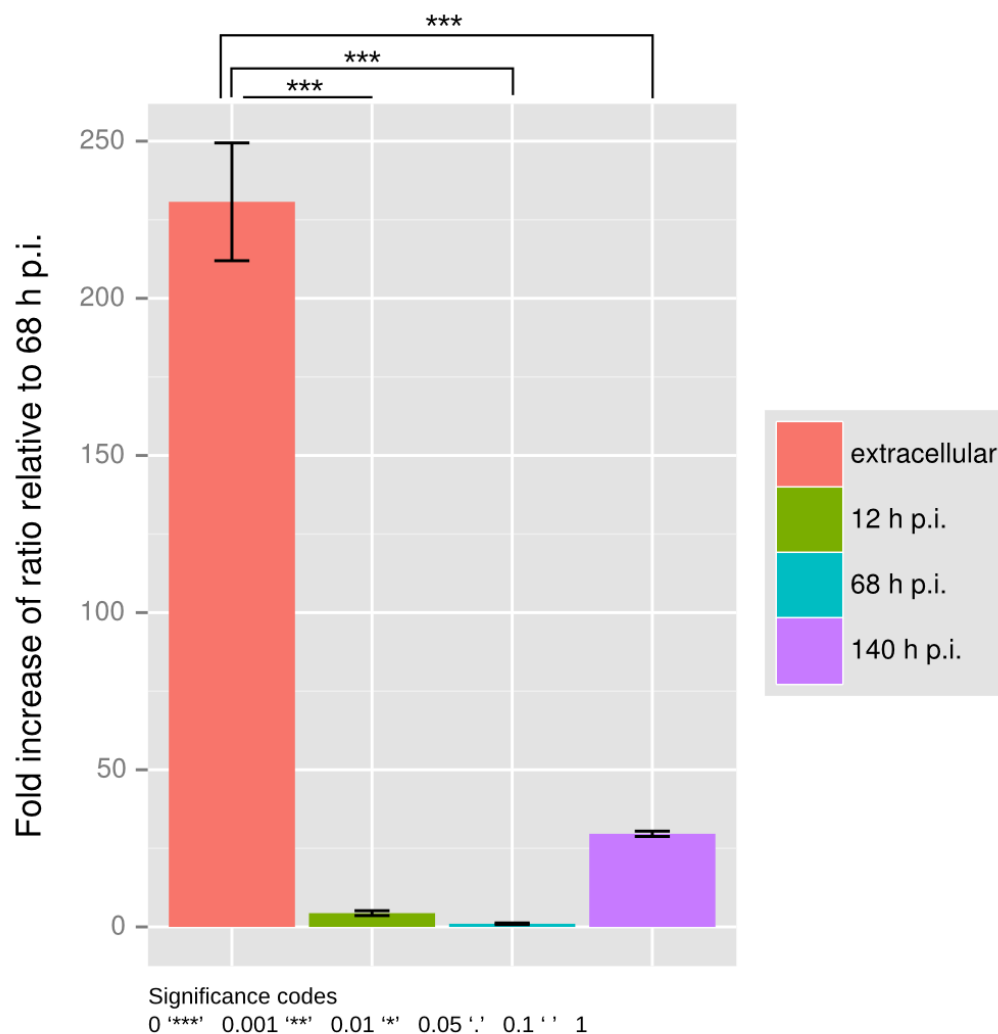
**Figure 3.16** Relative amounts of Aasi_1074 transcripts were plotted as the fold increase of Aasi_1074 to Aasi_1396 ratios relative to time point 68 h *p.i.*, where the lowest ratios were observed. In extracellular *A. asiaticus* (red), the Aasi_1074 to Aasi_1396 ratio was 231-fold higher than at 68 h *p.i.* (turquoise), while at 12 h *p.i.* (green), only a 4-fold increased ratio and at 140 h *p.i.* (purple), a 30-fold higher ratio was observed. Error bars are standard deviations of biological replicates. Statistical significance was determined by one-way ANOVA and post-hoc Tukey's range test.

Eventually, the qPCR products of all standards and negative controls and one replicate of each sample were analysed using agarose gel electrophoresis. Gel images for the assays targeting Aasi_1074 and Aasi_1396 are shown in Figure 3.17a and b, respectively. The results from the gel electrophoresis correspond with the data obtained from the qPCR itself. All standards except the lowest and all samples applied to the gel showed the same band, coinciding with the length of the targets. Only for the standards with lowest concentrations, which contained less than 2 target copies and were not amplified in the qPCR as well, no target bands were observed in both assays. In the Aasi_1074 targeted assay, a signal was recorded for the qPCR-NTCs, but melt curve analysis indicated unspecific products, which could be further confirmed by the absence of target bands on the gel. For some of the no-reverse transcriptase controls, gel electrophoresis revealed the presence of specific PCR products, which is also in accordance with the qPCR results, where the identical replicates of the same samples were quantified close to or even beyond the limit of detection of the qPCR.
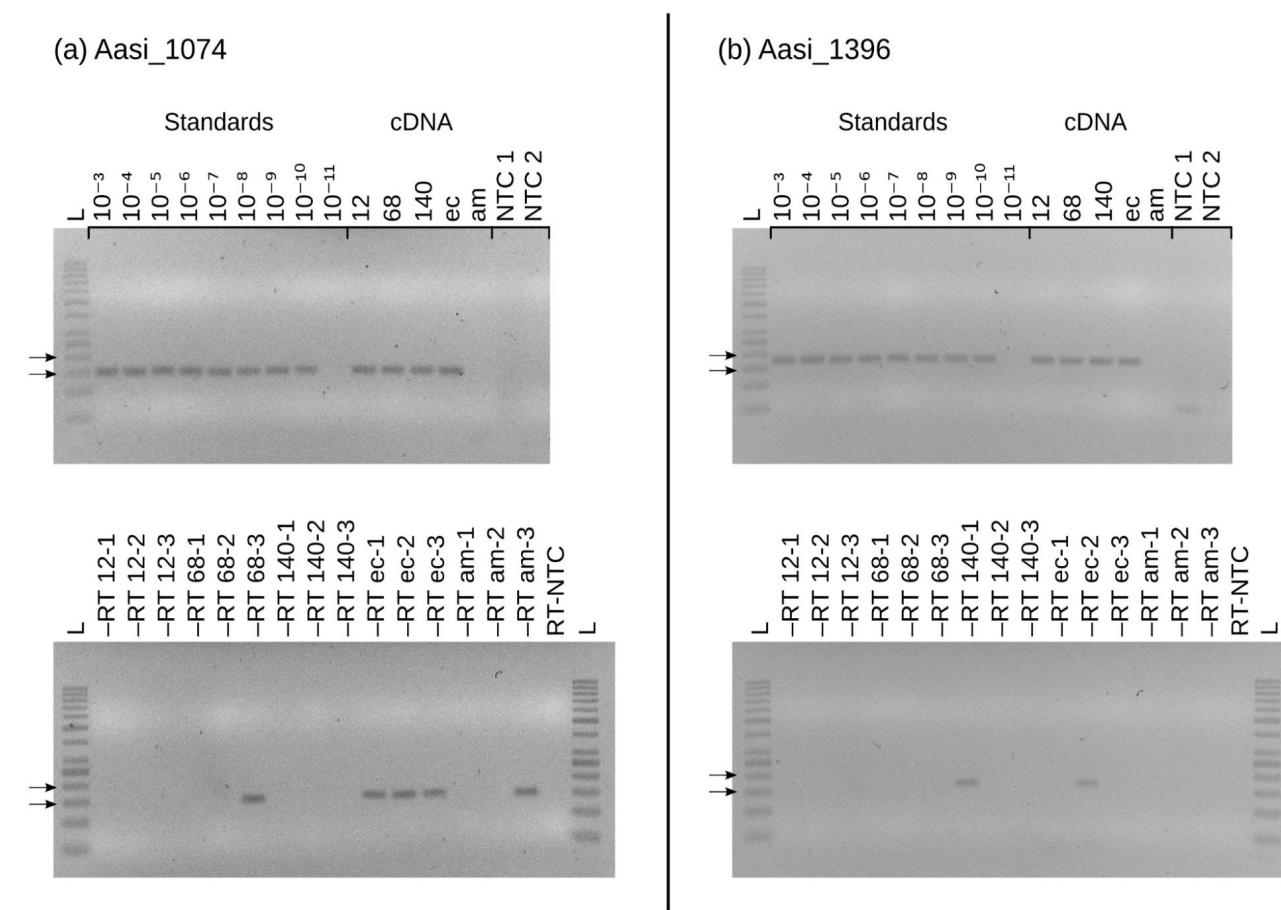
**Figure 3.17** Agarose gel electrophoresis of qPCR products (2.5 % agarose, 120 V, 60 min). *L* GeneRuler™ 50 bp DNA Ladder, arrows are 150 and 200 bp; *$10^{-3}$–$10^{-11}$* standard dilution series; *12, 68, 140* cDNA samples from time points 12, 68, and 140 h *p.i.*; *ec* cDNA from extracellular A. asiaticus; *am* no-target control: cDNA from symbiont-free *Acanthamoeba* sp.; only one replicate per sample was loaded on the gel; *NTC* no-template control of the qPCR assay (*NTC 1* PCR grade water, *NTC 2* commercially available RNase-free water used for RNA work); −*RT* no-reverse transcriptase controls, sample and number of biological replicate (1-3) are indicated with the same abbreviations as for cDNA; *RT-NTC* no-template control of the reverse transcription step. qPCR efficiencies and standard curve quality indicators are given in figure 3.15. **(a)** Aasi_1074 targeted qPCR assay. Target bands have a size of 141 bp. **(b)** Aasi_1396 targeted qPCR assay. Target bands are 167 bp. Bands at the bottom of some NTC lanes most likely represent primer dimers.

## 3.6. Ultrastructure of *A. asiaticus*

Transmission electron microscopy (TEM) images of *A. asiaticus* in its extracellular stage were already available from a previous study (unpublished material by Thomas Penz, personal communication; Tsao, 2011). During this diploma thesis, samples from defined infection time points were prepared for additional microscopic analysis to gain further insights into the ultrastructure of *A. asiaticus*. Besides standard TEM, cryo-electron microscopy (cryo-EM) of extracellular *A. asiaticus* and a phage sheath preparation was done for improved visualisation of the prophage-like intracellular structures.

### 3.6.1. Attachment of *A. asiaticus* to amoebal host cells

In samples taken at an early stage of the infection cycle, 17 h *p.i.*, during the attachment of *A. asiaticus* to its prospective host, cytoplasmic fibril-like structures could be detected microscopically, which most probably represent the prophage tail sheath (Figure 3.18a). Similar structures were already observed

in extracellular stages of *A. asiaticus* in the beforementioned study. However, only in a very small fraction of all analysed cells, such prophage tail sheath-like structures were found. This can be explained by the required sample preparation for TEM, which involves the preparation of thin sections that allow only the visualisation of one randomly selected plane of a three-dimensional sample. Structures located in a different region of the cell will always remain undetected. For the same reason, it is difficult to accurately determine the dimensions of the presumable prophage tail sheath. The length of the observed structures was at least 200 nm, and a bundle of several prophage tail sheaths was apparently assembled and anchored on a base plate.
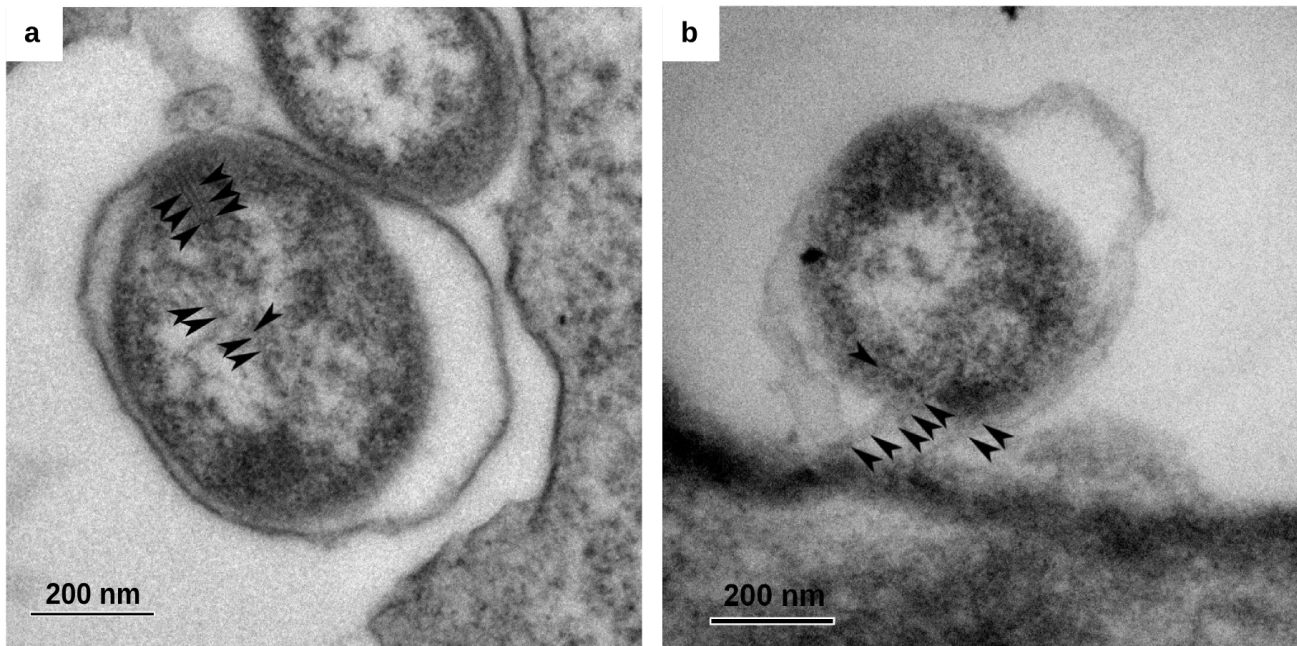


**Figure 3.18** Transmission electron microscopy images of *A. asiaticus* during attachment to the *Acanthamoeba* host at 17 h *p.i.* **(a)** Arrowheads mark cytoplasmic, fibril-like structures which most likely represent the prophage tail sheath assembled in bundles and anchored to the inner membrane. **(b)** Prophage tail-like structures extending on the outside of an *A. asiaticus* cell towards the cell membrane of the *Acanthamoeba* host. Images were recorded by Dr. Rok Kostanjšek (University of Ljubljana).

For some *A. asiaticus* cells located close to the surface of amoebal cells, very faint, elongated structures were seen (Figure 3.18b) that extended outside the bacterial cell and seemed to be in contact with the eukaryotic host cell membrane. These thin structures could represent parts of the prophage-like apparatus in extended conformation.

## 3.6.2. Intracellular prophage-like structures

Cryo-EM has the advantage over conventional TEM techniques that no sectioning is required during sample preparation. Images are recorded from a plunge-frozen three-dimensional sample so that intracellular structures can be conserved *in situ*. Cryo-EM was applied for visualisation of the intracellular prophage-like structures in extracellular *A. asiaticus*. Images are presented in Figure 3.19. As with standard TEM, fibril-like structures resembling the prophage tail sheaths were detected assembled in bundles and seemed to be anchored on a base plate, which was located close to the inner

cell membrane of *A. asiaticus* (Figure 3.19a). In contrast to standard TEM, prophage-like structures were found in a large proportion of all analysed cells, since the technique involves image recording as a tilt series for visualisation of different parts of the same sample. Figure 3.19b and c show two images recorded from the same sample showing two *A. asiaticus* cells, but at different angles.
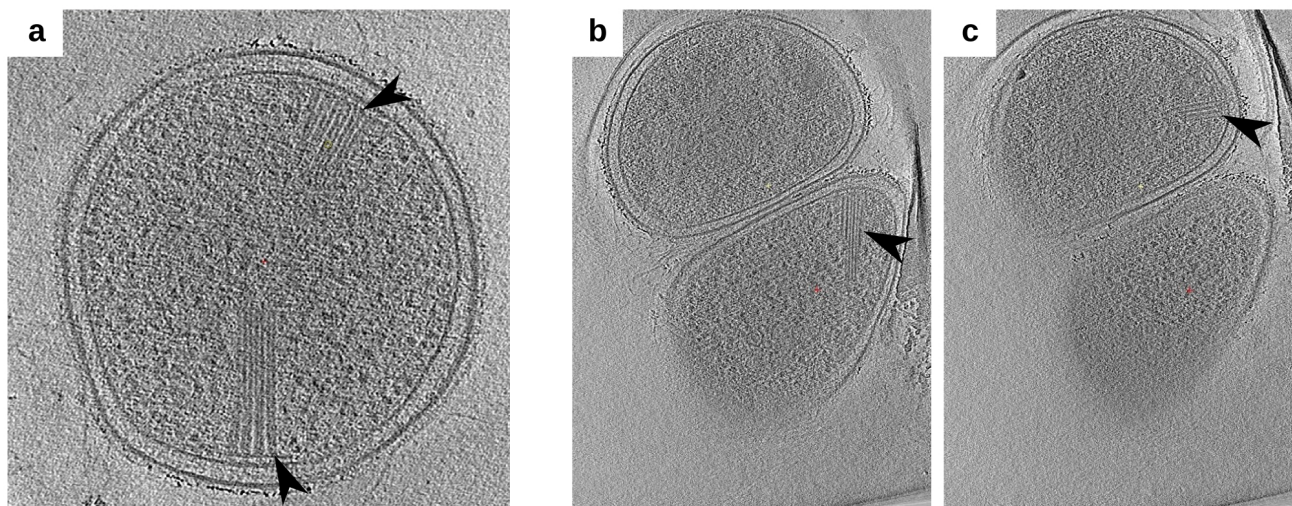


**Figure 3.19** Cryo-electron microscopy images of extracellular *A. asiaticus*. Cytoplasmic, fibril-like structures were detected intracellularly, which appeared in bundles and anchored to the inner cell membrane. Sample preparation, staining, plunge-freezing, and image recording were done by Mag. Karin Aistleitner (Department of Microbial Ecology, University of Vienna) and Dr. Martin Pilhofer (California Institute of Technology).

### 3.6.3. Microscopic analysis of sheath purification

Negative staining and subsequent imaging of purified prophage tail sheaths with conventional TEM (Figure 3.20a and b) revealed straight, hollow, tubular structures with a minimal length of 200 nm and a diameter of 4–6 nm. In the final microscopic analysis with cryo-EM (Figure 3.20 c and d), images recorded at different angles showed a striped pattern on the outside of the tubular structures, suggesting a helical organisation of the prophage tail sheath.

**Figure 3.20 (a)** and **(b)** negative staining and **(c)** and **(d)** cryo-electron microscopy images of purified prophage tail sheaths. Images were recorded by Dr. Martin Pilhofer (California Institute of Technology).
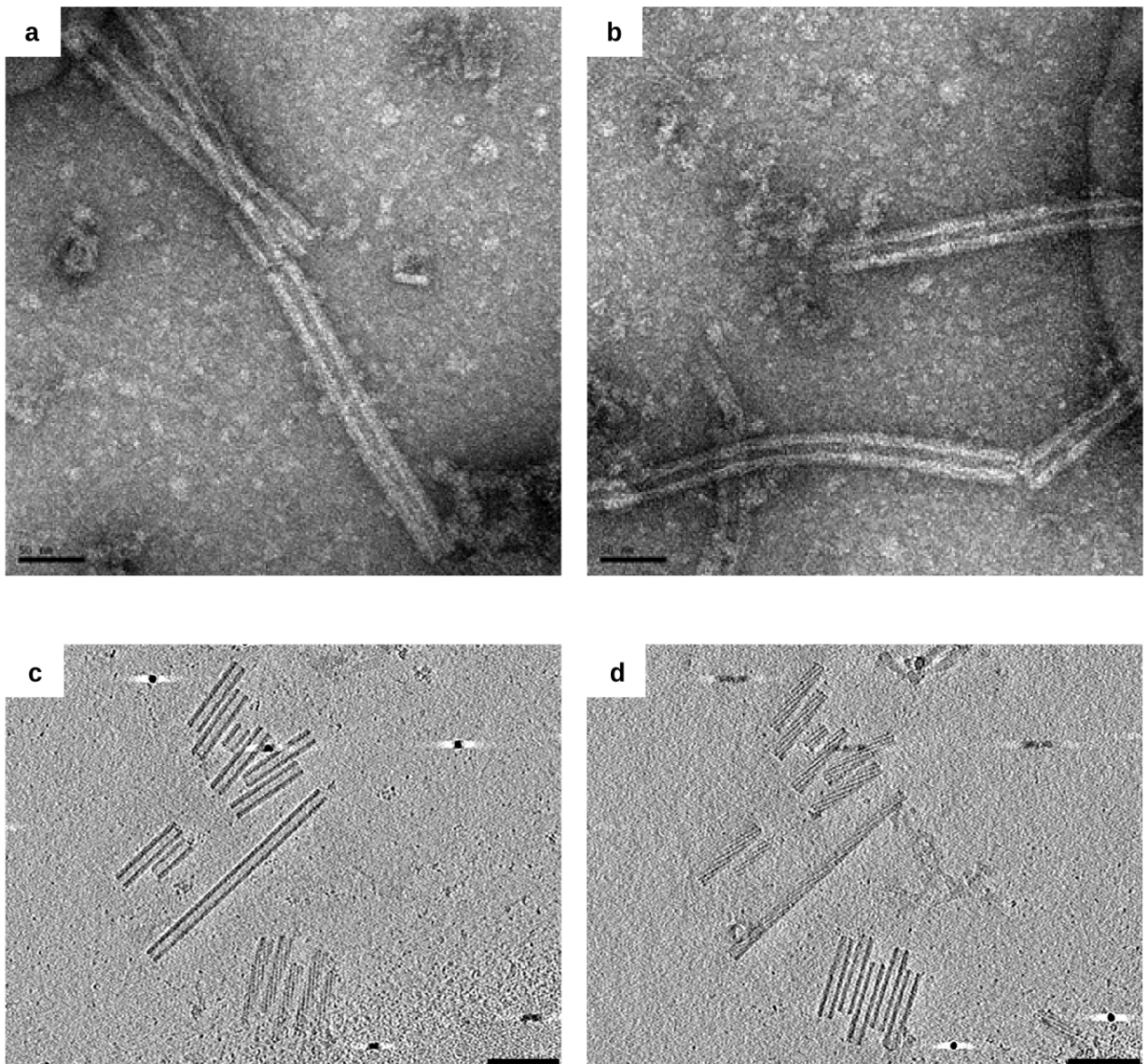
# Chapter 4. Discussion

## 4.1. Heterologous expression of selected afp proteins

To establish the link between selected proteins from the antifeeding prophage (afp)-like gene cluster of *Amoebophilus asiaticus* and fibril-like cytoplasmic structures discovered microscopically in extracellular infection intermediates, the prophage tail sheath (Aasi_1074) and VgrG homologue (Aasi_1080) were cloned for heterologous protein expression in *E. coli*. The long-term goal was to produce specific antibodies for immunofluorescence, thus allowing detection and intracellular localisation of the proteins. An essential prerequisite for the production of antibodies is that the target proteins are available in their native conformation and functional. This presupposes that the expression vector contains the insert in full length and correct orientation, without any frame shift mutations or base substitutions. Frame shift mutations would cause a completely different translation than the intended product by changing the reading frame, which potentially shifts also the stop codon and leads to premature or delayed abortion of the translation. In any case, the resulting translated product is most likely not functional. Base substitutions may seem to have less dramatic effects at first view, but still they can also lead to conversion of an amino acid codon into a stop codon (nonsense mutation), which causes an early abortion of the translation and truncation of the protein. Apart from this, single base substitutions can at least affect the functionality of the translated protein by changing the meaning of a codon to a different amino acid (missense mutation). Depending on the biochemical properties of the one amino acid being replaced and the other amino acid being incorporated instead of it, the consequences of such a mutation can be very different. If the properties of the two amino acids are largely identical, the protein may even retain its functionality, however, a decrease or even loss of function is equally possible, and it is difficult to predict what will be the case. Ultimately, in a silent mutation, the base exchange does not alter the codon meaning so that the same amino acid as in the original sequence will be incorporated. Although this does not change the functionality of the protein, the expression level can at least be affected.

With $2.2 \times 10^{-5}$ errors per nt per PCR cycle, the error rate of the commonly used standard recombinant *Taq* Polymerase is relatively high (Tindall & Kunkel, 1988). The probability for it to work flawlessly for the amplification of Aasi_1074 and Aasi_1080, which both have a length over 1500 nt, is rather low. Therefore, different commercially available high-fidelity polymerases were chosen for the amplification of the target sequences. Additional proofreading activity of the polymerase, or enzyme mix, can further reduce the risk for undesired errors during PCR. Amplification with Thermo Scientific's High Fidelity PCR Enzyme Mix, which consists of a mixture of standard *Taq* DNA Polymerase and a thermostable polymerase with proofreading activity and (according to the manufacturer's indications) has a four times lower error rate than standard *Taq* DNA Polymerase, was not successful. The reasons for this failure are unclear; since a parallel control reaction with standard *Taq* polymerase did work, it was assumed that the enzyme mix might have been decrepit due to long and/or inappropriate storage. The second high-fidelity polymerase used in this study, TaKaRa™ Ex Taq™ DNA Polymerase (TaKaRa Biotechnology), is also reported to have a 4.5× lower mutation rate than standard recombinant *Taq* DNA Polymerase, combined with an additional 3′→5′ proofreading activity for improved fidelity. With this polymerase, PCR products for Aasi_1074 were obtained (the amplification of Aasi_1080 was not attempted) and cloned into pET-21b and pGEX-4T-3. Sequencing of two clones from each expression vector revealed that the inserts all had one or two base substitutions which altered the codon meaning to a different amino acid. Notwithstanding the

# DISCUSSION

supposedly low error rate of the TaKaRa™ Ex Taq™ DNA Polymerase, base substitutions can and will happen. Depending on the PCR cycle in which they occur, the fraction of erroneous copies can vary in a broad range and may still allow successful cloning of the target gene. In the case of Aasi_1074, however, all sequenced pET-21b and pGEX-clones contained errors. One possible explanation might be that the prophage tail sheath exhibits such a high degree of toxicity that this even affects the propagation of pCR-TOPO-XL® plasmids in *E. coli*, although only low levels of expression occur in this cloning step. This would promote the selection for plasmids with defective inserts and translation products with reduced functionality. Although the available expression vectors (Aasi_1074, amplified with TaKaRa™ Ex Taq™ DNA Polymerase, in pET-21b and pGEX-4T-3) all contained base substitutions and did not meet the high requirements for the production of antibodies, heterologous expression of the faulty proteins was attempted in *E. coli* BL21. With both vectors, the expression of a protein of the correct size could be achieved. Nevertheless, the mutations represent a considerable element of uncertainty. Based only on the amino acid sequence, any predictions of structural and/or functional changes of the translation products can only be speculative. It was therefore decided not to use these proteins for further steps.

As an alternative to the previously used TaKaRa™ Ex Taq™ DNA Polymerase, Aasi_1074 and Aasi_1080 were finally amplified with Phusion® DNA Polymerase (New England Biolabs), which is a *Pyrococcus furiosus*-like enzyme fused with a processivity-enhancing domain, also has $3´{\rightarrow}5´$ exonuclease activity and a $50\times$ lower error rate than standard *Taq* DNA Polymerase. The quality of the PCR products was verified by sequencing the pCR-XL-TOPO® plasmids; no base substitutions were observed. However, in the second cloning step from pCR-XL-TOPO® into pET-21b and pGEX-4T-3, it was not possible to obtain growth of *E. coli* transformants. The reason for this could either be problems with the ligation of the expression vector and insert, or the transformation of the plasmids. Two different enzymes were tested for ligation, Thermo Scientific's T4 DNA ligase and NEBNext® Quick T4 Ligase (New England Biolabs), but with both the result was negative. In addition to *E. coli* BL21, two other expression strains (C41 and C43) were tested, which both did not show growth of transformants. Since it could be verified by PCR with T7 primers that the ligation itself was successful, it was concluded that the absence of recombinant *E. coli* was caused by restrained uptake or early loss of the plasmid. This is in accordance with the previous observation of a bias towards plasmids with defective inserts. Taken together, the results strongly suggest that both prophage tail sheath and VgrG homologue of *A. asiaticus* are toxic for *E. coli*.

One common strategy for the expression of toxic proteins in vectors based on IPTG induction is to use expression media containing glucose or other inhibitors of the lac operon, making use of the so-called glucose effect, or catabolite repression. In the presence of glucose (or other lac repressors), basal expression under control of the lac promoter occurs only at low levels, which allows tighter regulation of the lac operon (Grossman *et al.*, 1998). It is also possible to introduce a lac repressor on the same or a second, compatible plasmid. Still, some highly toxic proteins cannot be expressed with these approaches, and even if cloning becomes possible, the induced expression of higher levels of the protein may not work. Also, a broad range of host strains and vectors for protein expression in *E. coli* exists to choose from. *E. coli* C41 and C43, originally described by Miroux & Walker (1996), are two mutant strains derived from BL21 which are often used for the overexpression of recombinant proteins to circumvent toxicity-associated problems (Dumon-Seignovert *et al.*, 2004). However, even with C41 and C43, it was not possible to clone proteins from the afp of *A. asiaticus*. These two particular strains were used for practical reasons, since they were available at the Department of Microbial Ecology. It has to be noted that in the original publication (Miroux & Walker, 1996), they were mainly evaluated

for the expression of toxic membrane proteins and different globular proteins, but not with proteins similar to the prophage tail sheath and VgrG homologue. Because it was beyond the scope and temporal constraints of the work for this diploma thesis, further *E. coli* strains and vectors or even alternative expression systems to *E. coli* were not tested.

## 4.2. RNA extraction and RT-qPCR assay development for prophage tail sheath gene expression study

### 4.2.1. Evaluation of RNA extraction

Purity and integrity of RNA are crucial for any successful quantitative real-time PCR (RT-qPCR) approach (Fleige & Pfaffl, 2006). The state-of-the-art method for the evaluation of RNA quality and quantity is microfluidics-based gel electrophoresis, e.g. with the Experion™ Automated Electrophoresis System (Bio-Rad; Fleige & Pfaffl, 2006). Also in this study, the Experion™ system was the method of choice for checking the integrity of DNase-treated RNA samples. While RNA integrity assessment can theoretically be done with standard, non-denaturing agarose gel electrophoresis as well (a less expensive alternative), the main drawback of this method is its low sensitivity. Apart from that, the migration behaviour of non-denatured RNAs of similar sizes can be different depending on their secondary structure, which may hinder a clear differentiation between single bands. Denaturing electrophoresis on agarose gels is a feasible alternative, as long as sufficiently high amounts of RNA are available to be applied to the gel (Fleige & Pfaffl, 2006). Another method for RNA quality assessment is polyacrylamide gel electrophoresis (Zheng *et al.*, 1996; Alm & Stahl, 2000). However, microfluidics-based gel electrophoresis is superior to all other methods in terms of sensitivity, which is a practical advantage if only limited amounts of RNA are available. Furthermore, it provides comprehensive information about both quality and quantity of the nucleic acids in one step. Indicators for degradation are on the one hand an elevated threshold baseline, and on the other hand a decreased 28S:18S ratio (for eukaryotic RNA) or 23S:16S ratio (for prokaryotic RNA; Mueller *et al.*, 2004). High ratios of around 2:1 benchmark good RNA integrity. RNA extracted from a culture of *Acanthamoeba* sp. infected with *A. asiaticus* comes with the challenge that it contains both prokaryotic and eukaryotic RNA in unknown proportions. Usually, the 16S and 23S rRNA peak in prokaryotic and 18S and 28S rRNA peak in eukaryotic samples are automatically recognised by the Experion™ software, depending on the selected option, but the available version has no preset for rRNA-based analysis of mixed samples. In case of samples containing both prokaryotic and eukaryotic RNA (12, 68, and 140 h *p.i.*), the 23S to 16S rRNA ratio could therefore not be determined reliably. Since the peaks were in general very distinct and sharp in all samples, with the only exception being the 28S rRNA peak, and the 23S to 16S rRNA ratio in prokaryotic samples was between 1.76 and 1.79, it was inferred that the overall RNA integrity was sufficient. Broad, less pronounced 28S rRNA indicate slight degradation of longer RNAs, which is in accordance with the fact that longer RNAs are more prone to degradation than short ones.

In addition to high integrity, RNA extracts should be free of proteins, as can be measured by the absorbance at 260 and 280 nm (Pfaffl, 2005). The absorbance at 260 nm provides a first estimation of RNA quantity as well, but if substantial amounts of co-extracted genomic DNA are present in not-yet DNase treated samples, the RNA concentration can be easily overestimated. The 260:280 ratio is an indicator for RNA purity in terms of protein contaminations. A ratio over 1.8 is considered to represent acceptable RNA quality (Manchester, 1996). In recent years, however, the reliability of this method has been questioned because the sensitivity is so low that even relatively high protein concentrations

contribute only little to the overall ratio (Bustin & Nolan, 2004b). For example, even a ratio of 1.8 still corresponds to up to 40 % protein, and a ratio of 1.94 to 30 % protein. Apart from protein contaminations, also residual traces of phenol, which is often used for nucleic acids extraction, become apparent in the 260:280 ratio. A ratio of close to two is considered as good (Sambrook & Russell, 2000). Since the TRIzol® reagent (Life Technologies), which was used for RNA isolation, is a commercially available ready-made reagent for guanidinium thiocyanate-phenol-chloroform extraction, traces of phenol were likely to be found within the extracts. For all measured samples, the 260:280 ratio was between 1.90 and 2.08, which indicates a high quality and absence of large quantities of proteins and/or phenol. Genomic DNA, which is inevitably co-extracted during RNA isolation, was removed by direct DNase I digestion of RNA extracts. Traces of DNA in the samples will influence the outcome of the subsequent RT-qPCR, since gDNA and reverse transcribed RNA (i.e., cDNA) are both amplified during the qPCR reaction. Standard agarose gel electrophoresis is again not sensitive enough to reliably detect remnants of DNA in RNA samples. The DNase-treated samples were therefore applied to standard PCR and later also included in the qPCR analysis (without prior cDNA synthesis) to verify the absence of gDNA. In standard PCR and subsequent agarose gel electrophoresis, visible bands on the gel would be a clear sign of DNA contaminations. In qPCR, the Cq-values have to be equal to or higher as the Cq values of the NTCs, and in the ideal case beyond the detection limit of the qPCR. For all samples, no considerable amounts of contaminating gDNA were detected by either method, therefore no further evaluation of the RNA extraction pipeline was necessary.

## 4.2.2. Development and evaluation of RT-qPCR assays

(RT-)qPCR is one of the most powerful and versatile techniques in molecular biology for a broad range of applications based on the detection and quantification of nucleic acids, albeit it comes with several potential pitfalls. Nonetheless, or even precisely because of this, it is often underestimated how important careful evaluation of a newly designed (RT-)qPCR assay is to ensure the reliability and scientific relevance of the results. Bustin *et al.* (2009) proposed a set of recommendations, called MIQE (an acronym for "Minimum Information for Publication of Quantitative Real-Time PCR Experiments") guidelines, which deal with critical steps in design and implementation of (RT-)qPCR-based analyses and provide a list of information that should be made available in publications. In addition to appropriate preparation and storage of samples, these guidelines address parameters for reverse transcription of RNA, target information, primer design, assay validation, and conclusive data analysis.

Fluorescent dyes are required for any qPCR-based approach to enable quantification of nucleic acids during the PCR reaction, and two major categories exist to choose from: (1) unspecific DNA-binding dyes (e.g. SYBR Green I) and (2) sequence-specific labeled oligonucleotides, i.e. primers and probes. While the latter type comes with the additional possibility for multiplexing, in a low-throughput singleplex analysis, like in this study, SYBR Green I is often the method of choice because it is less expensive and allows faster qPCR assay development. Two SYBR Green I based assays targeting the prophage tail sheath (Aasi_1074) and the beta-subunit of the RNA polymerase (Aasi_1396) as reference gene were designed, evaluated, and used for relative quantification of Aasi_1074 transcripts. However, as SYBR Green I binds unspecifically to any double-stranded DNA, the specificity of such assays has to be evaluated with great care. Prerequisite for any specific PCR or qPCR are target-specific primers, which has to be taken into account already during primer design. Additionally, a no-target control (cDNA reverse transcribed from RNA from symbiont-free *Acanthamoeba* sp.) was analysed with qPCR to exclude unspecific binding of the primers. The selection of no-target controls depends on the experimental system, and since in this case a culture consisting exclusively of *Acanthamoeba* sp. and

one endosymbiont was analysed, no further controls were regarded necessary. Primer optimisation with focus on concentrations and annealing temperature is another crucial point; it is known that poor primer optimisation reduces the quality of a qPCR assay (Nolan *et al.*, 2006). Both assays were thoroughly optimised by evaluating different primer annealing temperatures and primer concentrations. Melting curves were performed after each qPCR run to check the specificity. This is done by gradually increasing the temperature after the qPCR itself is completed and recording the fluorescence during the whole time. Since the temperature at which dsDNA denatures is dependent on its molecular composition, each dsDNA fragment present in the qPCR mix after amplification will result in denaturation and thereby a sudden decrease in fluorescence at a characteristic temperature. When plotting the negative first derivative of the fluorescence curves against temperature, this phenomenon becomes apparent as distinct melt peaks for each individual amplification product. These peaks then allow differentiation between target and unspecific products such as primer dimers. For none of the cDNA samples or qPCR standards, unspecific PCR products were observed. One out of two different NTCs (prepared with PCR grade water) resulted in unspecific PCR products in the Aasi_1074 targeted assay but not in the Aasi_1396 targeted assay, although the same aliquot of water was used. The second NTC (purchased RNase-free water used for RNA work) was sometimes amplified with high Cq values in the Aasi_1074 targeted assay and always remained negative in the Aasi_1396 targeted assay. It was concluded that the observed unspecific products were most likely caused by an excess of primers when no target was added, and had no relevant influence on the qPCR results.

A well-optimised qPCR assay is characterised by a linear standard curve covering a broad dynamic range and high amplification efficiencies close to 100 %. Theoretically, efficiencies over 100 % are hardly possible, but still they can occur due to pipetting errors or other inaccuracies. Amplification efficiency must be assessed by means of calibration curves (Bustin *et al.*, 2009), consisting of serial dilutions of DNA standards with defined concentrations and/or target copy numbers. Plasmids, PCR amplicons, synthesised oligonucleotides, gDNA, and cDNA can all be employed for this purpose. In the beginning of this study, gDNA from *Acanthamoeba* sp. + *A. asiaticus* was intended to be used for practical reasons, as it was readily available. But it turned out that extended storage of (diluted) gDNA standards at –20 °C over several days or weeks drastically impaired the quality of the calibration curves, and independent from storage time, the reproducibility was not good. As an alternative, pCR-XL-TOPO® plasmids with the respective gene or fragment of the gene were successfully established as standards. Circular plasmids are most commonly used as qPCR standards, though it has been shown that they can lead to overestimation of the actual target copy numbers (Hou *et al.*, 2010). This relies on the fact that circular plasmids usually occur in supercoiled form (Hayes, 2003), which can suppress the qPCR reaction compared to relaxed target DNA (Chen *et al.*, 2007). Instead, linearised plasmids and PCR amplicons are suggested as more suitable types of qPCR standard. Hou *et al.* (2010) did not observe a consistent effect on the amplification efficiency, comparing the evaluation with circular and linear standards, but pointed out that differences in the efficiencies can be observed in some cases. Overestimation of target copy numbers has to be avoided in particular if an absolute quantification is desired. Relative quantification, however, is based on differences in the ratio of target to reference gene (or transcript) copies and thus not influenced by this potential overall bias in the calculation of absolute copy numbers. Also the determination of linear dynamic range and detection limit of the qPCR would not be affected. Taken together, it was decided that the practical advantages (easy availability and no additional linearisation or PCR step before use) outweighed the drawback that no absolute quantification of target mRNAs was possible, since this was not the scope of this study anyway. The Aasi_1074 assay showed an amplification efficiency of 88.1 % (qPCR standard curve quality indicator: $R^2 = 0.999$) in a dynamic range from $1.2 \times 10^8$ to $1.2 \times 10^1$ copies, and the assay

targeting Aasi_1396 had an amplification efficiency of 87.6 % (qPCR standard curve quality indicator: $R^2$ = 0.998) in a range from $1.5 \times 10^8$ to $1.5 \times 10^1$ copies. Both assays were similar in their performance, which is desirable in case of a relative quantification with two independent assays.

Another challenge of RT-qPCR based approaches is that both steps, reverse transcription and qPCR, can be inhibited by a variety of exogenous or endogenous substances (Bustin & Nolan, 2004a; Bustin, 2005; Nolan *et al.*, 2006). Inhibition is a concentration dependent phenomenon. Inhibitors are often co-extracted with RNA; purification steps can surely decrease the amount of inhibitory substances, but a complete removal is a visionary aspiration. Since the reverse transcription has been shown to introduce considerable variation into the RT-qPCR in its entirety, it is advisable to conduct the reaction in technical duplicates or triplicates and adjust the total RNA concentration so that it is the same in all samples (Ståhlberg *et al.*, 2004). This is commonly achieved by dilution of the RNA extracts, however, it has to be considered that also potential inhibitory substances will be diluted with this strategy. A simple approach to assess inhibitory effects of the reverse transcription, if the available RNA amount is not extremely limited, is to use a dilution series of RNA extracts to find a dilution range where no inhibition occurs (Ståhlberg *et al.*, 2003). To reduce the amount of inhibitors within RNA extracts to a minimum, an additional ethanol precipitation step was performed after DNase I treatment. A dilution series of one selected sample was reverse transcribed and analysed with Aasi_1396 targeted qPCR. Only when 5 µL of undiluted RNA extract (= 1713.5 ng) were applied to reverse transcription in 25 µL reaction volume, inhibition was observed. A dilution to a concentration of 100 ng µL$^{-1}$ was selected for the final protocol, as higher RNA template amounts seemed to be reverse transcribed with slightly better efficiency than lower amounts.

Following reverse transcription, no buffer exchange was done prior to the qPCR analysis. Consequently, inhibitory reaction components within the reverse transcription mix would still be present and influence the qPCR reaction. qPCR inhibition was investigated by analysing a cDNA dilution series of one reverse transcribed sample with the Aasi_1396 targeted assay. Again, with the only exception being the highest applied amount of cDNA (undiluted reverse transcription reaction mix, 10 % of the total qPCR reaction volume), a good linear correlation between the amount of cDNA and Aasi_1396 copy numbers indicated the absence of inhibitors, or at least only neglectable effects on qPCR performance. For practical reasons, a 10-fold dilution was used in the final protocol. Addressing the problem of inhibition is of course primarily important for absolute quantification, and the effect on the overall results is less pronounced in case of relative quantification. However, in the Aasi_1396 targeted RT-qPCR assay, inhibition was observed neither during reverse transcription nor in the subsequent qPCR step over a broad range.

## 4.3. The role of the putative afp during infection

A variety of amoeba-associated bacteria shows a biphasic lifestyle with two morphologically and physiologically distinct stages. Well-studied examples include the human pathogen *Legionella pneumophila* and members of the order *Chlamydiales*, such as *Protochlamydia amoebophila*, *Parachlamydia acanthamoebae*, and *Simkania negevensis* (Harb *et al.*, 2000; Molofsky & Swanson, 2004; Horn, 2008). In general, these bacterial endosymbionts exhibit an extracellular infectious stage and an intracellular stage which replicates inside the amoebal host. Following attachment to and entry into the host cells, intracellular replication occurs until the symbionts are released from the host to start a new cycle of infection. *P. amoebophila*, *P. acanthamoebae*, and *S. negevensis* were originally recovered from soil samples, nasal swab, and as a contaminant in human cell culture, respectively

(Kahane *et al.*, 1995; Amann *et al.*, 1997; Fritsche *et al.*, 2000; Collingro *et al.*, 2005). Despite being isolated from substantially different sources, not closely related and different in their ways of interaction with the amoebal host (Horn, 2008), they all share the unique chlamydial developmental cycle. The cycle starts with the uptake of the extracellular, infectious stage, the elementary bodies (EBs), by phagocytosis and is followed by differentiation of EBs into reticulate bodies (RBs), which then replicate within the amoebal host through binary fission. The RBs can at a certain point re-differentiate back into EBs, which are then released either by host cell lysis or in vesicles. During intracellular replication, the bacteria can occur either in multiple larger inclusions, as it is observed for example in *P. acanthamoebae* (Greub & Raoult, 2002), or in single cell inclusions, like in the case of *P. amoebophila* (Collingro *et al.*, 2005). Apart from thriving intracellularly in inclusions, surrounded by a host-derived membrane, both *P. acanthamoebae* and *P. amoebophila* have also been detected directly in the cytoplasm of the amoebae (Fritsche *et al.*, 2000; Greub & Raoult, 2002). While members of the *Chlamydiales* usually are obligate endosymbionts and metabolically highly dependent on their amoebal host (Horn, 2008), *Legionella pneumophila* is primarily a human pathogen which has been reported to occur either planktonic or in biofilms within aquatic systems (Rogers & Keevil, 1992; Rogers *et al.*, 1994). In addition, *L. pneumophila* facultatively infects and multiplies within amoebae or other protozoa, where it is surrounded by a host-derived membrane in phagosomes in a similar way as chlamydiae (Abu-Kwaik, 1996). With reference to this facultative inhabitation of amoebae, *L. pneumophila* also shows a biphasic lifestyle, consisting of an extracellular transmissive phase and an intracellular replicative phase, which re-differentiates back to the transmissive form before release through host cell lysis (Molofsky *et al.*, 2004; Weissenmayer *et al.*, 2011).

With *A. asiaticus*, the life cycle of an amoeba endosymbiont belonging to the phylum of the *Bacteroidetes* was described for the first time. Remarkably, *A. asiaticus* also exhibits a biphasic lifestyle with an extracellular, infectious stage and an intracellular, replicative stage (Tsao, 2011). The life cycle starts with an extracellular, coccoid, infectious intermediate, which is taken up by phagocytosis by the amoebal host. However, once internalised, *A. asiaticus* is not surrounded by host-derived membranes as it is seen for members of the *Chlamydiales* and *L. pneumophila*. Instead, the symbiont resides directly within the cytoplasm (Horn *et al.*, 2001) in a similar way as *Rickettsia* spp. (Hackstadt, 1998). During intracellular replication, *A. asiaticus* undergoes a morphological differentiation from a short, coccoid rod to a more elongated shape (Tsao, 2011). In later stages of the infection, the shape of *A. asiaticus* changes again to short rods, indicating the transition back to the infectious intermediate. It has been shown that intracellularly replicating *A. asiaticus* has a significantly lower degree of infectivity than the extracellular intermediate (Tsao, 2011). At the end of each cycle, *A. asiaticus* is released by host cell lysis.

Such close dependency between a bacterial endosymbiont and its eukaryotic host as it is the case for *A. asiaticus* requires mechanisms for interaction with the host. Obligate intracellular bacteria usually possess at least one of the currently known six types of secretion systems for the delivery of effectors to the host (Tseng *et al.*, 2009). A common mechanism for host cell interaction of all members of the *Chlamydiaceae* is the type III secretion system (T3SS; Peters *et al.*, 2007), which has been shown to be present also in the genomes of the beforementioned examples *P. amoebophila* and *S. negevensis* (Horn *et al.*, 2004; Peters *et al.*, 2007). *L. pneumophila* utilises a type IV secretion system to deliver effector proteins to the host (Vogel *et al.*, 1998). Genome analysis of *A. asiaticus* revealed a large repertoire of putative effector proteins, but no complete type I–VI secretion system or other known functional secretion device is encoded in the genome (Schmitz-Esser *et al.*, 2010). However, a cluster of 13 genes

DISCUSSION

(Aasi_1072 to Aasi_1806) with predicted operon structure is found in the *A. asiaticus* genome which resembles a derived type VI secretion system, but shows even stronger similarity and is largely syntenic to the afp gene cluster of the insect pathogen *Serratia entomophila* (Penz *et al.*, 2010). It has been proposed by Penz *et al.* (2010) that the putative afp of *A. asiaticus* might be used as a protein secretion device. Interestingly, cytoplasmic fibril-like structures were detected by transmission electron microscopy in extracellular *A. asiaticus* after release from the amoebae through host cell lysis, and also at an early stage of the infection cycle during attachment to the host (this study and additional unpublished data; Thomas Penz, Department of Microbial Ecology; personal communication). These fibril-like structures are assumed to represent the phage tail sheath of the afp, since no other proteins are encoded in the genome of *A. asiaticus* which might account for similar structures. Bundles of several prophage tail sheaths seemed to be anchored on a base plate at the inside of the cell wall. In this study, *A. asiaticus* cells and purified prophage particles were visualised with cryo-electron microscopy for a more detailed analysis of the ultrastructure of the prophage than with traditional transmission electron microscopy. The analysis revealed straight, apparently hollow, tubular structures with a minimal length of 200 nm and a diameter of 4–6 nm. A striped pattern on the outside of the tubes suggests helical organisation of the prophage tail sheath. It is remarkable that the purified phage particles showed structural similarity to the phage tail like structures of the T6SS of Vibrio cholerae (Basler *et al.*, 2012). Indeed, it has been suggested that phage-tail associated protein complexes such as afp-like prophages share a common evolutionary origin with T6SS (Leimann *et al.*, 2009). The prophage-like structures were found in a large proportion of all cells present within the samples, however, in the intracellular intermediate of *A. asiaticus*, no such structures were observed. To show a possible involvement of the putative afp in the process of infecting the amoebal host, the expression of one selected protein from the afp-like gene cluster, the prophage tail sheath (Aasi_1074), was analysed at different time points of the infection cycle in this study. It could be demonstrated that the prophage tail sheath is expressed differentially in the intracellular, replicative and extracellular, infectious intermediate of *A. asiaticus*. The relative amount of prophage tail sheath transcripts was highest in the extracellular stage, significantly lower already during the attachment of *A. asiaticus* to the amoebal host, and lowest in an intracellular intermediate at 68 hours *post infection*. Towards the end of the infection cycle, the transcript level was again rising. Taken together with the observation of filamentous, prophage-like structures being present only in the extracellular but not intracellular stage of *A. asiaticus*, these results strongly suggest an important role of the putative prophage in the infection process.

In *S. entomophila*, the afp is presumably used as a protein secretion apparatus to deliver toxins to the host (Hurst *et al.*, 2004; Hurst *et al.*, 2007). Apart from *S. entomophila*, also *Photorhabdus* sp. and several marine bacteria, including many members of the *Bacteroidetes*, encode similar toxin-delivering prophages (Persson *et al.*, 2009). In a similar way, the putative afp of *A. asiaticus* could be used as a device to either deliver effectors encoded directly within the afp-like gene cluster to the host, or as a more general protein secretion system.

## 4.4. Outlook

In this study, the differential expression of the prophage tail sheath in the intracellular, replicative and the extracellular, infectious intermediate of *A. asiaticus* could be shown. Based on these first insights regarding the expression of proteins of the putative secretion device of *A. asiaticus* at different time points of the infection cycle, it would be interesting to extend this endeavour to a wider range of proteins presumably important for interaction with the host. The work conducted for this diploma

thesis was embedded in a larger and still ongoing project at the Department of Microbial Ecology, which, among others, aims to study the complete metatranscriptome of *A. asiaticus* in key stages of the infection cycle. This approach will lead to a far more comprehensive understanding of the mechanisms for host interaction and reveal further details regarding the infection cycle.

Since the cloning of selected afp proteins was hindered by the occurrence of most likely toxicity-associated problems, the production of antibodies for immunofluorescence based on the heterologously expressed proteins was not possible. Consequently, the connection between the afp-like gene cluster and microscopically observed putative prophage-like structures still has to be verified. As an alternative to further evaluation of the conditions for heterologous expression of the target proteins, peptide antibodies were ordered. However, as the time frame for antibody production and preparation steps for immunofluorescence substantially exceeded the temporal limitations, it was never planned to do immunofluorescence during this thesis, but in follow-up work. In addition to enabling verification of the identity of microscopically detected prophage-like structures, immunofluorescence also promises to better visualise the intracellular localisation of the putative secretion system.

Agnes Harreither

# Chapter 5. Summary

Symbioses between organisms have played a crucial role during evolution, starting with the origin of eukaryotic organelles by endosymbiotic uptake, and they were essential for the generation of biological diversity. Free-living amoebae, ubiquitous protozoa with great significance in a variety of terrestrial and aquatic ecosystems, are known to commonly harbour bacterial endosymbionts. These associations between amoebae and bacteria serve as important model systems to study the establishment of an intracellular lifestyle and symbiotic relationships between bacteria and protists in general.

*Amoebophilus asiaticus* is an obligate endosymbiont of free-living amoebae belonging to the genus *Acanthamoeba*. The complete genome of *A. asiaticus* was sequenced recently and provided novel insights into the mechanisms of interactions between host and symbiont. Its small genome size and a very limited repertoire of genes for essential biosynthetic pathways point towards a close symbiotic association and strict dependency on the amoeba host. Surprisingly, none of the currently known type I–VI secretion systems needed for the delivery of putative effector proteins to the host cytoplasm is present in the genome of *A. asiaticus*. However, *A. asiaticus* encodes a cluster of 13 genes with predicted operon structure and weak similarity to a derived type VI secretion system, which closely resembles the antifeeding prophage (afp) of the insect pathogen *Serratia entomophila*. It was previously shown that *A. asiaticus* exhibits a biphasic lifestyle with two morphologically different stages. Remarkably, the extracellular intermediate has a much higher degree of infectivity than the intracellular, replicative stage. Transmission electron microscopy analysis of extracellular, infectious *A. asiaticus* revealed bundles of filamentous cytoplasmic structures, which could represent the putative antifeeding prophage. These structures were not detected in the intracellular, replicative stage of *A. asiaticus*.

In this study, a (reverse transcription) quantitative real-time PCR (RT-qPCR) based approach was used to analyse the expression of one representative gene of the afp-like cluster of *A. asiaticus* at different time points of the infection cycle. Two RT-qPCR assays targeting the prophage tail sheath gene and, as a reference gene, the beta-subunit of the RNA polymerase, were developed, evaluated, and extensively optimised. Application of the RT-qPCR assays in infection experiments demonstrated that the prophage tail sheath gene was differentially expressed in the extracellular versus the intracellular stage of *A. asiaticus*. The relative amount of prophage tail sheath transcripts was highest in the extracellular stage and lowest during intracellular replication, at an exemplary time point of 68 hours *post infection* (231-fold lower than in extracellular *A. asiaticus*).

To establish the missing link between the afp-like gene cluster of *A. asiaticus* and microscopically observed structures, two selected proteins, the prophage tail sheath and the homologue of the needle tip protein VgrG, were cloned for heterologous expression in *Escherichia coli*. As a long-term goal, it was planned to produce antibodies for immunofluorescence against the purified proteins. Despite multiple optimisation steps of the experimental conditions, it was not possible to successfully express the target proteins, suggesting that they might be toxic for *E. coli*.

Additionally, infection experiments were conducted to prepare samples for conventional transmission electron microscopy and cryo-electron microscopy. *A. asiaticus* cells from different infection time points and a purification of prophage particles were visualised (microscopic analysis was done by collaboration partners at the University of Ljubljana and the California Institute of Technology).

SUMMARY

Straight, hollow, tubular prophage-like structures with a minimal length of 200 nm, a diameter of 4–6 nm and presumable helical organisation were detected in a large fraction of extracellular, but not in intracellular *A. asiaticus*. This observation coincides well with the RT-qPCR results and, taken together, both strongly support a possible involvement of the putative prophage in the infection process.

Agnes Harreither

# Chapter 6. Zusammenfassung

Symbiosen zwischen verschiedenen Organismen spielten während der Evolution eine entscheidende Rolle. Bereits für die Entstehung eukaryotischer Organellen war die endosymbiotische Aufnahme von Bakterien ausschlaggebend; auch die biologische Diversität wurde durch vielfältige Erscheinungsformen der Symbiosen geprägt. Freilebende Amöben, eine weit verbreitete Gruppe einzelliger Lebewesen mit großer Bedeutung in terrestrischen und aquatischen Lebensräumen, sind dafür bekannt, bakterielle Endosymbionten zu besitzen. Diese Assoziationen zwischen Amöben und ihren bakteriellen Symbionten dienen als wichtige Modellsysteme für die Erforschung der Entwicklung einer intrazellulären Lebensweise und der Symbiose zwischen Bakterien und Protisten.

*Amoebophilus asiaticus* ist ein obligat intrazellulärer Symbiont von Akanthamöben. Die Sequenzierung seines Genoms lieferte neue Einblicke in die Interaktionsmechanismen zwischen Wirt und Symbiont. Die kleine Größe des Genoms und ein drastisch eingeschränktes Repertoire an Genen für essentielle Biosynthesewege deuten auf eine sehr enge symbiotische Beziehung und starke Abhängigkeit des bakteriellen Symbionten vom Wirt hin. Überraschenderweise findet sich im Genom von *A. asiaticus* keines der bekannten Typ I–VI Sekretionssysteme, die für den Transfer von Effektorproteinen in das Zytoplasma der Wirtszelle erforderlich sind. Dafür findet sich aber ein Cluster aus 13 Genen mit großer Ähnlichkeit zu dem „antifeeding" Prophagen (afp) der insektenpathogenen Bakterien *Serratia entomophila*. *A. asiaticus* besitzt einen zweistufigen Lebenszyklus mit einer extrazellulären, infektiösen und einer intrazellulären, nicht-infektiösen Phase, die sich auch morphologisch unterscheiden. Im Zytoplasma der extrazellulären, jedoch nicht der intrazellulären Form von *A. asiaticus* konnten mittels Transmissionselektronenmikroskopie Bündel aus filamentösen Strukturen nachgewiesen werden, bei denen es sich vermutlich um den Prophagen handelt.

In der vorliegenden Studie wurde ein quantitativer Echtzeit-PCR (qPCR) Ansatz gewählt, um die Expression eines Gens aus dem afp-Cluster von *A. asiaticus* zu unterschiedlichen Infektionszeitpunkten zu analysieren. Dafür wurden zwei qPCR Assays gegen das „prophage tail sheath"-Gen und das Gen für die Beta-Untereinheit der RNA Polymerase als Referenzgen entwickelt und sorgfältig optimiert. Es konnte gezeigt werden, dass das „prophage tail sheath"-Gen in den verschiedenen Stufen des Infektionszyklus differentiell exprimiert wird. Die relative Menge an „prophage tail sheath"-Transkripten war in der extrazellulären Phase am höchsten und während der intrazellulären Replikation, 68 Stunden nach Infektion, am geringsten (231-mal niedriger als in extrazellulärem *A. asiaticus*).

Um die fehlende Verbindung zwischen dem afp-Gencluster und den mikroskopisch sichtbaren filamentösen Strukturen herzustellen, wurden zwei ausgewählte Proteine kloniert, um sie in *Escherichia coli* exprimieren und aus den aufgereinigten Proteinen Antikörper für Immunfluoreszenz-Assays herstellen zu können. Trotz intensiver Evaluierung und Optimierung der experimentellen Bedingungen gelang es jedoch nicht, die Proteine erfolgreich zu exprimieren, was wahrscheinlich darauf zurückzuführen ist, dass diese toxisch für *E. coli* sind.

Zusätzlich wurden Infektionsexperimente durchgeführt, um Proben für Transmissionselektronenmikroskopie und Cryoelektronenmikroskopie vorzubereiten. Unterschiedliche Infektionszeitpunkte und eine Aufreinigung an Prophagen-Partikeln wurden fixiert (die mikoskopische Analyse wurde von Kollaborationspartnern an der Universität Ljubljana und dem California Institute of Technology durchgeführt). In einem großen Teil des extrazellulären, aber nicht des intrazellulären Stadiums von

## ZUSAMMENFASSUNG

*A. asiaticus* wurden gerade, röhrenförmige und vermutlich helikal organisierte Strukturen mit 200 nm Länge und 4–6 nm Durchmesser entdeckt. Diese Beobachtung deckt sich mit den Resultaten der qPCR. Zusammenfassend lässt sich sagen, dass die Ergebnisse der vorliegenden Arbeit erstmals plausible Hinweise auf eine Beteiligung des mutmaßlichen Prophagen am Infektionsprozess liefern.

Agnes Harreither

# Appendix A. Supplementary Materials and Methods

**Table A.1** Laboratory suppliers and manufacturers of equipment used in this study.

| Abbreviation | Full name and headquarters | Website |
| --- | --- | --- |
| AustrAlco | AustrAlco GmbH Österreichische Agrar-Alkohol HandelsgesmbH; Spillern, Austria | australco.at |
| Avantor | Avantor Performance Materials; Center Valley, PA, USA | avantormaterials.com |
| Beckman Coulter | Beckman Coulter Inc.; Brea, CA, USA | beckmancoulter.com |
| BINDER | BINDER GmbH; Tuttlingen, Germany | binder-world.com |
| Bioer Technology | Bioer Technology Co.; Hangzhou, China | bioer.com.cn/bioer/bioer_en |
| Bio-Rad | Bio-Rad Laboratories, Inc.; Hercules, CA, USA | bio-rad.com |
| Biostep | Biostep GmbH; Jahnsdorf, Germany | biostep.de |
| Biozym | Biozym Scientific GmbH; Hessisch Oldendorf, Germany | biozym.com |
| BRAND | BRAND GmbH + Co. KG; Wertheim, Germany | brand.de |
| Braun | B. Braun Melsungen AG; Melsungen, Germany | bbraun.com |
| Camspec | Spectronic Camspec Ltd.; Garforth, United Kingdom | spectronic.co.uk |
| Carl Roth | Carl Roth GmbH + Co. KG; Karlsruhe, Germany | carlroth.com |
| Citifluor | Citifluor Ltd.; Leicester, United Kingdom | citifluor.co.uk |
| Eppendorf | Eppendorf AG; Hamburg, Germany | eppendorf.com |
| Epson | Seiko Epson Corporation; Suwa, Nagano, Japan | epson.com |
| Fresenius Kabi | Fresenius Kabi AG; Bad Homburg, Germany | fresenius-kabi.com |
| GFL | GFL Gesellschaft für Labortechnik mbH; Burgwedel, Germany | gfl.de |
| Greiner Bio-One | Greiner Bio-One International AG; Kremsmünster, Austria | gbo.com |
| Hettich Lab Technology | Andreas Hettich GmbH & Co. KG; Tuttlingen, Germany | hettichlab.com |
| IKA-Werke | IKA®-Werke GmbH & Co. KG; Staufen, Germany | ika.com |
| Invitrogen | Part of Life Technologies | invitrogen.com |
| JOUAN Nordic A/S | JOUAN Nordic A/S; Allerød, Denmark | jouannordic.denmark-products.com |
| Life Technologies | Life Technologies Corporation; Carlsbad, CA, USA | lifetechnologies.com |
| Lonza | Lonza Group Ltd.; Basel, Switzerland | lonza.com |
| Marienfeld | Paul Marienfeld GmbH & Co. KG; Lauda-Königshofen, Germany | marienfeld-superior.com |
| Memmert | Memmert GmbH + Co. KG; Schwabach, Germany | memmert.com |
| Merck | Merck KGaA; Darmstadt, Germany | merckgroup.com |
| Millipore | EMD Millipore; Billerica, MA, USA | millipore.com |
| MP Biomedicals | MP Biomedicals LLC; Santa Ana, CA, USA | mpbio.com |
| Nalgene | Part of Thermo Fisher Scientific | nalgenunc.com |

## SUPPLEMENTARY MATERIALS AND METHODS

| | | |
|---|---|---|
| NEPA GENE | NEPA GENE Co. Ltd.; Ichikawa, Chiba, Japan | nepagene.jp |
| New Brunswick Scientific | New Brunswick Scientific; Enfield, CT, USA | nbsc.com |
| New England Biolabs | New England Biolabs Inc.; Ipswich, MA, USA | neb.com |
| Nunc | Part of Thermo Fisher Scientific | nuncbrand.com |
| Ohaus | Ohaus Corporation; Parsippany, NJ, USA | us.ohaus.com |
| Olympus | Olympus Corporation; Shinjuku, Tokyo, Japan | olympus-global.com |
| Oxoid | Part of Thermo Fisher Scientific | oxoid.com |
| Pall | Pall Corporation; Port Washington, NY, USA | pall.com |
| PEQLAB | PEQLAB Biotechnologie GmbH; Erlangen, Germany | peqlab.com |
| Qbiogene | Part of MP Biomedicals | qbiogene.com |
| QIAGEN | QIAGEN GmbH; Hilden, Germany | qiagen.com |
| Roche | F. Hoffmann-La Roche Ltd.; Basel, Switzerland | roche.com |
| Sartorius | Sartorius AG; Göttingen, Germany | sartorius.com |
| SCHOTT | SCHOTT AG; Mainz, Germany | schott.com |
| Scientific Industries | Part of Thermo Fisher Scientific | scientificindustries.com |
| Sigma-Aldrich | Sigma-Aldrich Co. LLC.; St. Louis, MO, USA | sigmaaldrich.com |
| Sterilin | Part of Thermo Fisher Scientific | sterilin.co.uk |
| Takara Biotechnology | Part of Takara Bio Inc. | *unavailable* |
| Takara Bio Inc. | Takara Bio Inc.; Otsu, Shiga, Japan | takara-bio.com |
| Tecan | Tecan Group Ltd.; Männedorf, Switzerland | tecan.com |
| Thermo Fisher Scientific | Thermo Fisher Scientific Inc.; Waltham, MA, USA | thermofisher.com |
| Thermo Scientific | Part of Thermo Fisher Scientific | thermoscientific.com |
| VWR | VWR International, LLC; Radnor, PA, USA | vwr.com |
| WTW | WTW Wissenschaftlich-Technische Werkstätten GmbH; Weilheim, Germany | wtw.de |
| Zeiss | Carl Zeiss AG; Oberkochen, Germany | corporate.zeiss.com |

## A.1. Step-by-step protocol for RNA extraction with TRIzol® Reagent

This protocol is based on the manufacturer's manual.

1. Harvest 50 mL of amoeba culture by centrifugation at 6409 × g for 3 min.
2. Completely remove supernatant by decanting and pipetting.
3. Quickly resuspend pellet in 750 μL of TRIzol® Reagent.
4. Transfer into a 2 mL FastPrep™ Lysing Matrix A tube, containing small beads only.
5. Lyse cells by bead beating for 30 s at 4.5 m s$^{-1}$.
6. Incubate at room temperature for 5 min.
7. Add 200 μL of chloroform per 750 μL TRIzol®.
8. Shake tubes vigorously by hand for a minimum of 15 s.
9. Incubate at room temperature for 3 min.
10. Centrifuge at 12000 × g for 15 min at 4 °C.
11. Transfer aqueous (upper) phase to a new 2 mL tube.
12. Add 500 μL of isopropanol per 750 μL TRIzol®.
13. Incubate at room temperature for 10 min.
14. Centrifuge at 12000 × g for 10 min at 4 °C to obtain the (gel-like) RNA pellet.
15. Wash pellet in 1 mL of 75 % ethanol.
16. Mix by vortexing.
17. Centrifuge at 7500 × g for 5 min at 4 °C.
18. Remove ethanol and air-dry pellet at room temperature for a maximum of 5 min.
19. Resuspend pellet in 100 μL of RNase free water.
20. Put on ice and store at –80 °C, or temporarily keep on ice and immediately proceed with DNase treatment (see Section A.2).

## A.2. Step-by-step protocol for the TURBO DNA-free Kit

This protocol, based on the manufacturer's recommendations, is designed for digestion of 10 μg nucleic acids in a reaction volume of 50 μL. All steps are performed at room temperature.

1. Dilute RNA with the appropriate amount of nuclease free water for a final reaction volume of 50 μL.
2. Add 0.1 volumes of 10× TURBO DNase Buffer.
3. Add 1.5 μL of TURBO DNase.
4. Mix gently.
5. Briefly spin down.
6. Incubate in the thermal cycler at 37 °C for 30 min.
7. Add another 1.5 μL of TURBO DNase.
8. Incubate in the thermal cycler at 37 °C for 30 min.
9. Add 0.2 volumes of vortexed DNase Inactivation Reagent.
10. Mix well.
11. Incubate for 5 min; mix 2–3 times during this time.
12. Centrifuge at 10000 × g for 90 s.
13. Transfer supernatant, containing the RNA, to a new 2 mL tube.
14. Put on ice and store at –80 °C, or temporarily keep on ice and immediately proceed with ethanol precipitation (see Section A.3).

## A.3. Step-by-step protocol for ethanol precipitation of RNA

The volumes given in this protocol are designed for precipitation of the complete amount of RNA recovered after DNase treatment (approximately 50 μL).

1. Fill up RNA with RNase-free water to a final volume of 200 μL.
2. Add 0.1 volumes of sodium acetate solution (3 mol L$^{-1}$).
3. Add 0.01 volumes of glycogen (helps to facilitate precipitation of nucleic acids).
4. Add 3 volumes of ethanol.
5. Incubate at –80 °C for 30 min.
6. Centrifuge at 21255 × g for 10 min at 4 °C.
7. Remove supernatant.
8. Wash pellet in 1 mL of 70 % ethanol.
9. Centrifuge at 21255 × g for 10 min at 4 °C.
10. Remove ethanol and air-dry pellet at room temperature for a maximum of 5 min.
11. Resuspend pellet in RNase-free water.
12. Put on ice.
13. Proceed with dilution of the RNA to a concentration of 100 ng μL$^{-1}$ and prepare aliquots:
    a) 3 μL for PCR to control for residual traces of endogenous DNA.
    b) 3 μL for Experion measurements.
    c) 20 μL (or more) for reverse transcription.
14. Store stocks and aliquots at –80 °C.

# Appendix B. Supplementary Results

## B.1. Screening of amoeba cultures

IS element specific PCR was performed with the primers ISCaa4F/ISCaa4R, targeting a 602 bp fragment of IS element ISCaa4, ISCAA5F/ISCaa5R, targeting a 423 bp fragment of ISCaa5, and ISCaa15F/ISCaa15R, targeting a 419 bp fragment of ISCaa15, for the identification of different *Amoebophilus asiaticus* strains. While ISCaa5 is found not only in *A. asiaticus* 5a2 but also in strain EIDS3 and US1, ISCaa15 is present only in two strains, 5a2 and EIDS3, and ISCaa4 is exclusive to strain 5a2. The PCR results (Figure B.1) are in accordance with this, since very distinct target bands for all three IS elements were observed for DNA from cultures presumably containing *A. asiaticus* 5a2, while only ISCaa5 and ISCaa15 primers resulted in target bands in DNA from strain EIDS3, and ISCaa5 in strain US1. Genomic DNA isolated from cultures of symbiont-free *Acanthamoeba* sp. resulted in weak target bands with all three primer pairs, which were slightly more pronounced for ISCaa4 and ISCaa5, and even fainter for ISCaa15. One explanation for the weak bands might be that cross contaminations occurred when handling DNA and/or PCR products. Contamination of the amoeba culture itself with *A. asiaticus* 5a2 is possible but rather unlikely, since (newly isolated) DNA from these supposedly symbiont-free amoebae was used as no-target control in qPCR as well and did not produce any wrong positive results. In addition, fluorescence *in situ* hybridisation (FISH; images not presented in this document) did not show any bacterial symbionts in the symbiont-free culture. For the no-template controls (PCR water) of the IS element PCR, no target bands were observed on the gel. Taken together, the presence of *A. asiaticus* and, in particular, strain 5a2, could be verified in the symbiont-containing cultures. Symbiont-free *Acanthamoeba* sp. cultures resulted in weak PCR target bands. But since the FISH results and later qPCR results did not support the finding of *A. asiaticus* in these cultures, it was concluded that the observed bands were most likely caused by cross contaminations during PCR and had no impact on the subsequent experimental steps.
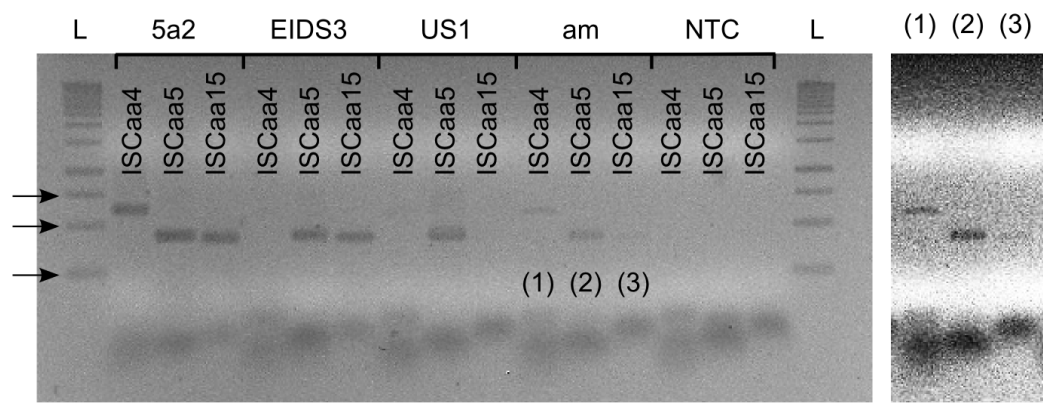
**Figure B.1** Agarose gelelectrophoresis of IS element PCR (1 % agarose, 120 V, 60 min). *L* GeneRuler™ 1 kb DNA Ladder; arrows highlight 250 bp, 500 bp, and 750 bp bands. *5a2, EIDS3, US1* DNA isolated from *Acanthamoeba* sp. harbouring different A. asiaticus strains (%a2, EIDS3, US1, respectively); *am* symbiont-free *Acanthamoeba* sp.; *NTC* no-template control; three lanes (1)-(3) are additionally shown with high contrast settings to highlight the presence of weak target bands.

# B.2. Evaluation of RNA extraction

The integrity of RNA extracts for RT-qPCR was assessed with an Experion™ Automated Electrophoresis system (Bio-Rad). Complete Experion™ results are presented in this section.
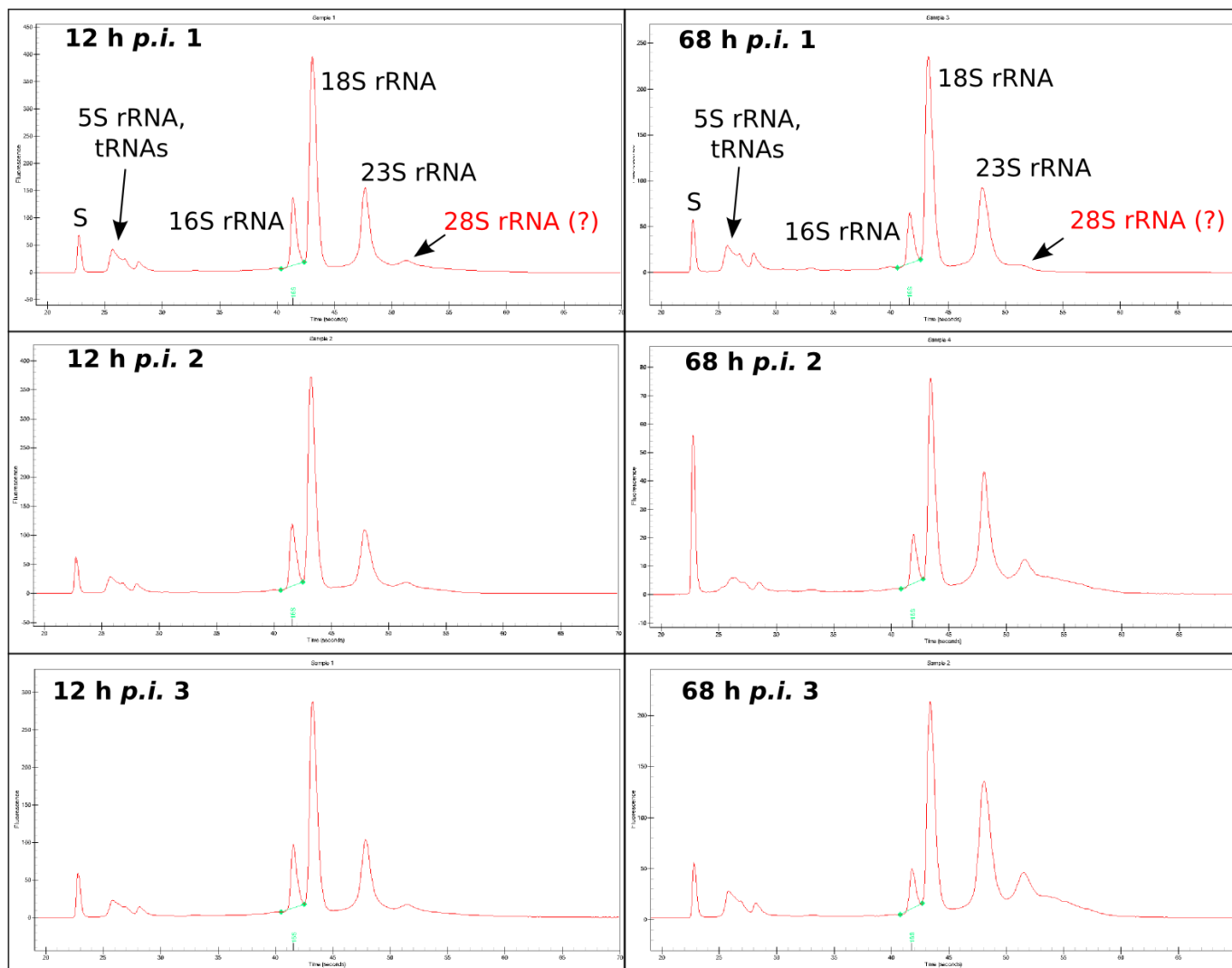


**Figure B.2** Electropherograms from the Experion™ analysis of RNA samples isolated from *Acanthamoeba* sp. infected with *A. asiaticus* 12 and 68 h *p.i. 1-3* biological replicates from the infection experiment; *S* signal peak of the Experion™ measurement; rRNA peaks are labeled accordingly. The small peak after the signal peak most likely consists of tRNAs and 5S rRNA. The 28S peaks are very flat and indicate degradation of large RNAs. All other rRNA peaks are very sharp and pronounced, indicating a very high overall quality of the RNA extracts.
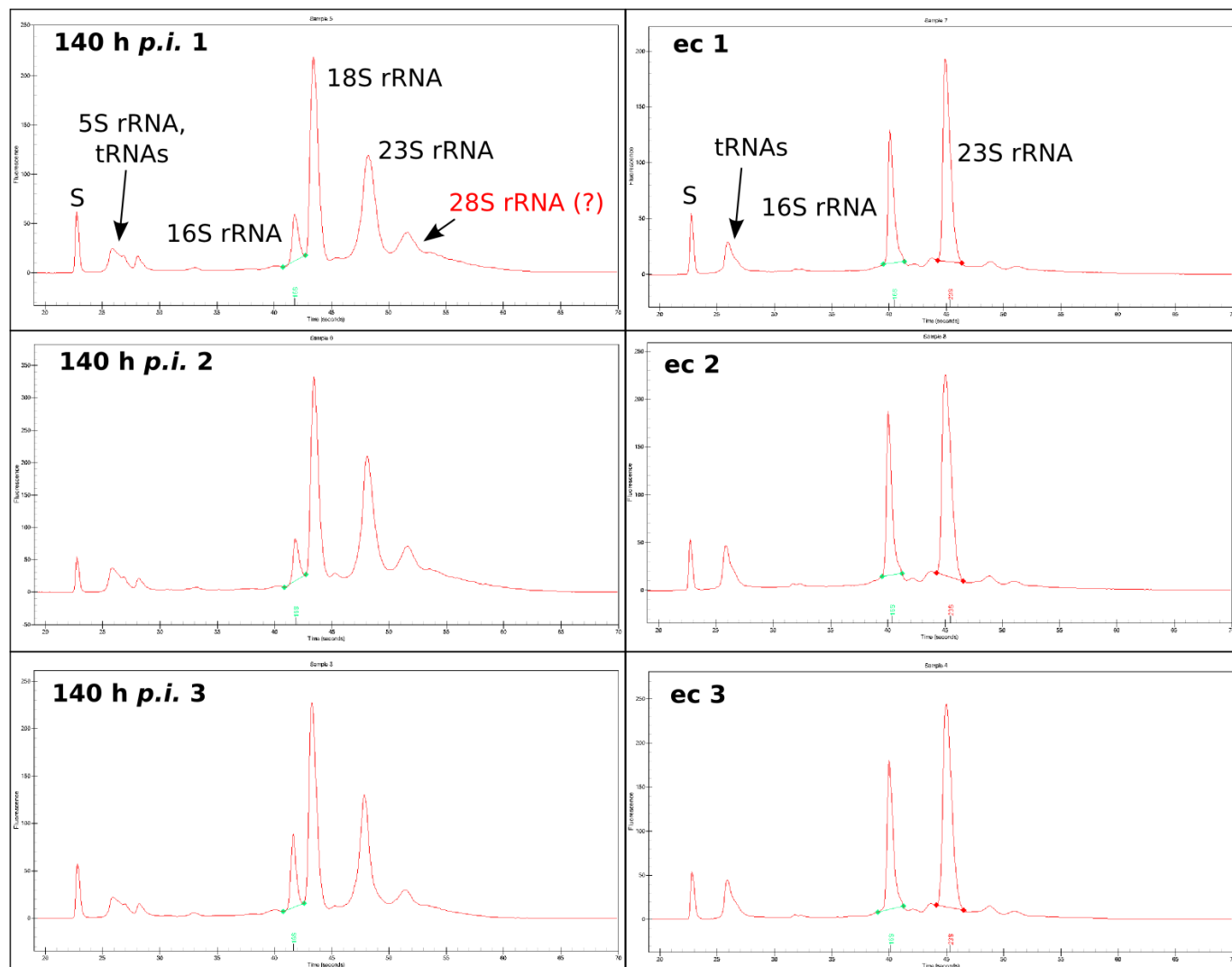
**Figure B.3** Electropherograms from the Experion™ analysis of RNA samples isolated from *Acanthamoeba* sp. infected with *A. asiaticus* 140 h *p.i.* and from extracellular *A. asiaticus*. *ec* extracellular *A. asiaticus*; *1-3* biological replicates from the infection experiment; *S* signal peak of the Experion™ measurement; rRNA peaks are labeled accordingly.
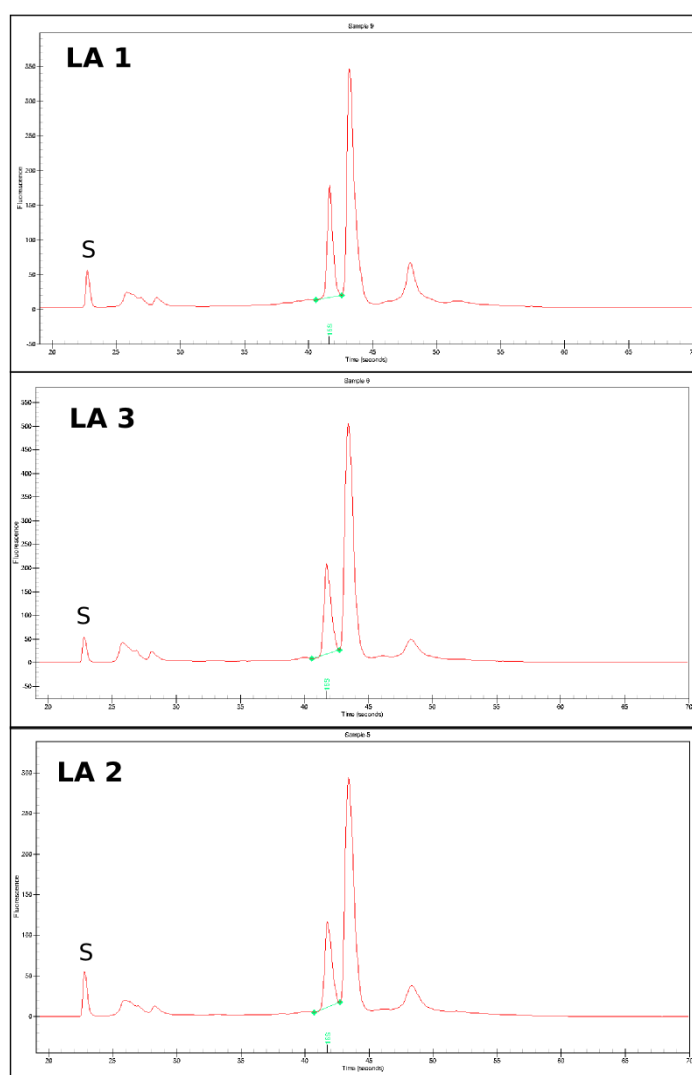
**Figure B.4** Electropherograms from the Experion™ analysis of RNA samples isolated from symbiont-free *Acanthamoeba* sp. *LA* RNA from symbiont-free amoebae; *1-3* biological replicates from the infection experiment; *S* signal peak.

# Appendix C. Sequences

## C.1. *A. asiaticus* prophage tail sheath gene clone

*A. asiaticus* prophage tail sheath (Aasi_1074) gene clone sequence including the flanking sequences of the pCR-XL-TOPO® vector from M13 Reverse to Forward primer. Used as standard in qPCR. Vector and insert sequences are given in 5′-to-3′ direction.

```
CAGGAAACAGCTATGACCATGATTACGCCAAGCTATTTAGGTGACGCGTTAGAATACTCAAGCTATGCATCAAGCTTGGTAC
CGAGCTCGGATCCACTAGTAACGGCCGCCAGTGTGCTGGAATTCGCCCTTGAGCTCCATGCCAGAAAATTTAAAAACTCCCG
GCGTATATATCGTCGAGAAGGACACCGGTGCCAATGCTGTGGTTCAGGTGGCAACTGCAGTTCCCGTTTTCATAGGATTTAC
CGAGCGGGCAGAAATCAATGGAAAATCTTTCCATATGAAGCCGGTGCATATTAACTCTTTATCTGAGTTTGAAATATTCTAT
GGAAAAGCACCTGTGCCTGTCTTTACCGTTAAACCTGCAGAAAAAGGAGGTGGAGATCTTAATATGAATGGACAAATGTATA
CCTTACAACAAAGTCCTTATTCAAAATTTTACCTATACAATAGTTTAAAATTATTTTTTGATAATGGTGGTGCAGATTGCTA
CATCATATCTATTGGACAATATGGTAAAGATCCACAACTGCTAGCAATTACCCCTGATACATTCAAAAAAGCAATAGATACC
TTAGCAGGCGAAGAAGTACCTACTATGTTGCTTATGCCCGACTCTCTGCTACTAGATGAAGAAGATTCTTCTTATTATTCTG
TACAAACATATGCTTTGCAACATTGTGGCAAATATATGGATAAAGTAGCGCTATTTGATATCTGGGGAAGTGGAGAAGAGCT
TCCATTAGGAGAAGACAAAAATAAATATGTAACTCGATTTAGAGAAATATAGGCTTAGACAACCTAACCTATGGTGCAGCG
TACTACCCTTGGGTTAAAACCAATATCATATCAATCAACGATATTGGATATGAGAACTTTAATTTAGATTCTTTAGAATCTC
TTATTAATGAAGCACACAAACCTATCCTGCACAATATCAAAACTGCTACTAGCGAAAAGGAGAAAAAATATTGGGATGCAGG
ACTTAAAAATGCTAGTAAAGAATATAAGCTTCTACGTAAAACTATAGCAGACAGACTTAATGTATTGCCAGCAGCACCAGCT
ATGGCAGGGTTGTACACGTACTGATAGAAGTAGAGGCGTATGGATAGCACCAGCTAACCAAAACCTAAATTCTGTTATTG
AGCCTGCTATTAAGATTACGCATGAAGATCAAGAAACTCTTAACGTAGATGCTATAAGCGGAAAATCTATTAATGCTATCCG
TGCATTTAGAGGAAGAGGATCTGCTATTGTTTGGGGGGCAAGAACGTTGGCAGGCAACAATGTAGAATGGCGCTATATTAAC
GTAAGGAGATTATTTATACTTATTGAACAGTCTATCAAACAAGCATCCTTCTCTGTTGTATTCCAACCTAACGTATCCATAA
CCTGGGCTATAGTAAAAGGAAGTATTGGTAACTTCTTAACCAACTTGTGGAGACAAGGTGCTTTAGTAGGAAACACTCCTTC
TGAAGCCTTTACAGTAAGCTGTGGACTTGGTGAAACTATGACTCAAGAAGACATTAATGAAGGTATCATGCGAATAAAAGTT
CAGGCAGCAGCTTCTAGACCAGCAGAGTTTATCGTCATTACATTTGAGCAAAAGATGGGCGGACAAGAAGGAGTCTCGAGA
AGGGCGAATTCTGCAGATATCCATCACACTGGCGGCCGCTCGAGCATGCATCTAGAGGGCCCAATTCGCCCTATAGTGAGTC
GTATTACAATTCACTGGCCGTCGTTTTAC
```

## C.2. *A. asiaticus* rpoB gene clone

*A. asiaticus* rpoB (Aasi_1396; partial sequence) gene clone sequence including the flanking sequences of the pCR-XL-TOPO® vector from M13 Reverse to Forward primer. Used as standard in qPCR. Vector and insert sequences are given in 5′-to-3′ direction.

```
CAGGAAACAGCTATGACCATGATTACGCCAAGCTATTTAGGTGACGCGTTAGAATACTCAAGCTATGCATCAAGCTTGGTAC
CGAGCTCGGATCCACTAGTAACGGCCGCCAGTGTGCTGGAATTCGCCCTTACTAGGTACGCCACCTGAAAAAAGAATTGATG
AAGGGCTACACAAAGTATTTAGAGAACACTTTCCCATAGAAGATTCCAGAGGAAATTTTGTACTAGAATTCATTGACTATAA
CCTTGATGCTCCTAAGTATGAACCCAGAGAATGTGTGGAAAGGGGAGTAACTTATTCTGTACCTCTTAAAGCAAAATTAAGG
CTACTACGTAATGATAATGATGATGATGAGTTTGAAACTATAGAGCAAGAAGTTTTTTTAGGCAATATTCCTTATATGACCT
CACAAGGCTCCTTTATAATCAATGGAGCAGAACGTGTGGTTGTCTCTCAAATACATAAATCTCCTGGCGTATTTTTTGCTCA
AAGTAAACACATTAGCGGTGCTAAGCTATACTCTGCTCGTATTATACCTTTCAAAGGTGCTTGGATAGAATTTGCTACGGAT
GTTAATAACATCATGTATGCCTATATAGACCGTAAGAAGAAATTCCCAATAACTACCCTTTTAAGGGCTATTGGCTATGGTA
CTGATAAAGAAATTTTAGACCTTTTTGAATTATCTGAAGAAATAAAGGTTACTAAATCTACTTTAAACCAACATATTGGTAG
AAAGTTGGCTGCAAGAGTACTTAGGTCTTGGTCCGAAGACTTTATAGATGAGGACACCGGTGAAGTTATTACACTAGATCGT
AATGAAGTGGTCTTAGAAAGAAACTCCATTCTTGATGAAACTGCTGTAGAGCTTATATTGCAGTCTGGCAGTTCTTCTGTTG
TATTGTATAGAGAAGATATTAATATTGCTGACTACGAAATTATATATAATACTTTACATAAAGATAATGCCAACTCCGAGAA
AGGGCGAATTCTGCAGATATCCATCACACTGGCGGCCGCTCGAGCATGCATCTAGAGGGCCCAATTCGCCCTATAGTGAGTC
GTATTACAATTCACTGGCCGTCGTTTTAC
```

Agnes Harreither

# Appendix D. Chemical formulas

$CaCl_2$
    calcium chloride

$Fe(NH_4)_2(SO_4)_2 \cdot 6\,H_2O$
    iron(II) ammonium sulfate (hexahydrate)

$H_2O$
    water

$HCl$
    hydrochloric acid

$KCl$
    potassium chloride
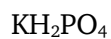
$KH_2PO_4$
    potassium dihydrogen phosphate

$MgCl_2$
    magnesium chloride

$MgSO_4$
    magnesium sulfate
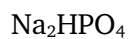
$Na_2HPO_4$
    sodium hydrogen phosphate

$Na_3C_6H_5O_7$
    sodium citrate
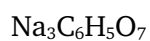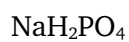
$NaH_2PO_4$
    sodium dihydrogen phosphate

$NaOH$
    sodium hydroxide

Agnes Harreither

# Glossary

| | |
|---|---|
| % (v/v) | volume/volume percentage |
| % (w/v) | weight/volume (or, more accurately, mass/volume) percentage |
| % (w/w) | weight/weight (or, more accurately, mass/mass) percentage |
| 16S rRNA | prokaryotic rRNA from the small ribosomal subunit |
| 18S rRNA | eukaryotic rRNA from the small ribosomal subunit |
| 23S rRNA | prokaryotic rRNA from the large ribosomal subunit |
| 28S rRNA | eukaryotic rRNA from the large ribosomal subunit |
| afp | antifeeding prophage |
| APS | ammonium persulfate |
| bp | base pairs (length unit for double-stranded nucleotide chains) |
| cDNA | complementary DNA |
| CI | cytoplasmic incompatibility |
| Cq | quantification cycle |
| DAPI | 4′,6-diamidino-2-phenylindole |
| DEPC | diethylpyrocarbonate |
| DNase | deoxyribonuclease |
| dNTP | deoxyribonucleotide |
| dsDNA | double-stranded DNA |
| DTT | Dithiothreitol |
| EDTA | ethylenediaminetetraacetic acid |
| FISH | fluorescence *in situ* hybridisation |
| FLUOS | 5(6)-Carboxyfluorescein-N-hydroxysuccinimide ester |
| gDNA | genomic DNA |
| GST | glutathione S-transferase |
| h *p.i.* | hours *post infection* |
| IPTG | isopropyl-β-D-1-thiogalactopyranoside |
| IS element | insertion sequence element |
| kb | kilobases (1 kb = 1000 bp) |
| LSM | laser scanning microscope |
| MCS | multiple cloning site |
| MOI | multiplicity of infection |
| mRNA | messenger RNA |
| nt | nucleotides (length unit for single-stranded nucleotide chains) |
| NTC | no-template control (e.g. in PCR or qPCR) |

GLOSSARY

| | |
|---|---|
| o/n | overnight |
| OD | optical density |
| PCR | polymerase chain reaction |
| PFA | paraformaldehyde |
| qPCR | quantitative real-time PCR |
| RNase | ribonuclease |
| rpm | revolutions per minute |
| rRNA | ribosomal RNA |
| RSD | relative standard deviation (i.e., standard deviation divided by arithmetic mean) |
| RT-PCR | reverse transcription PCR |
| RT-qPCR | reverse transcription qPCR |
| $R^2$ | coefficient of determination |
| SD | standard deviation |
| SDS | sodium dodecyl sulfate |
| SDS-PAGE | sodium dodecyl sulfate polyacrylamide gelelectrophoresis |
| T3SS | type three secretion system |
| T6SS | type six secretion system |
| TEM | transmission electron microscopy |
| tRNA | transfer RNA |
| USP | ubiquitin-specific protease |
| UV | ultraviolet |

# References

Al-Khodor, S.; Price, C. T.; Habyarimana, F.; Kalia, A. & Abu Kwaik, Y. (2008): **A Dot/Icm-translocated ankyrin protein of *Legionella pneumophila* is required for intracellular proliferation within human macrophages and protozoa.** *Molecular Microbiology* 70(4):908–923. doi:10.1111/j.1365-2958.2008.06453.x.

Alm, E. W. & Stahl, D. A. (2000): **Critical factors influencing the recovery and integrity of rRNA extracted from environmental samples: use of an optimized protocol to measure depth-related biomass distribution in freshwater sediments.** *Journal of Microbiological Methods* 40(2):153–162.

Altschul, S. F.; Gish, W.; Miller, W.; Myers, E. W. & Lipman, D. J. (1990): **Basic local alignment search tool.** *Journal of Molecular Biology* 215(3):403–410. doi:10.1016/S0022-2836(05)80360-2.

Amann, R. I.; Binder, B. J.; Olson, R. J.; Chisholm, S. W.; Devereux R. & Stahl, D. A. (1990): **Combination of 16S rRNA-targeted oligonucleotide probes with flow cytometry for analyzing mixed microbial populations.** *Applied and Environmental Microbiology* 56(6):1919–1925.

Amann, R.; Springer, N.; Schönhuber, W.; Ludwig, W.; Schmid, E. N.; Müller, D. & Michel, R. (1997): **Obligate intracellular bacterial parasites of acanthamoebae related to *Chlamydia* spp.** *Applied and Environmental Microbiology* 63(1):115–121.

Angot, A.; Vergunst, A.; Genin, S. & Peeters, N. (2007): **Exploitation of eukaryotic ubiquitin signaling pathways by effectors translocated by bacterial type III and type IV secretion systems.** *PLoS Pathogens* 3(1):e3. doi:10.1371/journal.ppat.0030003.

Artimo, P.; Jonnalagedda, M.; Arnold, K.; Baratin, D.; Csardi, G.; de Castro, E.; Duvaud, S.; Flegel, V.; Fortier, A.; Gasteiger, E.; Grosdidier, A.; Hernandez, C.; Ioannidis, V.; Kuznetsov, D.; Liechti, R.; Moretti, S.; Mostaguir, K.; Redaschi, N.; Rossier, G.; Xenarios, I. & Stockinger, H. (2012): **ExPASy: SIB bioinformatics resource portal.** *Nucleic Acids Research* 40(Web Server issue):W597–603. doi:10.1093/nar/gks400.

Basler, M.; Pilhofer, M.; Henderson, G. P.; Jensen, G. J. & Mekalanos, J. J. (2012): **Type VI secretion requires a dynamic contractile phage tail-like structure.** *Nature* 483(7388):182–186. doi:10.1038/nature10846.

Birtles, R.; Rowbotham, T.; Storey, C.; Marrie, T. & Raoult, D. (1997): **Chlamydia-like obligate parasite of free-living amoebae.** *The Lancet* 349(9056):925–926. doi:10.1016/S0140-6736(05)62701-8.

# REFERENCES

Birtles, R. J.; Rowbotham, T. J.; Michel, R.; Pitcher, D. G.; Lascola, B.; Alexiou-Daniel, S. & Raoult, D. (2000): **"*Candidatus* Odyssella thessalonicensis" gen. nov., sp. nov., an obligate intracellular parasite of *Acanthamoeba* species.** *International Journal of Systematic and Evolutionary Microbiology* 50(1):63–72. doi:10.1099/00207713-50-1-63.

Blumberg, D. D. (1987): **Creating a ribonuclease-free environment.** *Methods in Enzymology* 152:20–24.

Bozue, J. A. & Johnson, W. (1996): **Interaction of *Legionella pneumophila* with *Acanthamoeba castellanii*: uptake by coiling phagocytosis and inhibition of phagosome-lysosome fusion.** *Infection and Immunity* 64(2):668-673.

Bustin, S. A. & Nolan, T. (2004a): **Pitfalls of Quantitative Real-Time Reverse-Transcription Polymerase Chain Reaction.** *Journal of Biomolecular Techniques* 15(3):155–166.

Bustin, S. A. & Nolan, T. (2004b): **Template handling, preparation, and quantification.** In: *The Real-Time PCR Encyclopaedia A–Z of Quantitative PCR* (Bustin, S. A.), pp. 87–120. International University Line, La Jolla, CA, USA.

Bustin, S. A. (2005): **Real-time, fluorescence-based quantitative PCR: a snapshot of current procedures and preferences.** *Expert Review of Molecular Diagnostics* 5(4):493–498. doi:10.1586/14737159.5.4.493.

Bustin, S. A.; Benes, V.; Garson, J. A.; Hellemans, J.; Huggett, J.; Kubista, M.; Mueller, R.; Nolan, T.; Pfaffl, M. W.; Shipley, G. L.; Vandesompele, J. & Wittwer, C. T. (2009): **The MIQE guidelines: minimum information for publication of quantitative real-time PCR experiments.** *Clinical chemistry* 55(4):611–622. doi:10.1373/clinchem.2008.112797.

Caturegli, P.; Asanovich, K. M.; Walls, J. J.; Bakken, J. S.; Madigan, J. E.; Popov, V. L. & Dumler, J. S. (2000): **ankA: an *Ehrlichia phagocytophila* Group Gene Encoding a Cytoplasmic Protein Antigen with Ankyrin Repeats.** *Infection and Immunity* 68(9):5277–5283. doi:10.1128/IAI.68.9.5277-5283.2000.

Cazalet, C.; Rusniok, C.; Brüggemann, H.; Zidane, N.; Magnier, A.; Ma, L. *et al.* (2004): **Evidence in the *Legionella pneumophila* genome for exploitation of host cell functions and high genome plasticity.** *Nature Genetics* 36(11):1165–1173. doi:10.1038/ng1447.

Chen, J.; Kadlubar, F. F. & Chen, J. Z. (2007): **DNA supercoiling suppresses real-time PCR: a new approach to the quantification of mitochondrial DNA damage and repair.** *Nucleic Acids Research* 35(4):1377–88. doi:10.1093/nar/gkm010.

Collingro, A.; Toenshoff, E. R.; Taylor, M. W.; Fritsche, T. R.; Wagner, M. & Horn, M. (2005): **"*Candidatus* Protochlamydia amoebophila", an endosymbiont of *Acanthamoeba* spp.** *International Journal of Systematic and Evolutionary Microbiology* 55(5):1863–1866. doi:10.1099/ijs.0.63572-0.

Daims, H.; Brühl, A.; Amann, R.; Schleifer, K.-H. & Wagner, M. (1999): **The Domain-specific Probe EUB338 is Insufficient for the Detection of all *Bacteria*: Development and Evaluation of a more Comprehensive Probe Set.** *Systematic and Applied Microbiology* 22(3):434–444. doi: 10.1016/S0723-2020(99)80053-8.

Daims, H.; Stoecker, K. & Wagner, M. (2005): **Fluorescence in situ hybridization for the detection of prokaryotes.** In: *Molecular Microbial Ecology* (Osborn, A. M. & Smith, C. J.), pp. 213– 239. In: *Advanced Methods*. Taylor & Francis Group; Abingdon, United Kingdom. URL http:// www.taylorandfrancis.com/books/details/9781859962831/.

De Bary, H. A. (1879): **Die Erscheinung der Symbiose.** K.J. Trübner; Straßburg, Frankreich.

Dumon-Seignovert, L.; Cariot, G. & Vuillard, L. (2004): **The toxicity of recombinant proteins in *Escherichia coli*: a comparison of overexpression in BL21(DE3), C41(DE3), and C43(DE3).** *Protein Expression and Purification* 37(1):203–206. doi:10.1016/j.pep.2004.04.025.

Feinberg, A. P. & Vogelstein, B. (1983): **A technique for radiolabeling DNA restriction endonuclease fragments to high specific activity.** *Analytical Biochemistry* 132(1):6–13. doi:10.1016/0003-2697(84)90381-6.

Fleige, S. & Pfaffl, M. W. (2006): **RNA integrity and the effect on the real-time qRT-PCR performance.** *Molecular Aspects of Medicine* 27(2-3):126–139. doi:10.1016/j.mam. 2005.12.003.

Fritsche, T. R.; Horn, M.; Seyedirashti, S.; Gautom, R. K. & Schleifer, K. (1999): **In Situ Detection of Novel Bacterial Endosymbionts of *Acanthamoeba* spp. Phylogenetically Related to Members of the Order *Rickettsiales*.** *Applied and Environmental Microbiology* 65(1):206–212.

Fritsche, T. R.; Horn, M.; Wagner, M.; Herwig, R. P.; Schleifer, K.; Romesh, K. & Gautom, R. K. (2000): **Phylogenetic Diversity among Geographically Dispersed *Chlamydiales* Endosymbionts Recovered from Clinical and Environmental Isolates of *Acanthamoeba* spp.** *Applied and Environmental Microbiology* 66(6):2613–2619. doi:10.1128/AEM.66.6.2613-2619.2000.

Glare, T. R.; Corbett, G. E. & Sadler, T. J. (1993): **Association of a Large Plasmid with Amber Disease of the New Zealand Grass Grub, *Costelytra zealandica*, Caused by *Serratia entomophila* and *Serratia proteamaculans*.** *Journal of Invertebrate Pathology* 62(2):165–170. doi:10.1006/jipa.1993.1091.

Greub, G. & Raoult, D. (2002): **Crescent Bodies of *Parachlamydia acanthamoeba* and Its Life Cycle within *Acanthamoeba polyphaga*: an Electron Micrograph Study.** *Applied and Environmental Microbiology* 68(6):3076–3084. doi:10.1128/AEM.68.6.3076.

Grossman, T. H.; Kawasaki, E. S.; Punreddy, S. R. & Osburne, M. S. (1998): **Spontaneous cAMP-dependent derepression of gene expression in stationary phase plays a role in recombinant expression instability.** *Gene* 209(1):95–103. doi:10.1016/S0378-1119(98) 00020-1.

REFERENCES

Habyarimana, F.; Al-Khodor, S.; Kalia, A.; Graham, J. E.; Price, C. T.; Garcia, M. T. & Kwaik, Y. A. (2008): **Role for the Ankyrin eukaryotic-like genes of *Legionella pneumophila* in parasitism of protozoan hosts and human macrophages.** *Environmental Microbiology* 10(6):1460–1474. doi:10.1111/j.1462-2920.2007.01560.x.

Hackstadt, T. (1998): **The diverse habitats of obligate intracellular parasites.** *Current Opinion in Microbiology* 1(1):82–87. doi:10.1016/S1369-5274(98)80146-X.

Harb, O. S.; Gao, L. & Abu, Y. (2000): **From protozoa to mammalian cells: a new paradigm in the life cycle of intracellular bacterial pathogens.** *Environmental Microbiology* 2(3):251–265. doi:10.1046/j.1462-2920.2000.00112.x.

Hausmann, B. (2012): **Substrate utilisation of sulfate-reducing microorganisms in a peatland.** University of Vienna; Vienna, Austria.

Hayes, F. (2003): **The function and organization of plasmids.** In: *E. coli Plasmid Vectors* (Casali, N. & Preston, A.), pp. 1–18, Humana Press Inc., Totowa, NJ, USA.

Hochuli, E.; Bannwarth, W.; Döbeli, H.; Gentz, R. & Stüber, D. (1988): **Genetic Approach to Facilitate Purification of Recombinant Proteins with a Novel Metal Chelate Adsorbent.** *Nature Biotechnology* 6(11):1321–1325. doi:10.1038/nbt1188-1321.

Horn, M.; Fritsche, T. R.; Gautom, R. K.; Schleifer, K. H. & Wagner, M. (1999): **Novel bacterial endosymbionts of *Acanthamoeba* spp. related to the *Paramecium caudatum* symbiont *Caedibacter caryophilus*.** *Environmental Microbiology* 1(4):357–367. doi:10.1046/j.1462-2920.1999.00045.x.

Horn, M.; Wagner, M.; Mu, K.; Schmid, E. N.; Fritsche, T. R.; Schleifer, K. & Michel, R. (2000): ***Neochlamydia hartmanellae* gen. nov., sp. nov. (*Parachlamydiaceae*), an endoparasite of the amoeba *Hartmannella vermiformis*.** *Microbiology* 146:1231–1239.

Horn, M.; Harzenetter, M. D.; Linner, T.; Schmid, E. N.; Müller, K. D.; Michel, R. & Wagner, M. (2001): **Members of the *Cytophaga-Flavobacterium-Bacteroides* phylum as intracellular bacteria of acanthamoebae: proposal of "*Candidatus* Amoebophilus asiaticus."** *Environmental Microbiology* 3(7):440–449. doi:10.1046/j.1462-2920.2001.00210.x.

Horn, M.; Fritsche, T. R.; Linner, T.; Gautom, R. K.; Harzenetter, M. D. & Wagner, M. (2002): **Obligate bacterial endosymbionts of *Acanthamoeba* spp. related to the beta-*Proteobacteria*: proposal of "*Candidatus* Procabacter acanthamoebae" gen. nov., sp. nov**. *International Journal of Systematic and Evolutionary Microbiology* 52(2):599–605.

Horn, M.; Collingro, A.; Schmitz-Esser, S.; Beier, C. L.; Purkhold, U.; Fartmann, B.; Brandt, P.; Nyakatura, G. J.; Droege, M.; Frishman, D.; Rattei, T.; Mewes, H.-W. & Wagner, M. (2004): **Illuminating the evolutionary history of chlamydiae.** *Science* 304(5671):728–730. doi:10.1126/science.1096330.

Horn, M. (2008): **Chlamydiae as symbionts in eukaryotes.** *Annual Review of Microbiology* 62:113–131. doi:10.1146/annurev.micro.62.081307.162818.

Hou, Y.; Zhang, H.; Miranda, L. & Lin, S. (2010): **Serious overestimation in quantitative PCR by circular (supercoiled) plasmid standard: microalgal pcna as the model gene.** *PloS One* 5(3):e9545. doi:10.1371/journal.pone.0009545.

Hunter, M. S.; Perlman, S. J. & Kelly, S. E. (2003): **A bacterial symbiont in the *Bacteroidetes* induces cytoplasmic incompatibility in the parasitoid wasp *Encarsia pergandiella*.** *Proceedings of the Royal Society of London. Series B: Biological Sciences* 270(1529):2185–90. doi:10.1098/rspb.2003.2475.

Hurst, M. R. H.; Glare, T. R. & Jackson, T. A. (2004): **Cloning *Serratia entomophila* Antifeeding Genes − a Putative Defective Prophage Active against the Grass Grub *Costelytra zealandica*.** *Journal of Bacteriology* 186(15):5116-5128. doi:10.1128/JB.186.15.5116.

Hurst, M. R. H.; Beard, S. S.; Jackson, T. A. & Jones, S. M. (2007): **Isolation and characterization of the *Serratia entomophila* antifeeding prophage.** *FEMS Microbiology Letters* 270(1):42–48. doi:10.1111/j.1574-6968.2007.00645.x.

Hybiske, K. & Stephens, R. S. (2008): **Exit strategies of intracellular pathogens.** *Nature Reviews Microbiology* 6(2):99–110. doi:10.1038/nrmicro1821.

Inkscape contributors (2011): **Inkscape.** URL http://inkscape.org/.

Jackson, T. A. (1995): **Amber disease reduces trypsin activity in midgut of *Costelytra zealandica* (*Coleoptera; Scarabaeidae*) larvae.** *Journal of Invertebrate Pathology* 65(1):68-69.

Jackson, T. A.; Huger, A. M. & Glare, T. R. (1993): **Pathology of Amber Disease in the New Zealand Grass Grub *Costelytra zealandica* (*Coleoptera: Scarabaeidae*).** *Journal of Invertebrate Pathology* 61(2):123–130. doi:10.1006/jipa.1993.1024.

Jackson, T. A.; Boucias, D. G. & Thaler, J.-O. (2001): **Pathobiology of Amber Disease, Caused by *Serratia* Spp., in the New Zealand Grass Grub, *Costelytra zealandica*.** *Journal of Invertebrate Pathology* 78(4):232–243. doi:10.1006/jipa.2002.5078.

Kahane, S.; Metzer, E. & Friedman, M. G. (1995): **Evidence that the novel microorganism "Z" may belong to a new genus in the family *Chlamydiaceae*.** FEMS Microbiology Letters 126(2):203–207. doi:10.1111/j.1574-6968.1995.tb07417.x.

Kimball, S.; Mattis, P. & the GIMP Development Team (2010): **GNU Image Manipulation Program.** URL http://www.gimp.org/.

Kubori, T.; Hyakutake, A. & Nagai, H. (2008): ***Legionella* translocates an E3 ubiquitin ligase that has multiple U-boxes with distinct functions.** *Molecular microbiology* 67(6):1307–1319. doi:10.1111/j.1365-2958.2008.06124.x.

REFERENCES

Kwaik, Y. A. (1996): **The phagosome containing *Legionella pneumophila* within the protozoan *Hartmannella vermiformis* is surrounded by the rough endoplasmic reticulum.** *Applied and Environmental Microbiology*. 62(6):2022–2028.

Leiman, P. G.; Basler, M.; Ramagopal, U. A.; Bonanno, J. B.; Sauder, J. M.; Pukatzki, S. *et al.* (2009). **Type VI secretion apparatus and phage tail-associated protein complexes share a common evolutionary origin.** *Proceedings of the National Academy of Sciences of the United States of America* 106(11):4154–4159. doi:10.1073/pnas.081336010.

LibreOffice contributors and/or their affiliates (2012): **LibreOffice Productivity Suite.** The Document Foundation. URL http://www.libreoffice.org/.

Mahillon, J. & Chandler, M. (1998). **Insertion Sequences.** *Microbiology and Molecular Biology Reviews*, 62(3):725–774.

Manchester, K. L. (1996): **Use of UV methods for measurement of protein and nucleic acid concentrations.** *Biotechniques* 20(6):968–970.

Margulis, L. (1981): **Symbiosis in cell evolution: life and its environment on the early Earth.** W. H. Freeman & Company; New York, NY, USA.

Miroux, B. & Walker, J. E. (1996). **Over-production of proteins in *Escherichia coli*: mutant hosts that allow synthesis of some membrane proteins and globular proteins at high levels.** *Journal of Molecular Biology* 260(3):289–298. doi:10.1006/jmbi.1996.0399.

Mohr, P. J.; Taylor, B. N. & Newell, D. B. (2012): **CODATA recommended values of the fundamental physical constants: 2010 (Web Version 6.3).** *Reviews of Modern Physics* 84(4):1527–1605. doi:10.1103/RevModPhys.84.1527. This database was developed by J. Baker, M. Douma, and S. Kotochigova. National Institute of Standards and Technology, Gaithersburg, MD 20899. URL http://physics.nist.gov/constants (accessed 2012-06-14).

Molmeret, M.; Horn, M.; Wagner, M. & Santic, M. (2005): **Amoebae as Training Grounds for Intracellular Bacterial Pathogens.** *Applied and Environmental Microbiology* 71(1):20–28. doi:10.1128/AEM.71.1.20.

Molofsky, A. B. & Swanson, M. S. (2004). **Differentiate to thrive: lessons from the *Legionella pneumophila* life cycle.** *Molecular Microbiology* 53(1):29–40. doi:10.1111/j.1365-2958.2004.04129.x.

Moran, N. A. (2006): **Symbiosis**. *Current Biology* 16(20):R866–R871. doi:10.1016/j.cub.2006.09.019.

Moran, N. A.; McCutcheon, J. P. & Nakabachi, A. (2008): **Genomics and evolution of heritable bacterial symbionts.** *Annual Review of Genetics* 42:165–190. doi:10.1146/annurev.genet.41.110306.130119.

Mueller, O.; Lightfoot, S. & Schroeder, A. (2004). **RNA Integrity Number (RIN) – Standardization of RNA Quality Control Application.** Application Note. Agilent Technologies, Santa Clara, CA, USA.

Munson, M. A.; Baumann, P. & Kinsey, M. G. (1991): ***Buchnera* gen. nov. and *Buchnera aphidicola* sp. nov., a taxon consisting of the mycetocyte-associated, primary endosymbionts of aphids.** *International Journal of Systematic Bacteriology* 41(4):566–568.

Newsome, A. L.; Baker, R. L.; Miller, R. D. & Arnold, R. R. (1985): **Interactions between *Naegleria fowleri* and *Legionella pneumophila*.** *Infection and Immunity* 50(2):449–452.

Newton, H. J.; Sansom, F. M.; Dao, J.; McAlister, A. D.; Sloan, J.; Cianciotto, N. P. & Hartland, E. L. (2007): **Sel1 repeat protein LpnE is a *Legionella pneumophila* virulence determinant that influences vacuolar trafficking.** *Infection and Immunity* 75(12):5575–5585. doi:10.1128/ IAI.00443-07.

Nielsen, H. (2011): **Working with RNA.** In: *RNA: Methods and Protocols* (Nielsen, H.), pp. 15–28. In: *Methods in Molecular Biology*, vol. 703 (Walker, J. M.). Springer Science+Business Media; New York, NY, USA. URL http://www.springerlink.com/content/t4u6038j71108161/.

Nijman, S. M. B.; Luna-Vargas, M. P. A.; Velds, A.; Brummelkamp, T. R.; Dirac, A. M. G.; Sixma, T. K. & Bernards, R. (2005): **A genomic and functional inventory of deubiquitinating enzymes.** *Cell* 123(5):773–786. doi:10.1016/j.cell.2005.11.007.

Nolan, T.; Hands, R. E. & Bustin, S. A. (2006). **Quantification of mRNA using real-time RT-PCR.** *Nature Protocols* 1(3):1559–1582. doi:10.1038/nprot.2006.236.

Pan, X.; Lührmann, A.; Satoh, A.; Laskowski-Arce, M. A. & Roy, C. R. (2008): **Ankyrin repeat proteins comprise a diverse family of bacterial type IV effectors.** *Science* 320(5883):1651–1654. doi:10.1126/science.1158160.

Parkhill, J.; Sebaihia, M.; Preston, A.; Murphy, L. D.; Thomson, N.; Harris, D. E. *et al.* (2003). **Comparative analysis of the genome sequences of *Bordetella pertussis*, *Bordetella parapertussis* and *Bordetella bronchiseptica*.** *Nature Genetics* 35(1):32–40. doi:10.1038/ ng1227.

Penz, T.; Horn, M. & Schmitz-Esser, S. (2010): **The genome of the amoeba symbiont "*Candidatus* Amoebophilus asiaticus" encodes an afp-like prophage possibly used for protein secretion.** *Virulence* 1(6):541–545. doi:10.4161/viru.1.6.13800.

Penz, T.; Schmitz-Esser, S.; Kelly, S. E.; Cass, B. N.; Müller, A.; Woyke, T.; Malfatti, S. A.; Hunter, M. S. & Horn, M. (2012): **Comparative Genomics Suggests an Independent Origin of Cytoplasmic Incompatibility in *Cardinium hertigii*.** *PLoS Genetics* 8(10):e1003012. doi:10.1371/journal. pgen.1003012.

REFERENCES

Persson, O. P.; Pinhassi, J.; Riemann, L.; Marklund, B.-I.; Rhen, M.; Normark, S.; González, J. M. & Hagström, A. (2009): **High abundance of virulence gene homologues in marine bacteria.** *Environmental Microbiology* 11(6):1348–1357. doi:10.1111/j.1462-2920.2008.01861.x.

Peters, J.; Wilson, D. P.; Myers, G.; Timms, P. & Bavoil, P. M. (2007): **Type III secretion à la Chlamydia.** *Trends in Microbiology* 15(6):241–251. doi:10.1016/j.tim.2007.04.005.

Pfaffl, M.W. (2005): **Nucleic acids: mRNA identification and quantification.** In: *Nucleic Acids, Encyclopedia of Analytical Science*, pp. 417–426. Academic Press.

R Development Core Team (2011): **R: A language and environment for statistical computing.** R Foundation for Statistical Computing; Vienna, Austria. URL http://www.r-project.org/.

Renatus, M.; Parrado, S. G.; D'Arcy, A.; Eidhoff, U.; Gerhartz, B.; Hassiepen, U.; Pierrat, B.; Riedl, R.; Vinzenz, D.; Worpenberg, S. & Kroemer, M. (2006): **Structural basis of ubiquitin recognition by the deubiquitinating protease USP2.** *Structure* 14(8):1293–1302. doi:10.1016/j.str. 2006.06.012.

Renesto, P.; Dehoux, P.; Gouin, E.; Touqui, L.; Cossart, P. & Raoult, D. (2003): **Identification and characterization of a phospholipase D-superfamily gene in rickettsiae.** *Journal of Infectious Diseases* 188(9):1276–1283. doi:10.1086/379080.

Rice, P.; Longden, I. & Bleasby, A. (2000): **EMBOSS : The European Molecular Biology Open Software Suite.** *Trends in Genetics* 16(6):2–3.

Rodríguez-Zaragoza, S. (1994): **Ecology of Free-Living Amoebae.** *Critical Reviews in Microbiology* 20(3):225–241. doi:10.3109/10408419409114556.

Rogers, J. & Keevil, C. W. (1992): **Immunogold and fluorescein immunolabelling of *Legionella pneumophila* within an aquatic biofilm visualized by using episcopic differential interference contrast microscopy.** *Applied and Environmental Microbiology* 58(7):2326–2330.

Rogers, J.; Dennis, P. J.; Lee, J. V. & Keevil, C. W. (1994): **Influence of Temperature and Plumbing Material Selection on Biofilm Formation and Growth of *Legionella pneumophila* in a Model Portable Water System Containing Complex Microbial Flora.** *Applied and Environmental Microbiology* 60(5):1585-1592.

Rowbotham, T. J. (1986): **Current views on the relationships between amoebae, legionellae and man.** *Israel Journal of Medical Sciences* 22(9):678–689.

Rozen, S. & Skaletsky, H. J. (2000): **Primer3 on the WWW for general users and for biologist programmers.** In: *Bioinformatics Methods and Protocols: Methods in Molecular Biology* (Krawetz, S. & Misener, S.), pp. 365–386. Humana Press, Totowa, NJ, USA.

Rytkönen, A. & Holden, D. W. (2007). **Bacterial interference of ubiquitination and deubiquitination.** *Cell Host & Microbe* 1(1):13–22. doi:10.1016/j.chom.2007.02.003.

Agnes Harreither

Sambrook, J. & Russell, D. W. (2000): **Molecular Cloning: A Laboratory Manual.** Cold Spring Harbor Laboratory; Cold Spring Harbor, NY, USA.

Sapp, J. (1994): **Evolution by Association: A History of Symbiosis.** Oxford University Press; Oxford, United Kingdom.

Sato, K.; Naito, M.; Yukitake, H.; Hirakawa, H.; Shoji, M.; McBride, M. J.; Rhodes, R. G. & Nakayama, K. (2010): **A protein secretion system linked to bacteroidete gliding motility and pathogenesis.** *Proceedings of the National Academy of Sciences of the United States of America* 107(1):276–281. doi:10.1073/pnas.0912010107.

Schmitz-Esser, S.; Toenshoff, E. R.; Haider, S.; Heinz, E.; Hoenninger, V. M.; Wagner, M. & Horn, M. (2008): **Diversity of bacterial endosymbionts of environmental acanthamoeba isolates.** *Applied and Environmental Microbiology* 74(18):5822–5831. doi:10.1128/AEM.01093-08.

Schmitz-Esser, S.; Tischler, P.; Arnold, R.; Montanaro, J.; Wagner, M.; Rattei, T. & Horn, M. (2010): **The genome of the amoeba symbiont "*Candidatus* Amoebophilus asiaticus" reveals common mechanisms for host cell interaction among amoeba-associated bacteria.** *Journal of Bacteriology* 192(4):1045–1057. doi:10.1128/JB.01379-09.

Schmitz-Esser, S.; Penz, T.; Spang, A. & Horn, M. (2011): **A bacterial genome in transition – an exceptional enrichment of IS elements but lack of evidence for recent transposition in the symbiont *Amoebophilus asiaticus*.** *BMC Evolutionary Biology* 11:270. doi:10.1186/1471-2148-11-270.

Seshadri, R.; Paulsen, I. T.; Eisen, J. A.; Read, T. D.; Nelson, K. E.; Nelson, W. C. *et al.* (2003): **Complete genome sequence of the Q-fever pathogen *Coxiella burnetii*.** *Proceedings of the National Academy of Sciences of the United States of America* 100(9):5455–5460. doi:10.1073/ pnas. 0931379100.

Siguier, P.; Filée, J. & Chandler, M. (2006): **Insertion sequences in prokaryotic genomes.** *Current Opinion in Microbiology* 9(5):526–531. doi:10.1016/j.mib.2006.08.005.

Ståhlberg, A.; Aman, P.; Ridell, B.; Mostad, P. & Kubista, M. (2003): **Quantitative real-time PCR method for detection of B-lymphocyte monoclonality by comparison of kappa and lambda immunoglobulin light chain expression.** *Clinical Chemistry* 49(1):51–59.

Ståhlberg, A.; Håkansson, J.; Xian, X.; Semb, H. & Kubista, M. (2004): **Properties of the reverse transcription reaction in mRNA quantification.** *Clinical Chemistry* 50(3):509–515. doi:10.1373/clinchem.2003.026161.

Sunagawa, S.; DeSantis, T. Z.; Piceno, Y. M.; Brodie, E. L.; DeSalvo, M. K.; Voolstra, C. R.; Weil, E.; Andersen, G. L. & Medina, M. (2009): **Bacterial diversity and White Plague Disease-associated community changes in the Caribbean coral *Montastraea faveolata*.** *The ISME Journal* 3(5):512–521. doi:10.1038/ismej.2008.131.

REFERENCES

Tan, H. M. (1999): **Bacterial catabolic transposons.** *Applied microbiology and biotechnology* 51(1):1–12.

Tindall, K. R. & Kunkel, T. A. (1988): **Fidelity of DNA synthesis by the *Thermus aquaticus* DNA polymerase.** *Biochemistry* 27(16):6008–6013. doi:10.1021/bi00416a027.

Tsao, H.-F. (2011): **Characterization of the infection cycle of the intracellular *Acanthamoeba* symbiont *Amoebophilus asiaticus*.** University of Vienna; Vienna, Austria.

Tseng, T.-T.; Tyler, B. M. & Setubal, J. C. (2009): **Protein secretion systems in bacterial-host associations, and their description in the Gene Ontology.** *BMC Microbiology* 9(Suppl 1):S2. doi:10.1186/1471-2180-9-S1-S2.

Vogel, J. P.; Andrews, H. L.; Wong, S. K. & Isberg, R. R. (1998): **Conjugative Transfer by the Virulence System of *Legionella pneumophila*.** *Science* 279(5352):873–876. doi:10.1126/science.279.5352. 873.

Voth, D. E.; Howe, D.; Beare, P. A.; Vogel, J. P.; Unsworth, N.; Samuel, J. E. & Heinzen, R. A. (2009): **The *Coxiella burnetii* ankyrin repeat domain-containing protein family is heterogeneous, with C-terminal truncations that influence Dot/Icm-mediated secretion.** *Journal of Bacteriology* 191(13):4232–4242. doi:10.1128/JB.01656-08.

Wagner, A. (2006): **Cooperation is fleeting in the world of transposable elements.** *PLoS Computational Biology* 2(12):e162. doi:10.1371/journal.pcbi.0020162.

Weissenmayer, B. A.; Prendergast, J. G. D.; Lohan, A. J. & Loftus, B. J. (2011): **Sequencing illustrates the transcriptional response of *Legionella pneumophila* during infection and identifies seventy novel small non-coding RNAs.** *PloS One* 6(3):e17570. doi:10.1371/journal.pone. 0017570.

Welchman, R. L.; Gordon, C. & Mayer, R. J. (2005): **Ubiquitin and ubiquitin-like proteins as multifunctional signals.** *Nature Reviews Molecular Cell Biology* 6(8):599–609. doi:10.1038/nrm1700.

Wernegreen, J. J. (2005): **For better or worse: genomic consequences of intracellular mutualism and parasitism.** *Current Opinion in Genetics & Development* 15(6):572–583. doi:10.1016/j.gde. 2005.09.013.

Wickham, H. (2009): **ggplot2: Elegant Graphics for Data Analysis.** Springer Science+Business Media, New York, NY, USA. URL http://ggplot2.org/.

Yang, G.; Dowling, A. J.; Gerike, U. & Waterfield, N. R. (2006): ***Photorhabdus* Virulence Cassettes Confer Injectable Insecticidal Activity against the Wax Moth.** *Journal of Bacteriology* 188(6):2254–2261. doi:10.1128/JB.188.6.2254.

Zchori-Fein, E. (2004): **Characterization of a *"Bacteroidetes"* symbiont in *Encarsia* wasps (*Hymenoptera: Aphelinidae*): proposal of *"Candidatus* Cardinium hertigii."** *International Journal of Systematic and Evolutionary Microbiology* 54(3):961–968. doi:10.1099/ijs.0.02957-0.

Zheng, D.; Alm, E. W.; Stahl, D. A. & Raskin, L. (1996): **Characterization of universal small-subunit rRNA hybridization probes for quantitative molecular microbial ecology studies.** *Applied and Environmental Microbiology* 62(12):4504–4513.

Zheng, J. & Leung, K. Y. (2007): **Dissection of a type VI secretion system in Edwardsiella tarda.** *Molecular Microbiology* 66(5):1192–206. doi:10.1111/j.1365-2958.2007.05993.x.

REFERENCES

Agnes Harreither

# Acknowledgements

First of all, I want to thank Thomas Penz for being an exceptional supervisor during this thesis. He always had an open ear for my questions and never got tired of encouraging me to carry on whenever I encountered some challenges.

I also want to thank Univ.-Prof. Dr. Michael Wagner, the head of our department, and Univ.-Prof. Dr. Matthias Horn, our group leader, for awakening my interest in the field of microbial ecology already in their lectures and giving me the opportunity to write my diploma thesis at DOME. In particular, I want to thank Univ.-Prof. Dr. Matthias Horn for giving me the chance to become a member of his group and all his encouragement during the last months.

Also, thanks to our collaboration partners, Dr. Rok Kostanjšek at the University of Ljubljana and Dr. Martin Pilhofer at the California Institute of Technology.

Working is always much nicer in a good atmosphere. Therefore, I want to thank all DOMiEs for making this intense time of my life so enjoyable and rich in variety. Also, thanks to the whole symbiosis group for a lot of fruitful scientific and non-scientific discussions and all the fun we had together. Thanks to Allen for patiently introducing me into the world of amoeba infections and lending me a helpful hand to take the most awesome CLSM pictures; to Alex for all his advices and support while writing my thesis; to Bela for the enthusiastic and helpful discussions about qPCR, statistics, and so many other science-related topics that I cannot even list them all here; to Karin for a lot of help with protein stuff, prophage purifications and fancy electron microscopy techniques; to our technician Martina Grill for all the sequencing and ordering, and for being awesome; and to all other DOMiEs for taking time to answer my questions.

Thanks a lot to all my fellow diploma, master & bachelor students – Andi, Bela, Brigitte, Claus, Esther, Feli, Florian and Florian, Jasmin, Jochen, Julia, Karim, Kathi, Madeleine, Martin, Michi, Mischa, Nici, Simone, Stefanie, Stephan, Tina, and Tomi – for the nice time inside and outside the lab, for countless coffee breaks and after-work pizza or drinks on the patio, and all the fun we had.

I also want to thank all my friends outside the DOMiEs for being patient with me whenever I arrived late or had no time at all "because I just had to finish off that last qPCR run".

Finally, I especially want to thank my parents for their boundless support and positive reinforcement in every aspect of my life – and for showing interest in my attempts to explain things about my thesis they didn't even know they wanted to know until I started explaining.

ACKNOWLEDGEMENTS

Agnes Harreither

# Curriculum Vitae

**Personal data**

| | |
|---|---|
| Name | Harreither, Agnes Katharina |
| Date of birth | March 18, 1987 |
| Place of birth | Vienna, Austria |
| Nationality | Austria |

**Education**

| | |
|---|---|
| 1993–1997 | Volksschule Putzendoplergasse, Vienna, Austria |
| 1997–2005 | Bundesgymnasium Alt Erlaa, Vienna, Austria |
| 2005 | Matura (high school diploma) at the Bundesgymnasium Alt Erlaa |
| since 2005 | Study of biology with focus on microbiology and genetics, University of Vienna, Austria |
| since 2011 | Diploma thesis at the Department of Microbial Ecology, University of Vienna, Austria |

**Teaching experience**

| | |
|---|---|
| 2012 | Tutor at the University of Vienna, Austria |

CURRICULUM VITAE

Agnes Harreither